From Dynamic Combinatorial "Hit" to Lead: *In vitro* and *in vivo* activity of compounds targeting the pathogenic RNAs that cause myotonic dystrophy

Leslie O. Ofori, Jason Hoskins, Masayuki Nakamori, Charles A. Thornton, and Benjamin L. Miller*

Departments of Dermatology, Chemistry, and Medicine, University of Rochester, Rochester, New York 14642

Benjamin_miller@urmc.rochester.edu

Supplementary information

INDEX:

Reagents and Materials. Commercially available reagents were obtained from Sigma Aldrich Chemical Co. (St. Louis, MO), TCI America (Portland, OR) Fisher Scientific, EMD Chemicals (Gibbstown, NJ) Advanced ChemTech (Louisville, KY) and Alfa Aesar and were used without further purification unless otherwise noted. Water used for reactions and aqueous workup was glass-distilled from a deionized water feed. Reagent grade solvents were used for all non-aqueous extractions. Reaction progress was monitored by analytical thin-layer chromatography (TLC) using EM silica gel 60 F-254 precoated glass plates (0.25 mm). Compounds were visualized on the TLC plates with a UV lamp (dual wavelength; λ=254 nm, λ =360 nm). Synthesized compounds were purified using flash column chromatography on EM silica gel 60 (230-400) mesh or alternatively via preparative reversed phase HPLC. Cell were cultured in Dulbecco's modified Eagle's medium (DMEM (GIBCO Cat# 11995)), supplemented with 10 % FBS and 1% pen-strep. MTT used for viability studies was purchased from CHEMICON, Inc.

Analysis. ^{1}H NMR spectra were recorded at 25 °C on either a Bruker Avance 400 (400 MHz) or Bruker Avance 500 (500 MHz) instrument and processed using MestReNova NMR processing software. Chemical shifts (δ) are reported in parts per million (ppm)

downfield from tetramethylsilane and referenced to the residual protium signal in the NMR solvents (D_2O, δ = 4.79). Data are reported as follows: chemical shift, multiplicity (s = singlet, d = doublet, t = triplet, m = multiplet and q = quartet), coupling constant (*J*) in Hertz (Hz) and integration. ^{13}C spectra were recorded at 25 °C on a Bruker Avance 500 instrument operating at 126 MHz. Chemical shifts (δ) are reported in ppm downfield from tetramethylsilane and referenced (except in D_2O) to the primary carbon resonance in the NMR solvent. FT-IR spectra were recorded on Shimadzu FT-IR spectrophotometer. High-resolution mass spectra (HRMS) were acquired at the university of Buffalo chemistry department mass spectrometry facility, Buffalo, NY or at the mass spectrometry facility of the University of California, Riverside. Low resolution mass spectra were recorded on Shimadzu LC/MS 2010 with APCI or electrospray ionization.

SYNTHESIS OF COMPOUNDS:

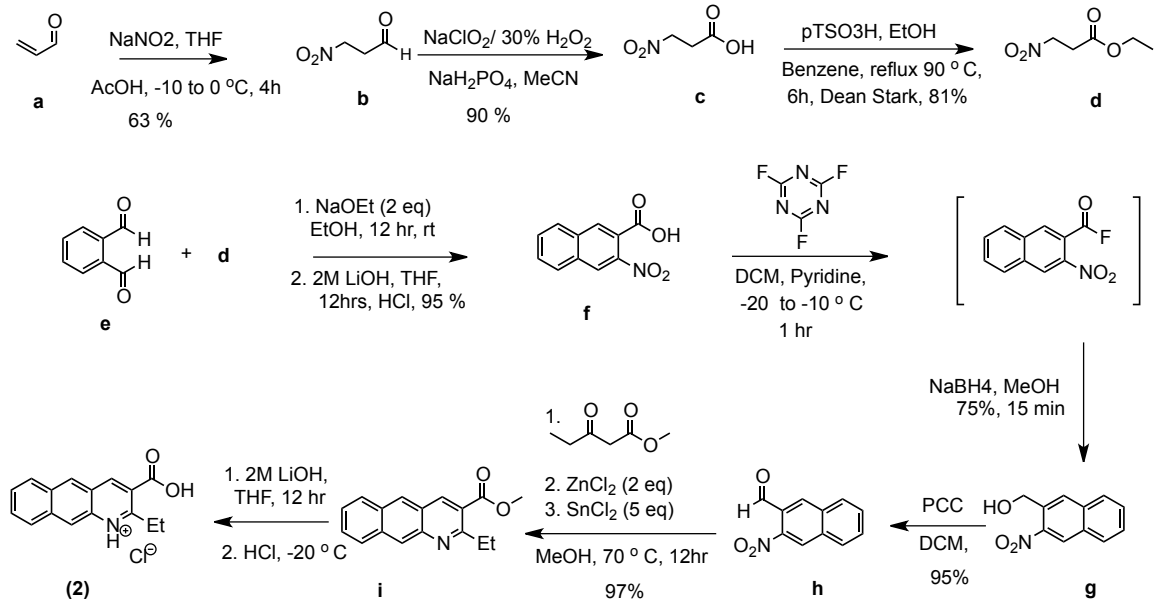

Supplementary Scheme 1. Synthesis of 2-ethyl benzo [*g*] quinoline carboxylic acid **(2)** starting from commercially available acrolein.

Ethyl-3-nitropropanoate **(d)** was prepared by following literature procedures[1] starting from commercially available acrolein (a). Spectral data were comparable to those reported in the literature (**Supplementary Scheme 1 a-d**). Ethyl-3-nitropropanoate **(d):** ^{1}H NMR (400 MHz, $CDCl_3$) δ: 4.62 - 4.39 (m, 2H), 4.03 (q, *J* = 7.1 Hz, 2H), 2.92 - 2.69 (m, 2H), 1.12 (t, *J* = 7.1 Hz, 3H). ^{13}C NMR (126 MHz, $CDCl_3$) δ: 169.64, 69.72, 61.22, 30.84, and 13.82.

3-Nitro-2-naphthoic acid **(f):** was synthesized by reacting O-phthaldialdehyde (e) with ethyl-3-nitropropionate using a method reported by Kienzel.[2] Spectral data were comparable to those reported in the literature**.** ^{1}H NMR (400 MHz, CD_3OD) δ: 8.38 (s, 1H), 8.30 (s, 1H), 8.01 (dd, *J* = 8.1, 4.6 Hz, 2H), 7.74 - 7.64 (m, 3H). ^{13}C NMR (126 MHz, CD_3OD) δ: 167.80, 146.75, 134.17, 133.47, 131.89, 130.36, 130.12, 129.61, 129.29, 124.94, 124.87. LRMS (ES-) calculated for $C_{11}H_6NO_4$ $(M-H)^-$ 216 found 216.

(3-Nitronaphthalen-2-yl) methanol **(g)** was prepared from (**f**) via a one-pot procedure for the conversion of carboxylic acids into alcohols[3]. Briefly, an oven dried two-neck round bottom flask equipped with a mechanical stirrer and a thermometer was cooled under N_2 gas. Pyridine (1.113 mL, 13.8 mmol) was added to a stirred solution of 3-nitro-2-naphthoic acid (3 g, 13.81 mmol) in dry CH_2Cl_2. The flask was cooled to -10 to -20 $^{\circ}$C in an acetone/dry ice bath, and then cyanuric fluoride (3.73 g, 27.63 mmol) was added in one portion. The mixture was then stirred vigorously at -10 to -20 $^{\circ}$C for 1 hour, diluted with CH_2Cl_2 and then 50 mL of ice-cold water was added. The aqueous phase was extracted (1 x100 mL) with CH_2Cl_2 and dried over $MgSO_4$. The solvent was concentrated under vacuum to a small volume (40 mL) in CH_2Cl_2, and then solid $NaBH_4$ (1.0451 g, 27.63 mmol) was added in one portion. Methanol (20 mL) was added in drops for over 15 minutes at ambient temperature. The reaction was quenched by addition of 50 mL 1 N aqueous H_2SO_4. The organic solvent was removed under vacuum and the aqueous phase diluted and extracted (2 x 40 mL) with ethyl acetate. The product was purified by flash column chromatography (silica gel) to yield 2.2 g (81%) of **g** as a bright yellow compound. ^{1}H NMR (400 MHz, CD_3OD) δ: 8.56 (s, 1H), 8.14 (s, 1H), 7.94 (dd, *J* = 24.5, 8.1 Hz, 2H), 7.61 (dt, *J* = 28.6, 7.1 Hz, 2H), 5.01 (s, 2H). ^{13}C NMR (126 MHz, CD_3OD)

δ: 147.14, 136.41, 134.23, 132.55, 130.67, 130.22, 129.17, 128.87, 128.70, 126.50, 62.41. LRMS (ES+) calculated for $C_{11}H_{10}NO_4$ $[M+H]^+$: 204 found: 204.

3-nitro-2-naphthaldehyde **(h)**: (3-nitronaphthalen-2-yl) methanol (3 g, 14.76 mmol) dissolved in 40 mL of dry CH_2Cl_2 was added slowly to a stirred solution of pyridinium cholorochromate[4] (4.77 g, 22.15 mmol) and celite (4.77 g) in CH_2Cl_2 under N_2 atmosphere at room temperature. The reaction was monitored by TLC until none of the starting material remained, and then diluted with 50 mL of ethyl acetate and filtered through a pad of Florisil. The filtrate was concentrated under vacuum and the product was purified by column chromatography using 20 : 80 ethyl acetate : hexane to yield 2.8 g (99 %) of a yellow crystalline compound. ^{1}H NMR (400 MHz, $CDCl_3$) δ: 10.46 (s, 1H), 8.62 (s, 1H), 8.41 (s, 1H), 8.05 (dd, J = 8.5, 5.0 Hz, 2H), 7.76 (dd, J = 6.2, 3.2 Hz, 2H). ^{13}C NMR (126 MHz, $CDCl_3$) δ: 188.19, 145.77, 134.18, 133.59, 132.09, 130.62, 130.47, 129.78, 129.62, 127.88, 125.97. LRMS (ES+) calculated for $C_{11}H_7NO_3$ $[M+H]^+$: 202 found: 202.

2-ethylbenzo[g]quinoline-3-carboxylic acid (**2**): A flame dried 100 mL 3-neck round bottom flask was equipped with a teflon-coated stir bar, thermometer, and a reflux condenser with N_2 inlet. The flask was charged with 1 g of 3 Å molecular sieves, 3-nitro-2-naphthaldehyde (1.5 g, 7.45 mmol), methyl propionylacetate (0.97 g, 7.45 mmol) and $ZnCl_2$ (2.03g, 14.9 mmol). Anhydrous methanol (50 mL) was added, flushed with a stream of N_2 and heated while stirring to an internal temperature of 70 °C for 1 hour. Next, $SnCl_2$ (7.1 g, 37.25 mmol) was added slowly in 3 portions, after which the reaction was stirred at 70 °C and allowed to reflux for 12 hours. After cooling to room temperature, the reaction was made alkaline by the addition of 50 mL K_2CO_3 (10 g dissolved in 50 mL of water) solution. Diethyl ether (50 mL) was added, and the mixture was then filtered through a pad of celite. The celite was washed (3 x 30 mL) with ether and the combined organics washed (3 x 50 mL) with brine and concentrated under vacuum to yield a red oily residue. This crude product was dissolved in 10 mL of THF and 40 mL of 2 M aqueous LiOH was added then stirred overnight at room temperature. After removal of the organic solvent under vacuum, the aqueous layer was chilled at -20

°C for 4 hours and then acidified to pH =1 with concentrated HCl. The precipitate formed was filtered, washed with 50 mL of water and dried under vacuum overnight to yield 1.7 g (94 %) of 2-ethylbenzo[*g*]quinoline-3-carboxylic acid as a yellow solid.

FT-IR (neat): 3375.2, 3358.8, 3341.44, 3319.75, 3052.62, 2936.42, 2539.11, 2521.27, 2447.5, 2159.16, 2097.93, 2026.56, 1974.01, 1880.95, 1876.13, 1690.97, 1686.15, 1670.72, 1661.56, 1638.42, 1634.56, 1583.45, 1536.2, 1458.08, 1405.53, 1278.72, 1254.61, 1232.43, 1183.25, 1141.78, 1084.4, 1053.06, 1053.06, 966.27, 898.28, 784.97, 751.22,686.61,619.59 cm^{-1}. ^{1}H NMR (500 MHz, CD_3OD) δ: 9.89 (s, 1H), 9.13 (s, 1H), 8.83 (s, 1H), 8.32 (dd, J = 11.0, 8.7 Hz, 2H), 7.85 (dddd, J = 9.5, 8.0, 6.7, 1.1 Hz, 2H), 3.72 (q, J = 7.6 Hz, 2H), 1.55 (t, J = 7.6 Hz, 3H). ^{13}C NMR (126 MHz, CD_3OD) δ: 167.20, 165.48, 152.46, 138.34, 134.92, 134.57, 133.00, 132.10, 130.46, 129.78, 129.44, 125.22, 124.31, 118.99, 28.97, and 14.45.

HRMS *m/z* calculated for $C_{16}H_{14}NO_2$ $[M+H]^+$: 252.1019; found: 252.1012.

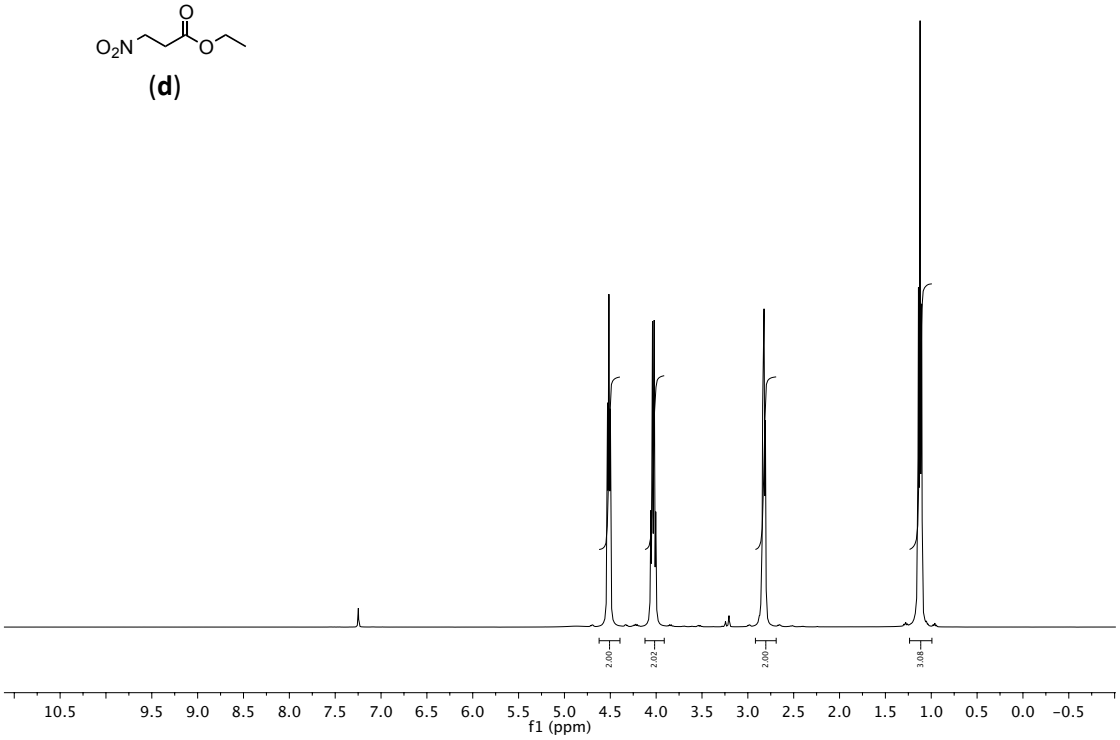
O
O_2N
O
(**d**)
2.00
2.02
2.00
3.08
10.5 9.5 9.0 8.5 8.0 7.5 7.0 6.5 6.0 5.5 5.0 4.5 4.0 3.5 3.0 2.5 2.0 1.5 1.0 0.5 0.0 −0.5
f1 (ppm)

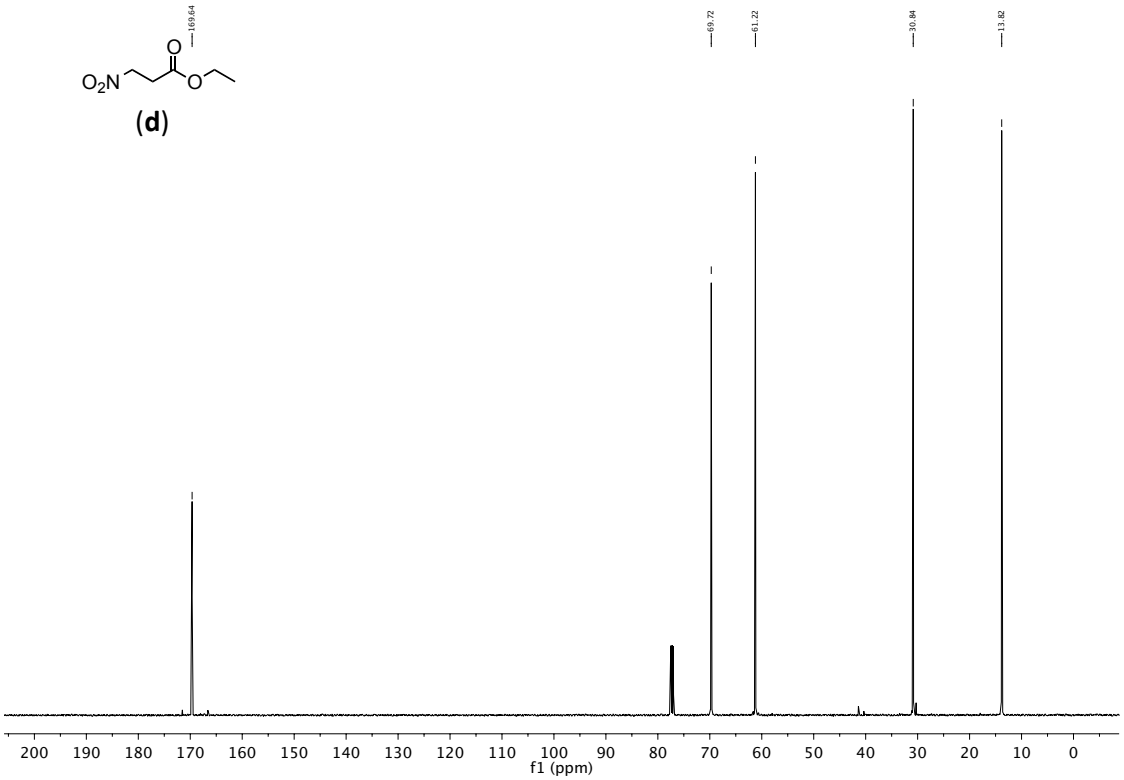
169.64
O
O_2N
O
(**d**)
69.72
61.22
30.84
13.82
200 190 180 170 160 150 140 130 120 110 100 90 80 70 60 50 40 30 20 10 0
f1 (ppm)

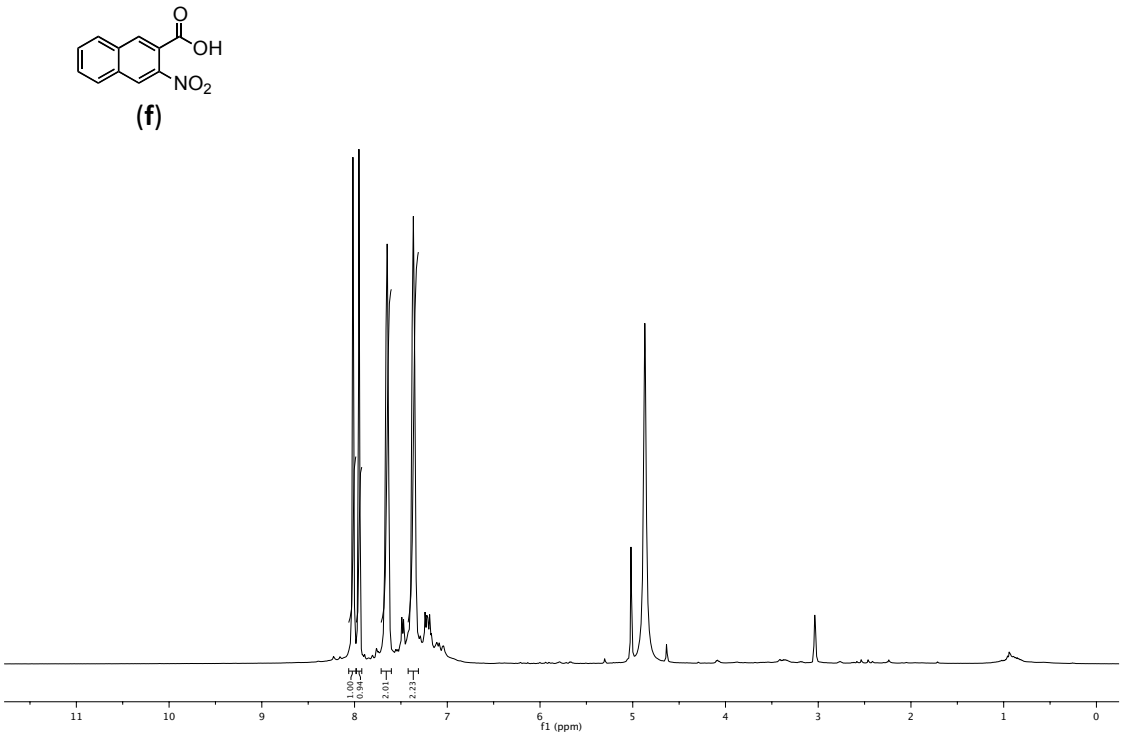
O
OH
NO2
(f)
1.00
0.94
2.01
2.23
11
10
9
8
7
6
5
4
3
2
1
0
f1 (ppm)

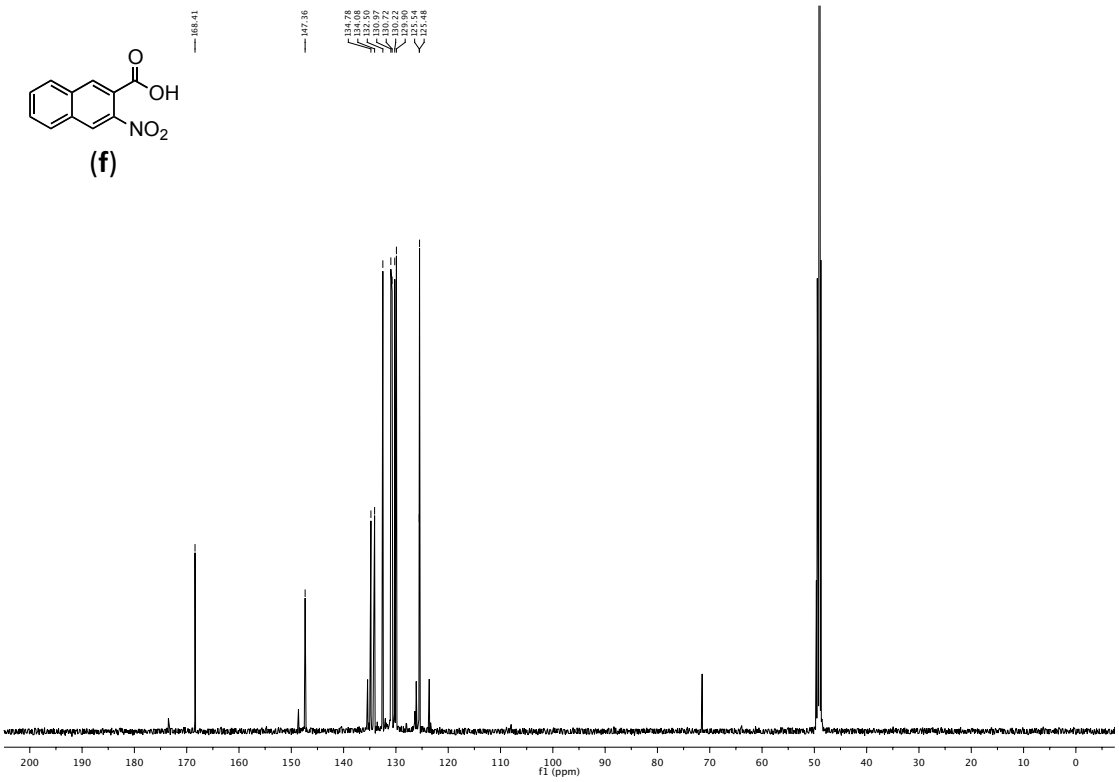
168.41
147.36
134.78
134.48
132.50
130.97
130.72
130.22
129.90
125.54
125.48
O
OH
NO2
(f)
200
190
180
170
160
150
140
130
120
110
100
90
80
70
60
50
40
30
20
10
0
f1 (ppm)

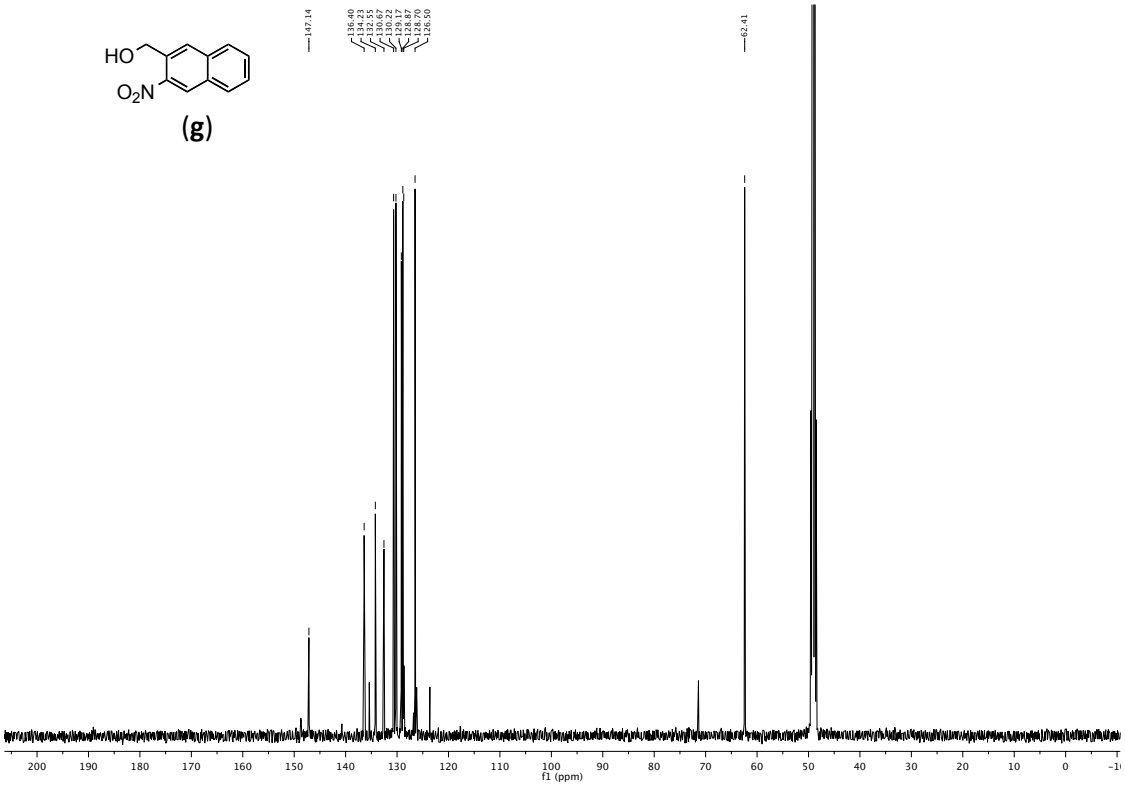
HO
O_2N
(g)
147.14
136.40
134.73
132.55
130.67
130.12
129.17
128.87
128.70
126.09
62.41
f1 (ppm)

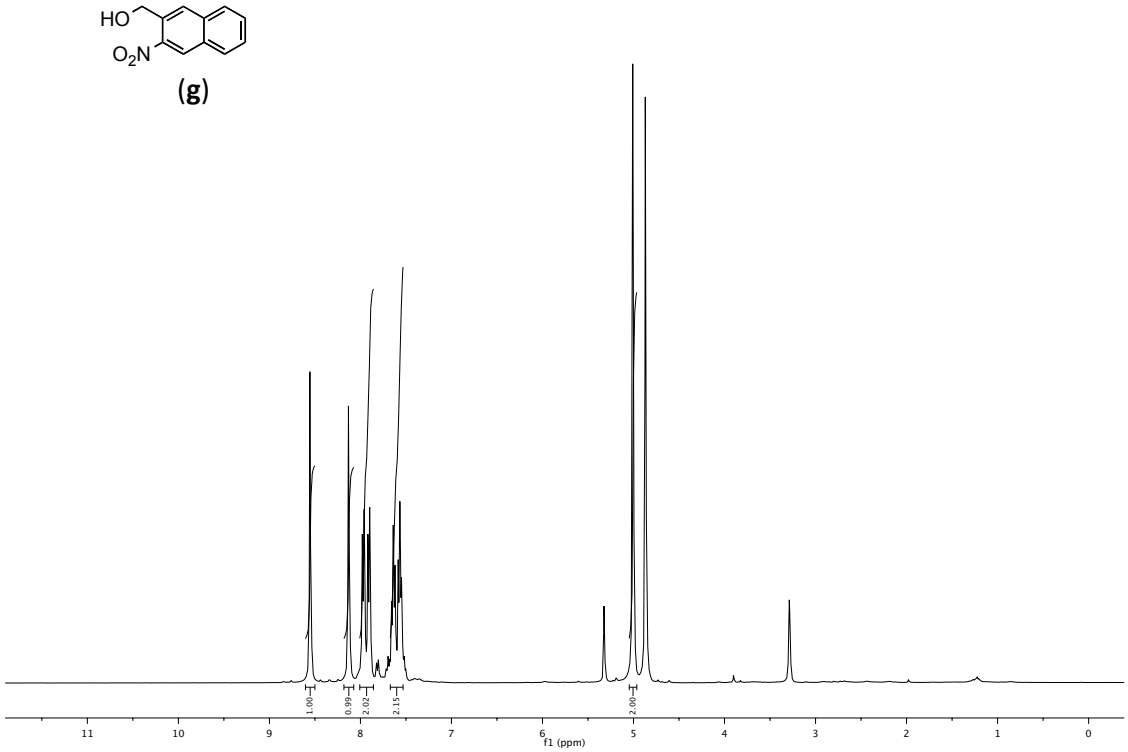
HO
O_2N
(g)
1.00
0.99
2.02
2.15
2.00
f1 (ppm)

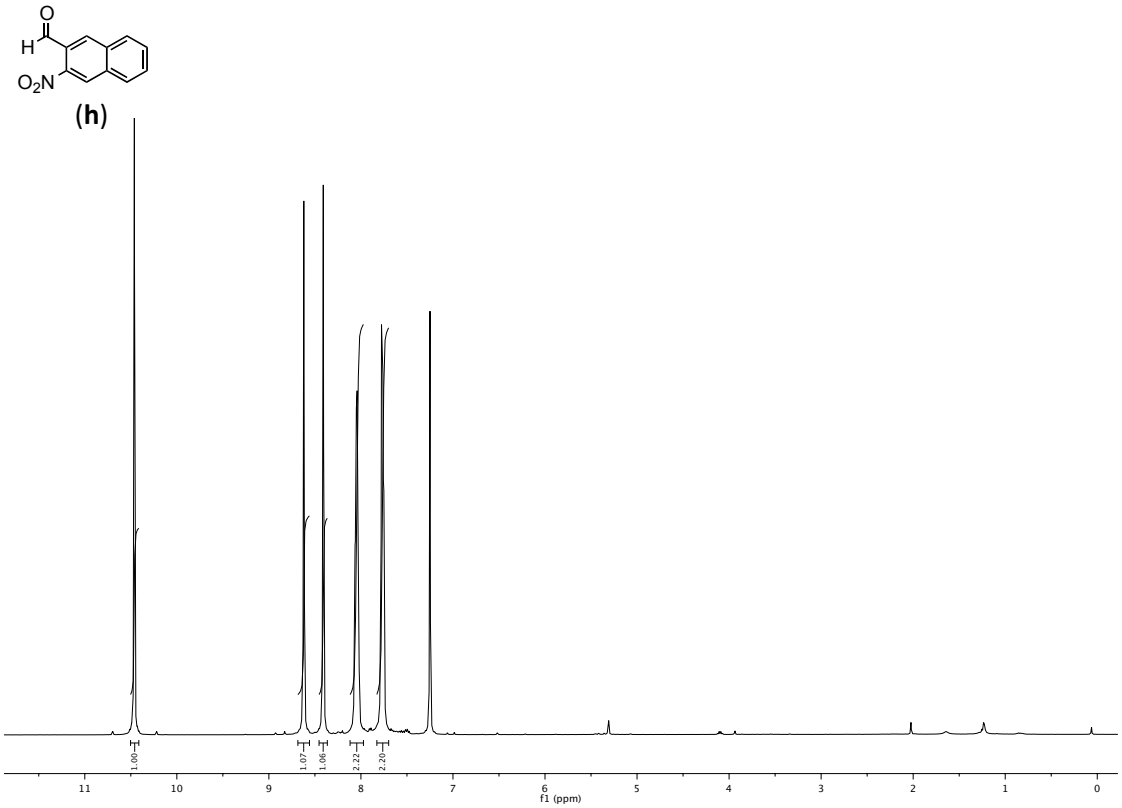
O
H
O_2N
(**h**)
1.00
1.07
1.06
2.22
2.20
11 10 9 8 7 6 5 4 3 2 1 0
f1 (ppm)

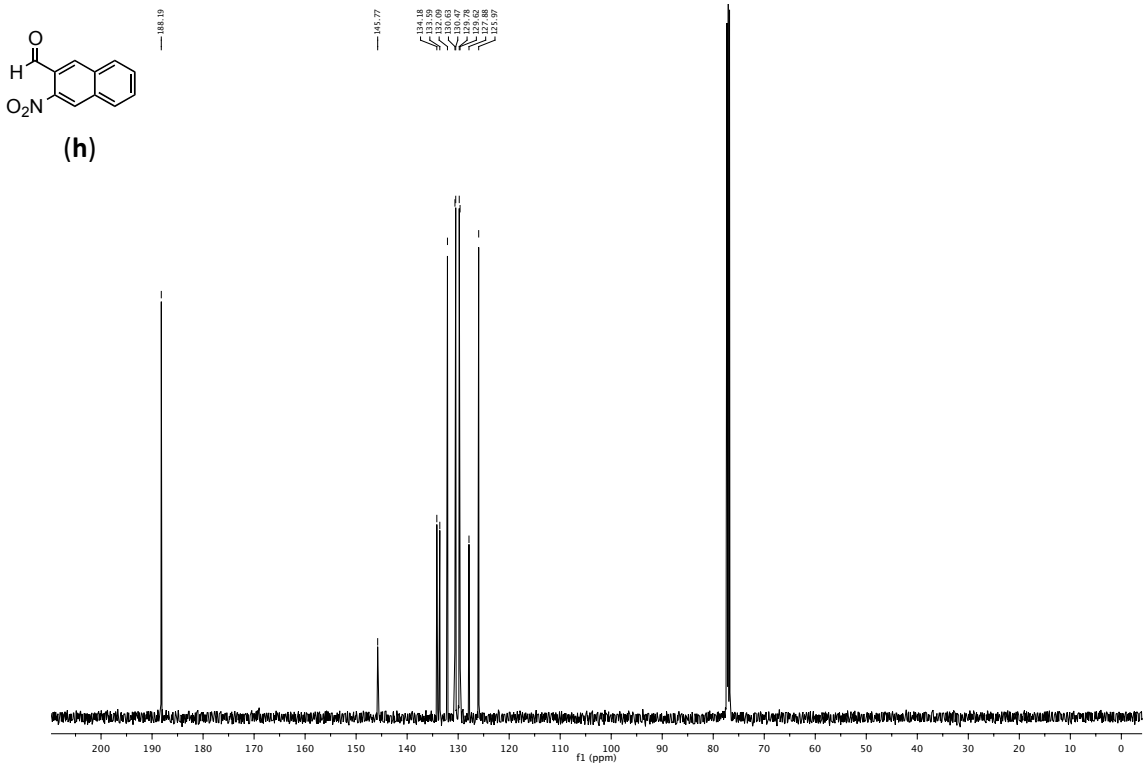
O
H
O_2N
(**h**)
188.19
145.77
134.18
133.59
133.09
132.32
130.63
130.47
130.16
129.76
129.62
127.88
127.79
125.97
200 190 180 170 160 150 140 130 120 110 100 90 80 70 60 50 40 30 20 10 0
f1 (ppm)

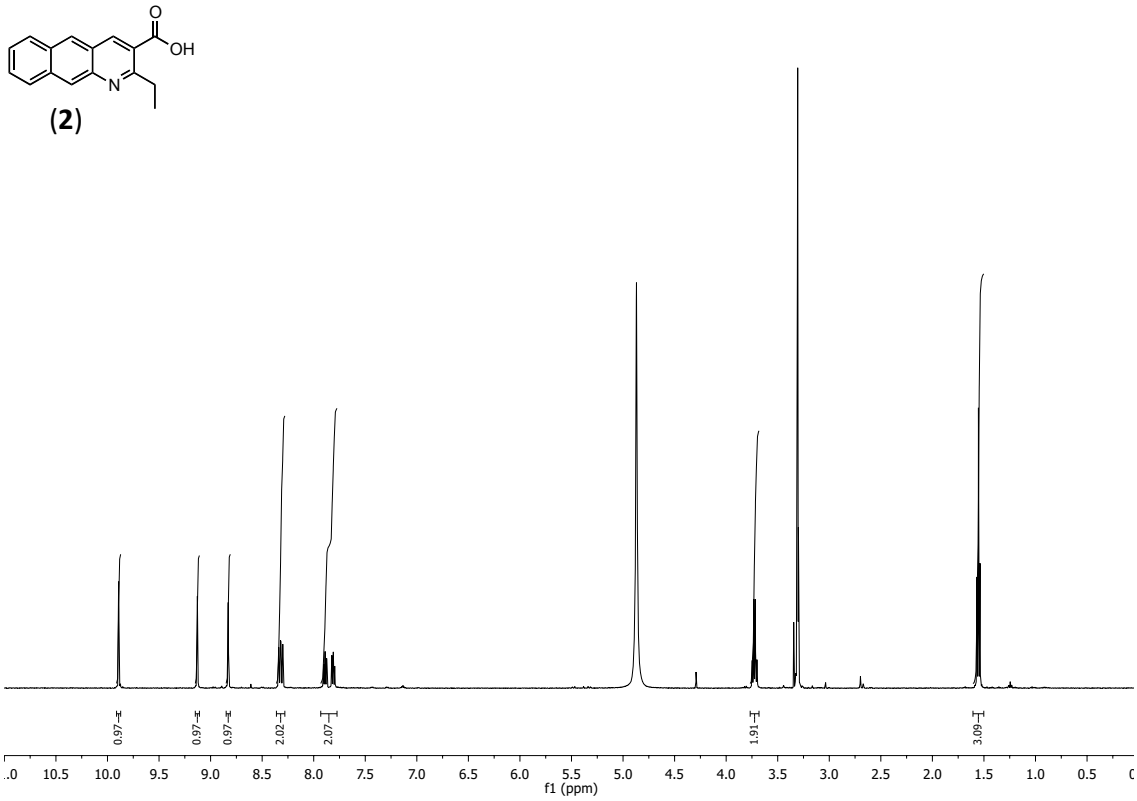
O
OH
N
(2)
0.97
0.97
0.97
2.02
2.07
1.91
3.09
10.5 10.0 9.5 9.0 8.5 8.0 7.5 7.0 6.5 6.0 5.5 5.0 4.5 4.0 3.5 3.0 2.5 2.0 1.5 1.0 0.5
f1 (ppm)

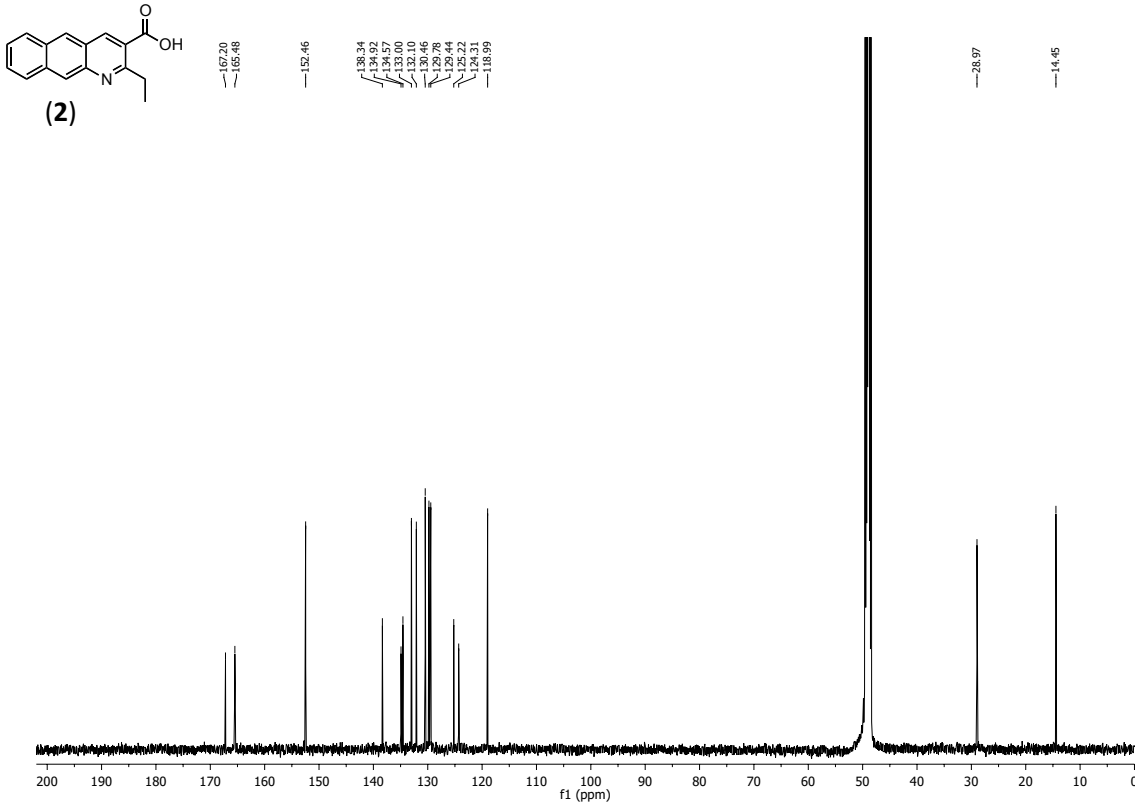
O
OH
N
(2)
167.20
165.48
152.46
138.34
134.92
134.57
133.10
132.10
130.46
129.78
129.44
125.22
124.31
118.99
28.97
14.45
200 190 180 170 160 150 140 130 120 110 100 90 80 70 60 50 40 30 20 10
f1 (ppm)

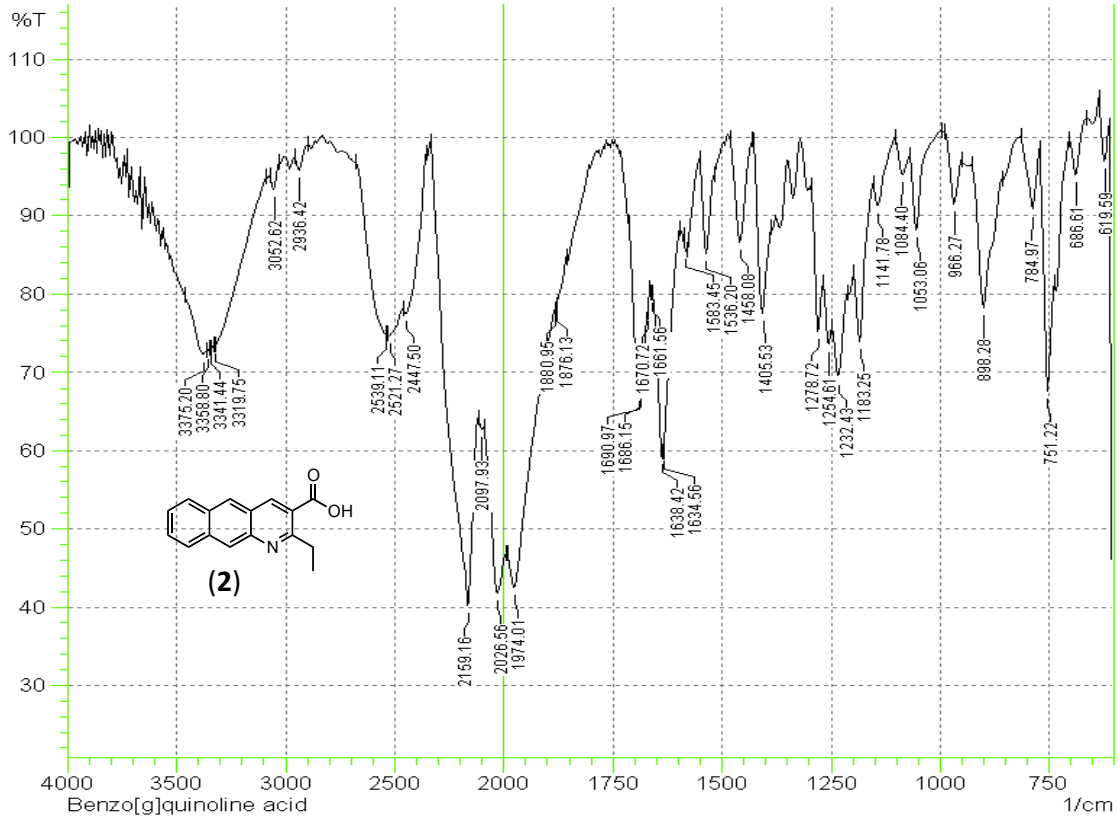
%T
110
100
90
80
70
60
50
40
30
3375.20
3358.80
3341.44
3319.75
3052.62
2936.42
2539.11
2521.27
2447.50
2159.16
2097.93
2026.56
1974.01
1880.95
1876.13
1690.97
1686.15
1670.72
1661.56
1638.42
1634.56
1583.45
1536.20
1458.08
1405.53
1278.72
1254.61
1232.43
1183.25
1141.78
1084.40
1053.06
966.27
898.28
784.97
751.22
686.61
619.59
O
OH
N
(2)
4000
3500
3000
2500
2000
1750
1500
1250
1000
750
Benzo[g]quinoline acid
1/cm

SYNTHESIS, ISOLATION AND SPECTRAL CHARACTERIZATION OF COMPOUNDS 3, 4, 5, 6, 7, 8, 9, 10, AND 11.

Compounds **3**, **4** and **5**: replacement of the disulfide in lead compound **1** with a non-labile olefin (C=C) bioisotere was performed according to procedures similar to those described in our recent report.[5] Briefly, resin bound monomer **3** (**Supplementary Scheme 2**) was synthesized using standard Fmoc methodology for solid phase peptide synthesis (SPPS). Wang resin (1.0 g, 100-200 μ mesh) was activated with 1,1'-carbonyldiimidazole (DIC, 3.3g, 10 mmol) in 12 mL of DMF for 12 h on a LabQuake rotator. The resin was then washed three times each with DMF, CH_2Cl_2 and again with DMF, followed by reaction with 1,3-diaminopropane (0.72 mL, 10 mmol) in DMF for another 12 h. After repeating the was cycle, the first amino acid (Fmoc-lys(boc)-OH, 3 mmol) was coupled to the resin using HBTU (1.14 g, 3 mmol) and DIPEA (0.85 mL, 5 mmol) in 12 mL DMF and rotating the mixture for 2 h. Following the wash cycle, Fmoc deprotection was accomplished using 12 mL of 20 % piperidine in DMF for 1 hour, followed again by the wash cycle. The remaining amino acids (Fmoc-L-allylglycine and Fmoc-L-proline) were similarly coupled to the growing peptide on the resin. 2-ethyl benzo[g]quinoline carboxylic acid (**2**) (0.502 g, 2 mmol) was coupled to the rest of the peptide using same SPPS conditions to synthesize resin-bound monomeric compound **3.**

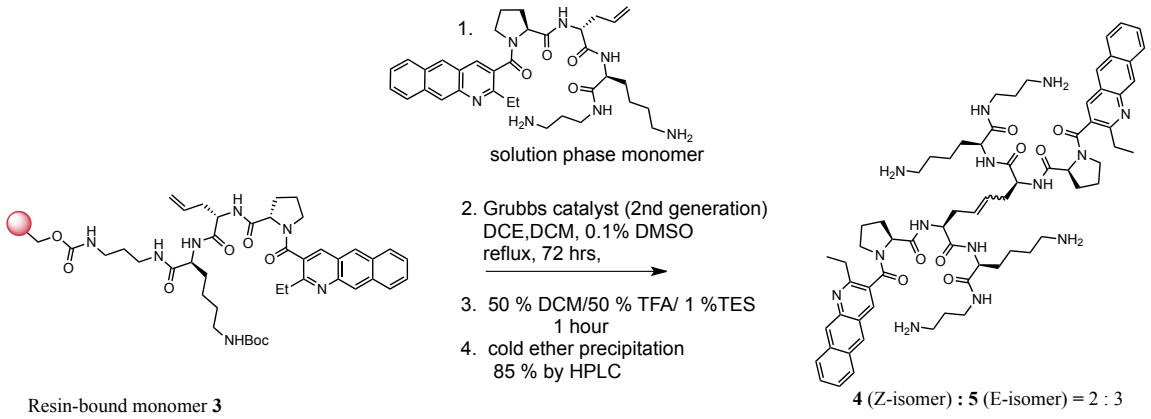

Supplementary scheme 2. Synthesis of compounds **4** and **5** using an olefin cross metathesis reaction.

Next, the resin was split into two equal parts of 0.50 g. One part was cleaved with 50 % TFA/1 % TES in 10 mL of CH_2Cl_2 for 1 h to obtain **3** as a yellow solid material (0.20 g) after removal of solvent. This cleaved product was used without purification as the solution component for the metathesis reaction. Both resin-bound and cleaved **3** were dried under vacuum overnight. The resin was allowed to swell in 10 mL dry CH_2Cl_2 for 10 min, washed (3 x 10 mL) with CH_2Cl_2 and then subjected to three 10 min washes with 0.8 M LiCl in DMF. Finally, the resin was washed (2 x 10 mL) with dry, degassed 1,2-dichloroethane and suspended in 5 mL of the same solvent in a 25 mL two-neck round bottom flask equipped with a reflux condenser and an N_2 inlet. The cleaved monomer **3** (0.20 g, 0.32 mmol) dissolved in 10 mL of a 1:4 mixture of CH_2Cl_2 and 1,2-dichloroethane (with two drops of DMSO to increase solubility) was added to the resin in the flask. The flask was maintained under a constant positive pressure of N_2 gas and a solution of Grubbs' second-generation metathesis catalyst (0.04 g, 0.05 mmol) dissolved in 1,2-dichloromethane (2 mL) was added. The reaction mixture was refluxed for 24 h, after which the catalyst was replenished with another 0.04 g portion and refluxed again for another 24 h. After repeating this cycle a second time, the reaction was cooled to room temperature and transferred into a standard solid-phase reaction vessel with filtering. The resin was washed with CH_2Cl_2 (3 x 10 mL), methanol (1 x 15 mL), and DMF (3 x 10 mL) and then suspended in 10 mL of DMF with 0.2 mL DMSO and rotated for 12 hours. Finally, the resin was washed with CH_2Cl_2 (3 x 10 mL) and subjected to a cleavage cocktail of 50 % TFA/50 % CH_2Cl_2/1 % TES for 1 h to obtain crude mixture **4** and **5** in a 3:2 isomer ratio. The isomers were separated using preparative reversed-phase-HPLC on a C18 column (Waters, XBridge™ Prep C18 5 μm OBD™, 19 X 250 mm) using a water-acetonitrile gradient with 0.1% TFA. While *E* and *Z* olefin geometries cannot be assigned definitively in the absent an X-ray crystal structure, we have proposed assignments based on three lines of evidence: chemical shifts of the olefin protons in the ^{1}H NMR spectra, analysis of the IR spectra, and the known selectivity of olefin cross-metathesis reactions. In ^{1}H NMR, the chemical shift of the olefin proton in the E-isomer is further downfield compared to the Z-isomer.[6,7] The infrared C=C stretch for the E-isomer shows absorbance at a higher frequency (1665 cm^{-1}) compared to the Z-isomer C=C stretch (1662 cm^{-1}). Also, the weak absorption at 971 cm^{-1} for the E-isomer is

consistent with spectra for trans 1,2-disubstituted alkenes.[8,9] The 3:2 isomer ratio is not surprising, since although the trans isomer is thermodynamically more favored in olefin metathesis reactions, this often provides only modest selectivity.[9]

HPLC trace for compound **3**

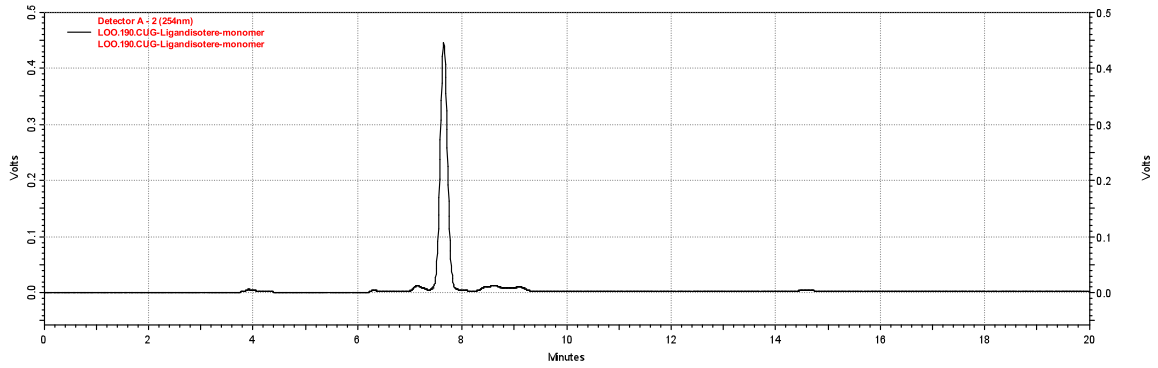

HPLC trace for crude mixture of **4** and **5**

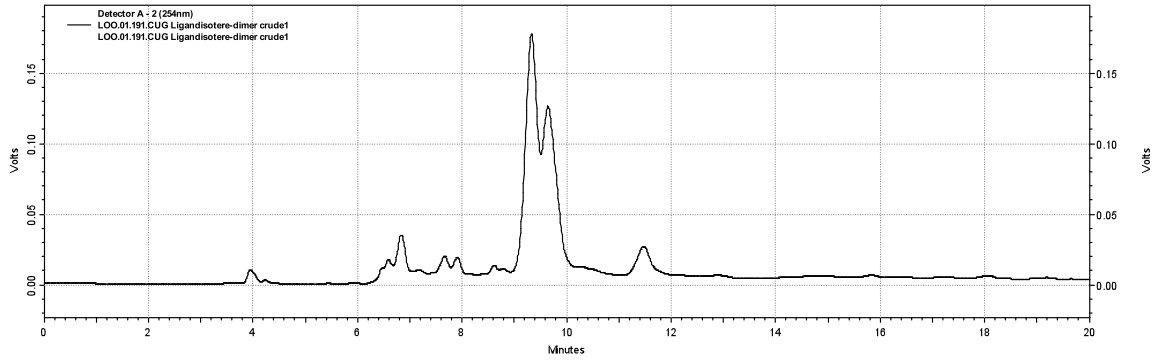

HPLC trace for compound **4** (minor *Z*-isomer)

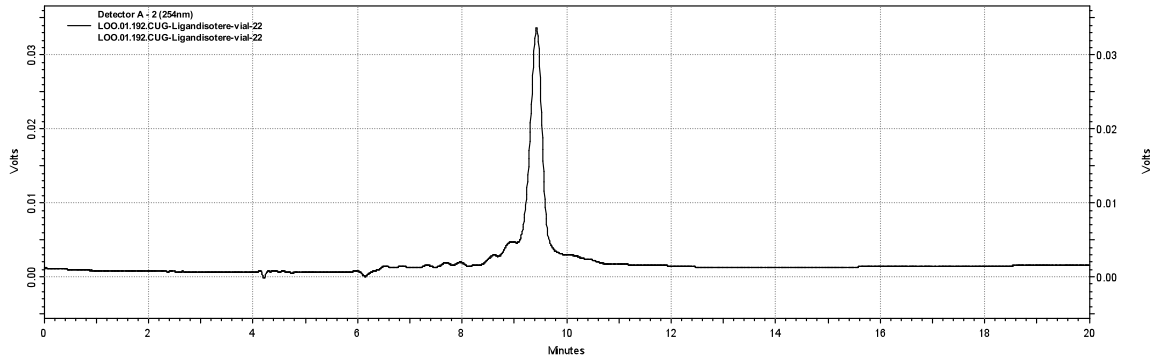

HPLC trace for compound **5** (major *E*-isomer)

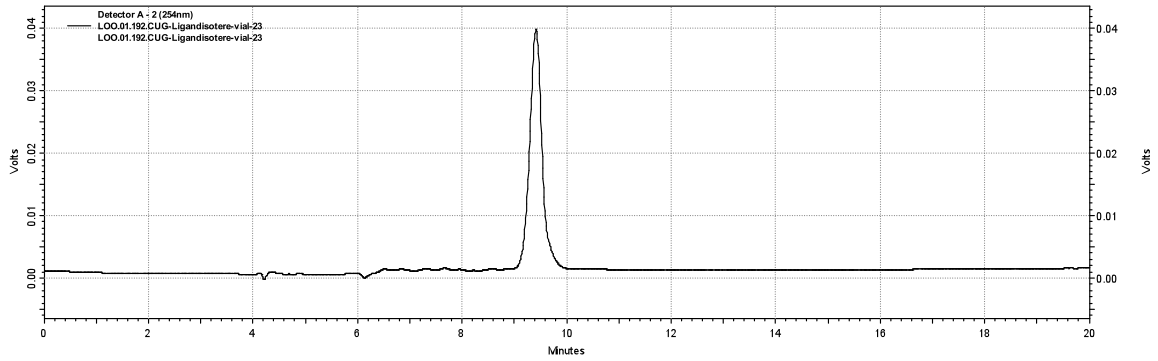

NMR SPECTRA (^{1}H and ^{13}C) FT-IR and HRMS OF COMPOUNDS 3, 4 and **5**

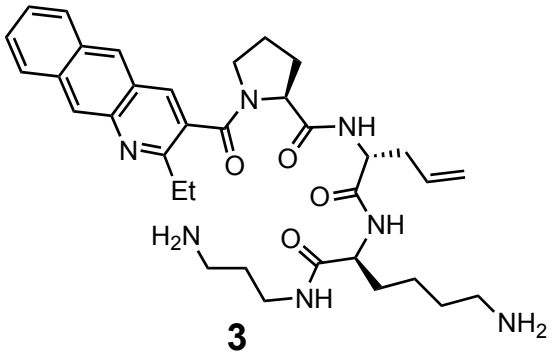

FT-IR (neat): 3654.37, 3117.23, 3080.59, 3041.53, 3016.94, 2944.13, 2934.01, 2532.36, 2520.79, 2488.97, 2449.43, 2159.16, 2097.93, 2027.05, 1974.01, 1904.09, 1875.16, 1854.43, 1660.6, 1654.81, 1646.61, 1638.42, 1631.67, 1628.77, 1581.52, 1518.84, 1430.12, 1405.05, 1194.82, 1176.5, 1126.35, 988.93, 924.32, 881.89, 833.67, 797.99, 748.8

^{1}H NMR (400 MHz, CD_3OD) δ: 9.24 (s, 1H), 8.89 (s, 1H), 8.76 (s, 2H), 8.22 (d, J = 4.8 Hz, 3H), 7.75 (dt, J = 14.3, 6.6 Hz, 3H), 5.91 (dq, J = 10.1, 6.8 Hz, 1H), 5.16 (dd, J = 36.1, 13.8 Hz, 3H), 4.73 (dd, J = 7.9, 5.3 Hz, 2H), 4.41 (dd, J = 15.6, 10.3 Hz, 2H), 4.26 (dd, J = 8.7, 5.2 Hz, 1H), 4.21 – 4.12 (m, 1H), 3.97 (d, J = 8.5 Hz, 1H), 3.84 (s, 2H), 3.60 (dd, J = 10.8, 6.6 Hz, 2H), 3.01 – 2.80 (m, 7H), 2.71 – 2.50 (m, 2H), 2.42 (dd, J = 12.2, 7.5 Hz, 2H), 2.20 – 1.92 (m, 6H), 1.90 – 1.55 (m, 12H), 1.55 – 1.30 (m, 9H).

^{13}C NMR (126 MHz, CD_3OD) δ: 174.48, 173.74, 173.45, 163.74, 137.06, 134.38, 134.00, 133.26, 130.71, 130.05, 129.97, 129.65, 129.59, 129.03, 124.90, 124.61, 118.34, 117.66, 62.88, 61.53, 54.70, 54.49, 54.36, 51.00, 40.17, 40.08, 40.05, 37.92, 37.83, 37.75, 36.62, 36.53, 35.94, 32.88, 31.99, 31.92, 30.85, 28.29, 28.24, 27.70, 27.65, 27.61, 25.75, 23.75, 23.50, 23.41, 13.76, 13.68, 13.62.

HRMS *m/z* calculated for $C_{35}H_{48}N_7O_4$ $[M+H]^+$: 630.3762, found: 630.3760

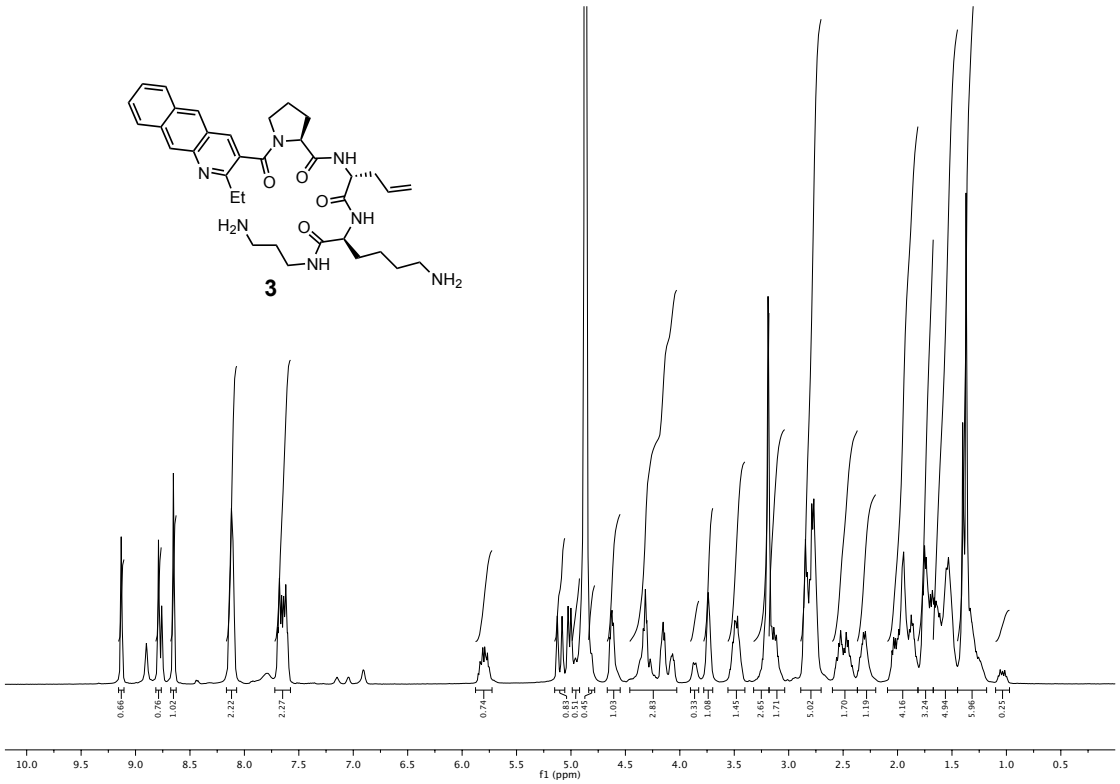
3
f1 (ppm)

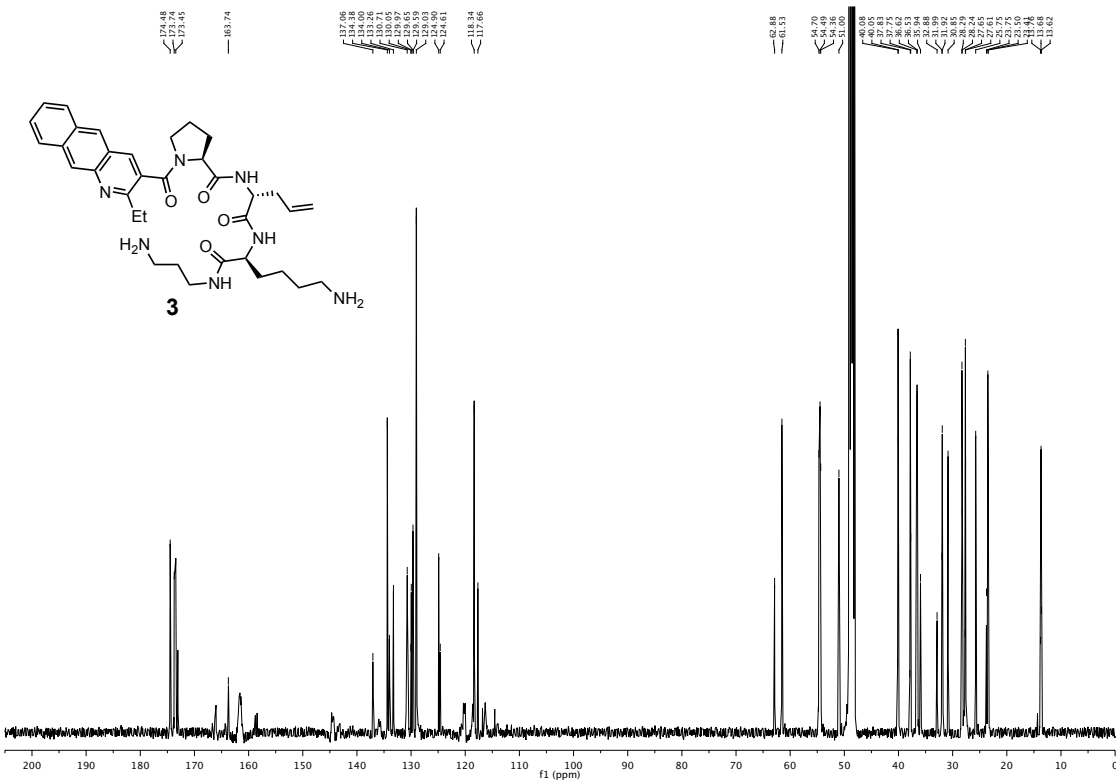
3
f1 (ppm)

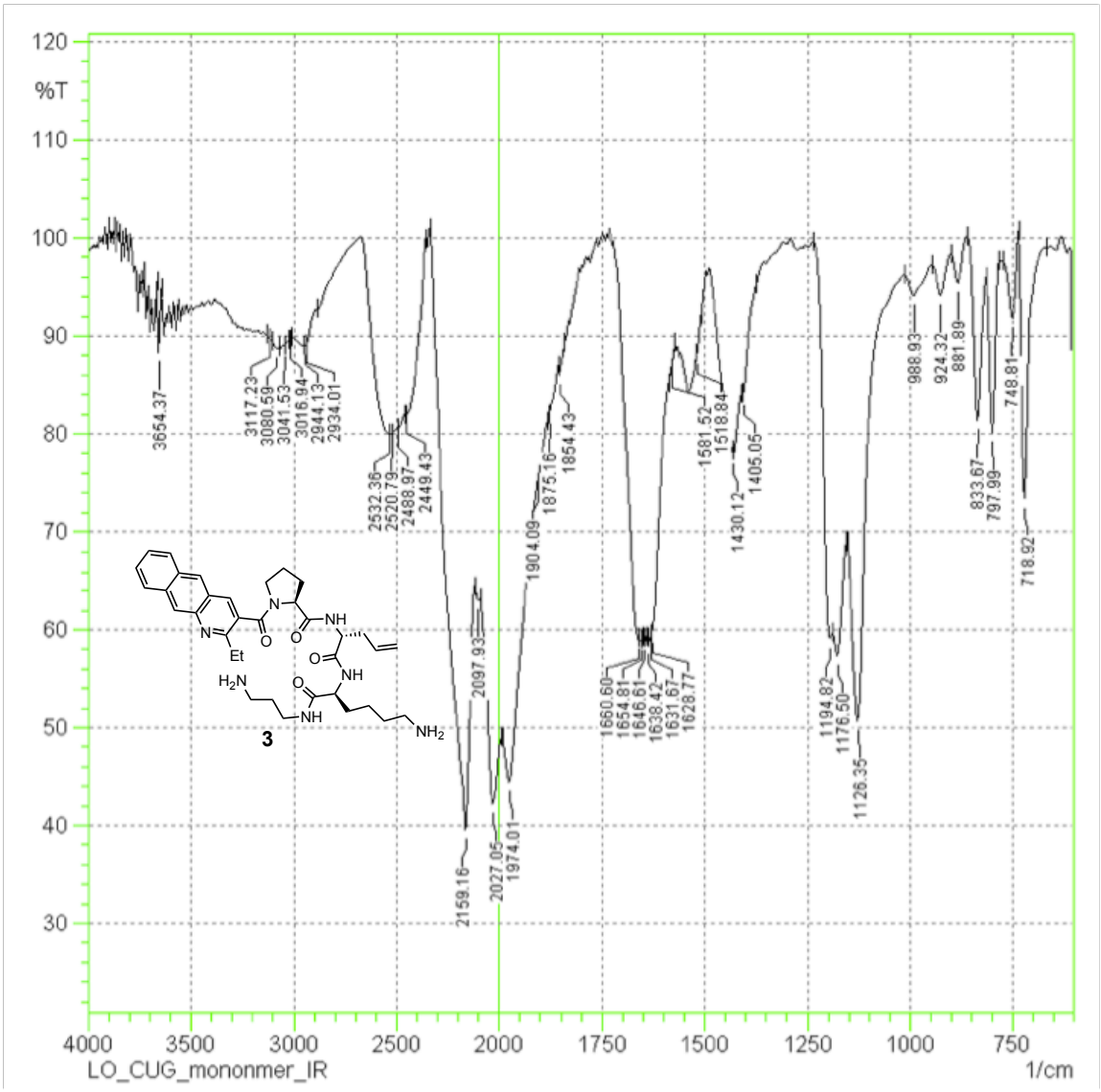
%T
1/cm
LO_CUG_mononmer_IR
3654.37
3117.23
3080.59
3041.53
3016.94
2944.13
2934.01
2532.36
2520.79
2488.97
2449.43
2159.16
2097.93
2027.05
1974.01
1904.09
1875.16
1854.43
1660.60
1654.81
1646.61
1638.42
1631.67
1628.77
1581.52
1518.84
1430.12
1405.05
1194.82
1176.50
1126.35
988.93
924.32
881.89
833.67
797.99
748.81
718.92
3

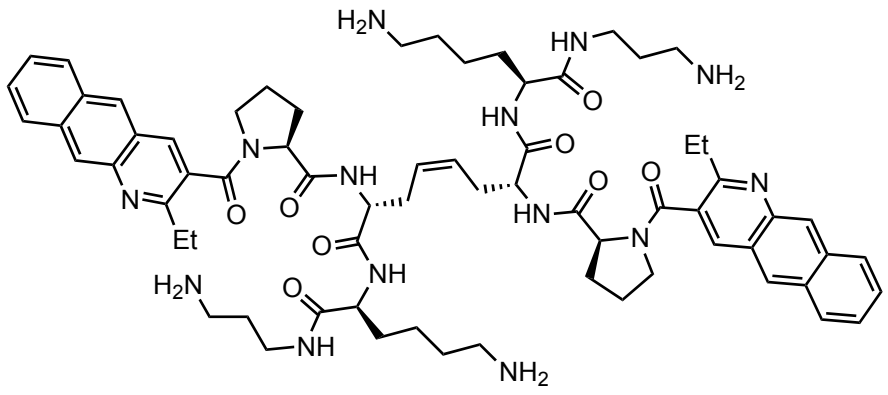

4

FT-IR (neat): 3461.02, 3284.07, 3271.53, 3059.86, 3056.96, 2947.99, 2671.71, 2560.33, 1662.04, 1649.99, 1645.17, 1535.71, 1532.34, 1433.98, 1433.98, 1181.8, 1127.8, 1061.74, 968.68, 880.93, 836.08, 798.96, 751.7, 719.4

^{1}H NMR (500 MHz, D_2O) δ: 8.50 (s, 1H), 7.71 (s, 1H), 7.41 (s, 1H), 7.16 (s, 2H), 6.97 (dd, J = 20.3, 17.0 Hz, 2H), 5.66 – 5.50 (m, 2H), 5.23 (d, J = 11.1 Hz, 1H), 5.15 (s, 1H), 5.13 (s, 1H), 4.58 – 4.45 (m, 2H), 4.31 – 4.14 (m, 2H), 3.43 (s, 1H), 3.29 (dt, J = 12.5, 5.9 Hz, 4H), 3.17 – 3.03 (m, 2H), 2.97 (dt, J = 19.3, 9.3 Hz, 10H), 2.54 (d, J = 14.9 Hz, 2H), 2.41 (s, 2H), 2.04 – 1.57 (m, 20H), 1.43 (t, J = 7.6 Hz, 10H), 1.21 (t, J = 7.7 Hz, 2H), 1.02 – 0.98 (m, 1H).

^{13}C NMR (126 MHz, D_2O) δ: 173.78, 173.73, 173.39, 173.19, 172.64, 172.50, 164.32, 163.79, 162.18, 159.98, 153.50, 144.50, 140.51, 139.93, 138.42, 137.12, 133.87, 132.70, 130.72, 129.08, 128.86, 128.71, 128.38, 128.27, 127.96, 127.75, 127.40, 127.10, 121.79, 116.30, 60.40, 60.22, 53.94, 53.75, 53.49, 53.18, 50.45, 49.85, 49.12, 48.63, 39.14, 39.10, 37.06, 37.01, 36.24, 36.16, 34.12, 30.66, 30.40, 29.92, 28.63, 26.64, 26.60, 26.38, 26.32, 26.26, 24.79, 24.65, 24.47, 22.13, 14.40, 13.43.

HRMS *m/z* calculated for $C_{68}H_{91}N_{14}O_8$ $[M+H]^+$: 1231.7139: found: 1231.7155.

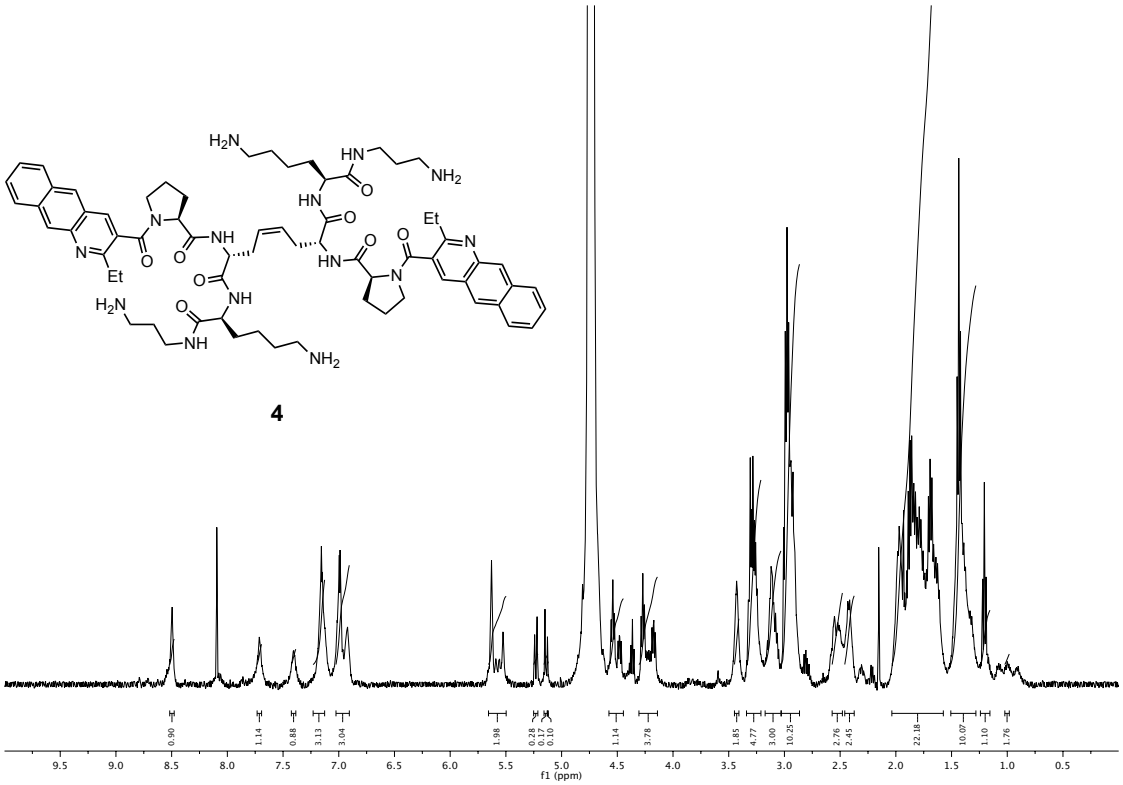
4
f1 (ppm)

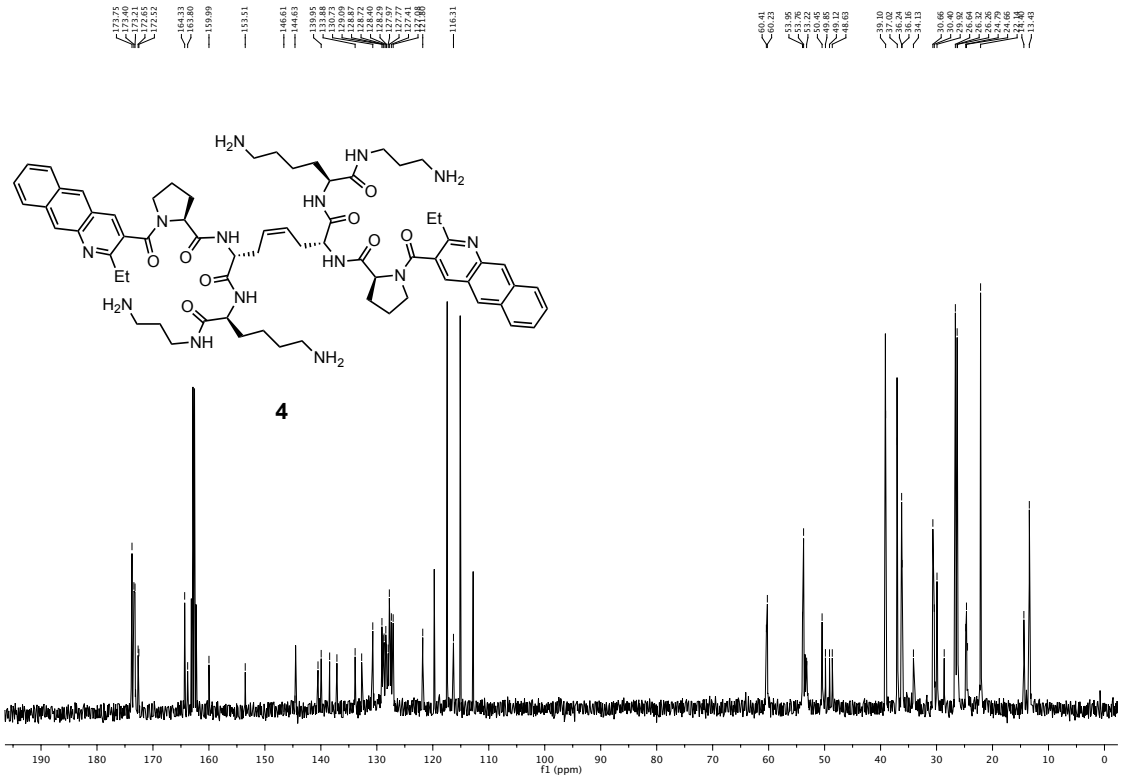
4
f1 (ppm)

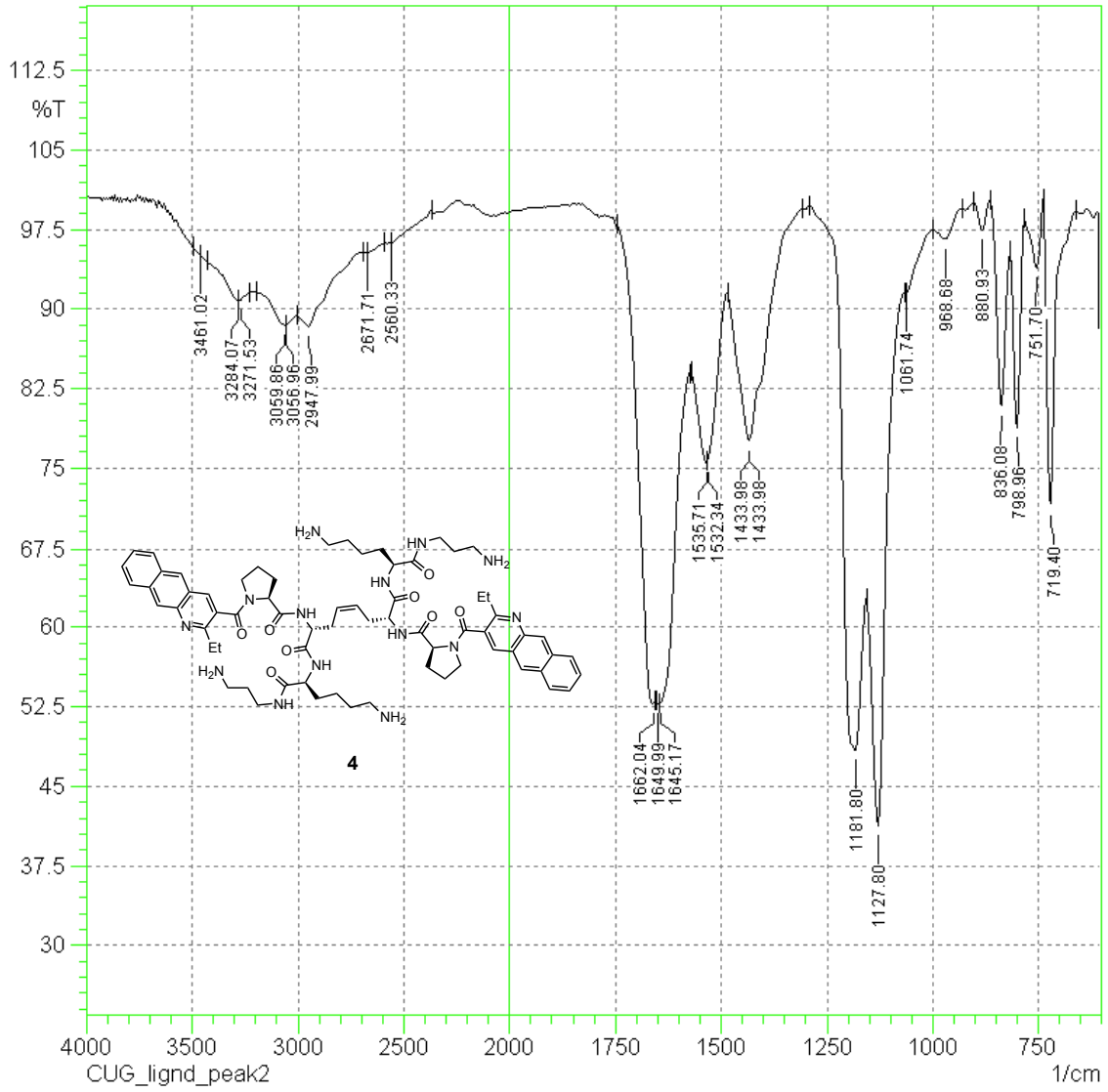
112.5
%T
105
97.5
90
82.5
75
67.5
60
52.5
45
37.5
30
3461.02
3284.07
3271.53
3059.86
3056.96
2947.99
2671.71
2560.33
1662.04
1649.99
1645.17
1535.71
1532.34
1433.98
1433.98
1181.80
1127.80
1061.74
968.68
880.93
836.08
798.96
751.70
719.40
4
4000
3500
3000
2500
2000
1750
1500
1250
1000
750
CUG_lignd_peak2
1/cm

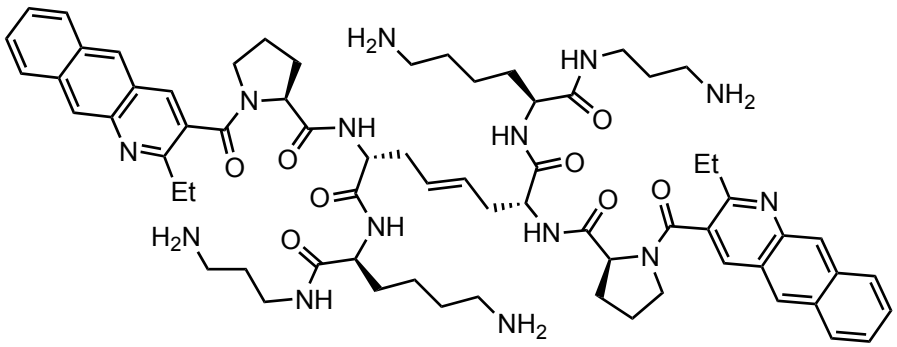

5

FT-IR (neat): 3285.03, 3271.53, 3054.55, 3048.77, 2945.58, 2675.08, 2557.43, 1665.42, 1648.54, 1533.79, 1431.57, 1193.85, 1179.39, 1127.32, 1062.22, 972.06, 881.41, 834.64, 798.47, 753.63, 719.4

^{1}H NMR (500 MHz, D_2O) δ: 8.56 (s, 1H), 7.74 (s, 1H), 7.36 (s, 1H), 7.19 – 7.12 (m, 3H), 7.11 – 7.07 (m, 1H), 7.02 – 6.94 (m, 3H), 6.94 – 6.90 (m, 1H), 5.67 (t, J = 4.4 Hz, 1H), 5.55 (s, 1H), 5.24 (d, J = 10.9 Hz, 1H), 5.14 (d, J = 10.9 Hz, 1H), 4.64 – 4.55 (m, 1H), 4.52 – 4.39 (m, 1H), 4.27 – 4.20 (m, 2H), 4.18 (d, J = 6.1 Hz, 1H), 4.11 (s, 1H), 3.43 (s, 2H), 3.29 (d, J = 9.1 Hz, 9H), 3.11 (s, 2H), 2.97 (dt, J = 23.5, 8.0 Hz, 19H), 2.69 (s, 2H), 2.62 (s, 2H), 2.41 (s, 2H), 2.01 – 1.91 (m, 8H), 1.90 – 1.74 (m, 17H), 1.74 – 1.61 (m, 13H), 1.41 (dd, J = 16.6, 8.8 Hz, 18H), 1.22 (t, J = 7.8 Hz, 2H).

^{13}C NMR (126 MHz, D_2O) δ: 173.86, 173.76, 173.35, 173.22, 173.14, 164.44, 164.39, 161.86, 160.13, 145.01, 144.50, 140.01, 139.76, 138.60, 137.31, 133.72, 132.55, 130.70, 129.01, 128.61, 128.20, 127.92, 127.72, 127.14, 127.07, 121.90, 116.29, 60.46, 60.25, 53.98, 53.03, 50.35, 48.67, 39.14, 37.06, 36.17, 30.63, 29.93, 26.65, 26.34, 24.68, 22.17, 14.24, 13.37.

HRMS *m/z* calculated for $C_{68}H_{91}N_{14}O_8$ $[M+H]^+$: 1231.7139: found: 1231.7156.

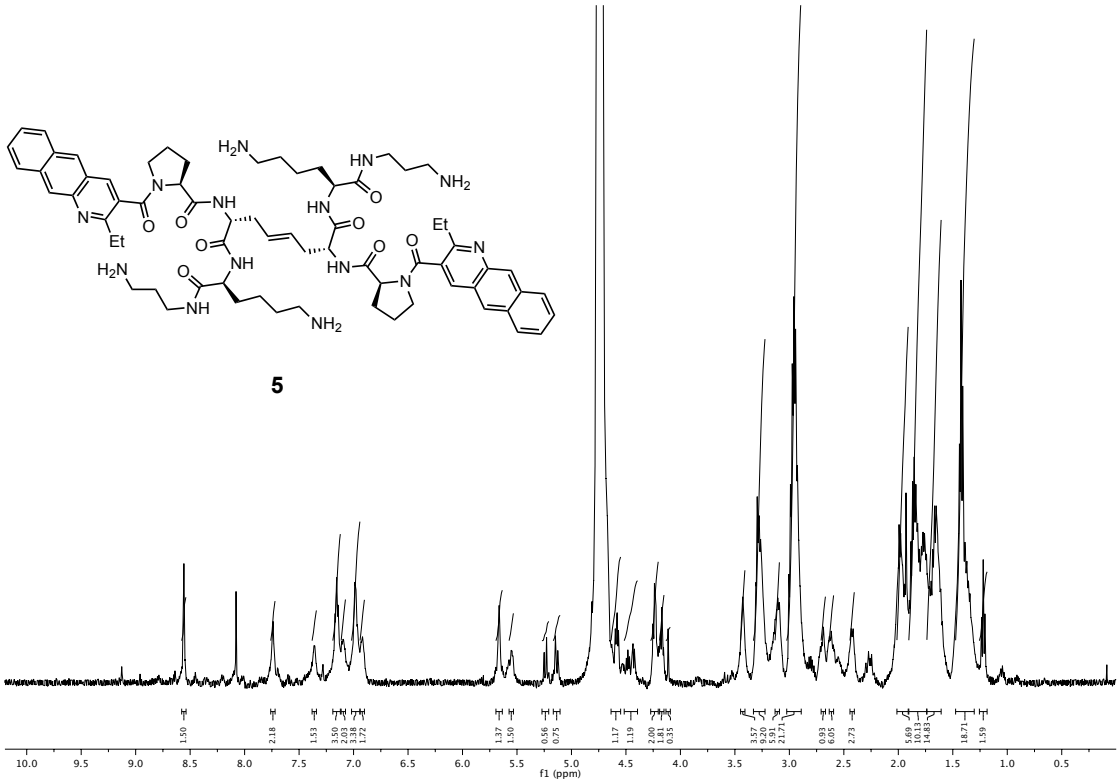
5
f1 (ppm)

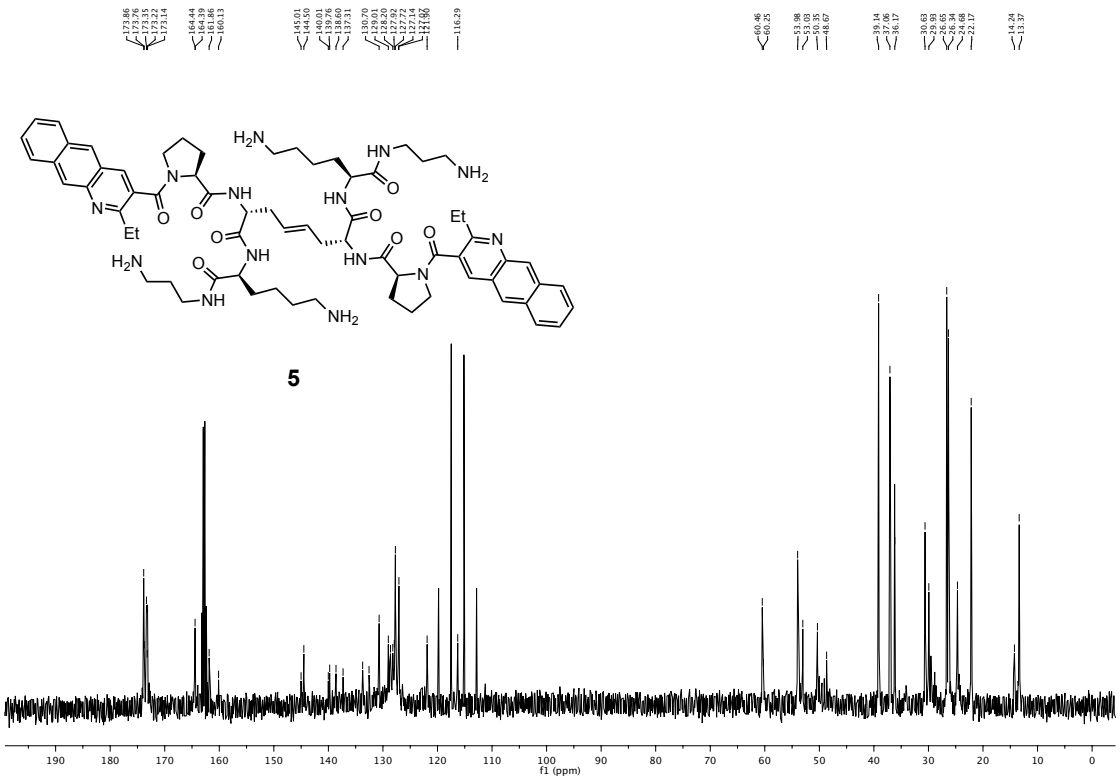
5
f1 (ppm)

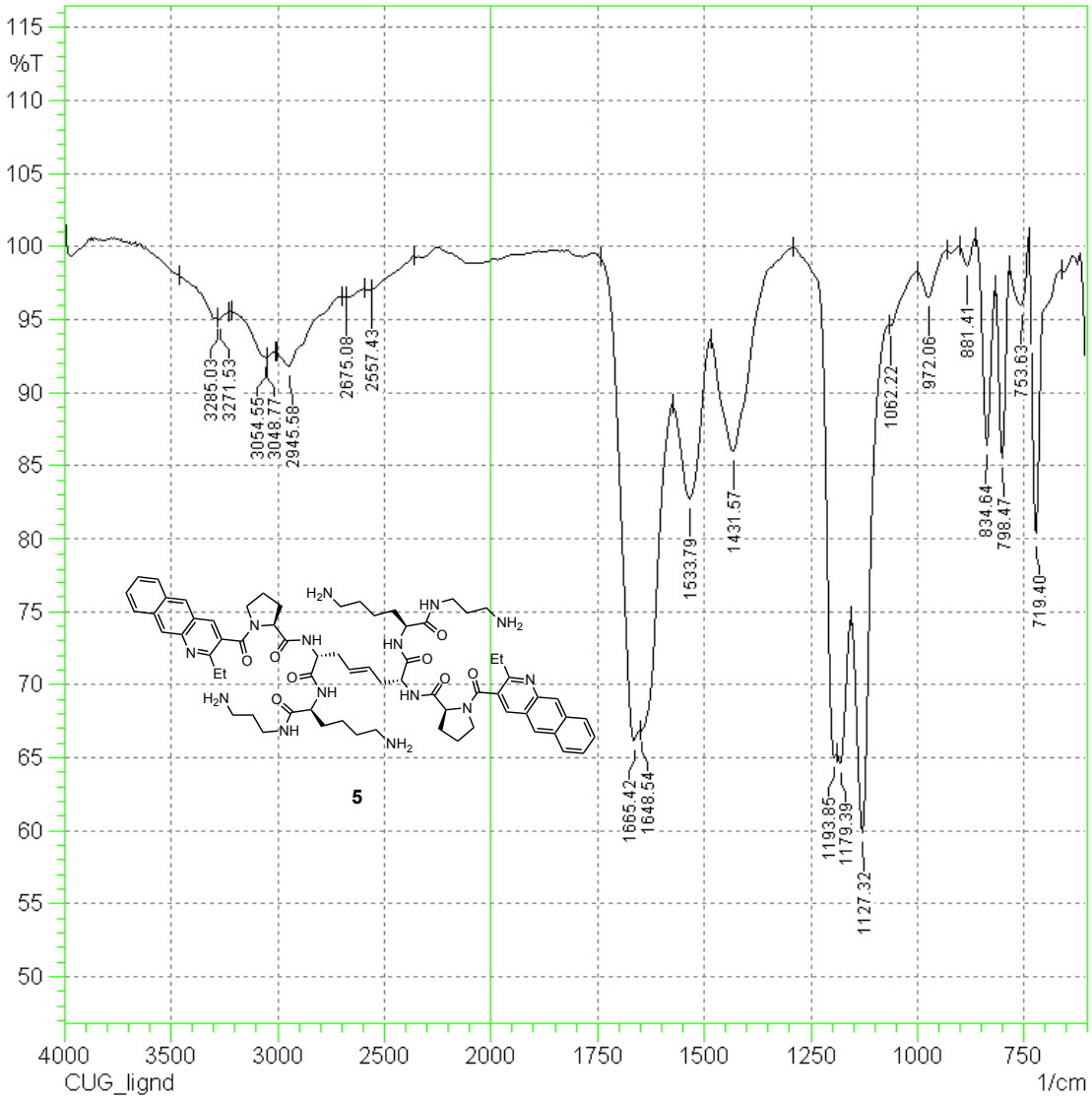
115
%T
110
105
100
95
90
85
80
75
70
65
60
55
50
4000
3500
3000
2500
2000
1750
1500
1250
1000
750
CUG_lignd
1/cm
3285.03
3271.53
3054.55
3048.77
2945.58
2675.08
2557.43
1665.42
1648.54
1533.79
1431.57
1193.85
1179.39
1127.32
1062.22
972.06
881.41
834.64
798.47
753.63
719.40
5

Compounds **6** and **7** were synthesized using the SPPS procedure described above to assemble the resin-bound monomer shown in **Supplementary Scheme 3**. However, the ethyl benzo[g]quinoline carboxylic acid heterocycle coupling step was eliminated. The resin-bound Fmoc protected monomer was then subjected to the olefin metathesis reaction in the presence of the Fmoc-monomer solution component as describe above. After the reaction was completed, the Fmoc group was removed with 20% piperidine in DMF before the peptidic product was cleaved from the resin with 50% TFA/50% CH_2Cl_2. The solvent was removed and the product was precipitate twice from cold diethyl ether. The crude mixture of **6** and **7** was purified and separated by reverse-phase preparative HPLC to obtain **6** and **7** in a *Z*:*E* geometrical isomer ratio of 1:2. The products were confirmed by mass spectrometry and olefin geometries were assigned as described above.

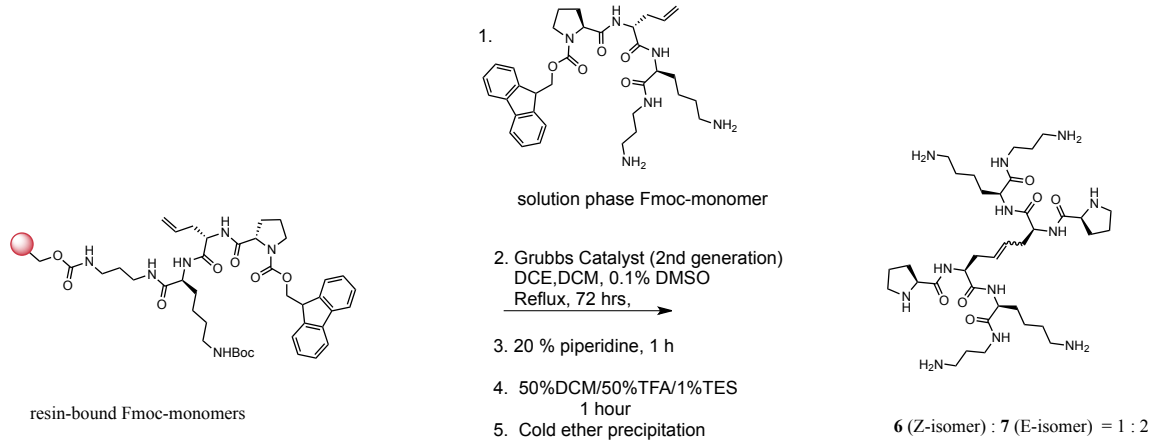

Supplementary Scheme 3: synthesis of analogs of lead compound lacking the benzo[g]quinoline heterocycle (**6** and **7)** by olefin metathesis.

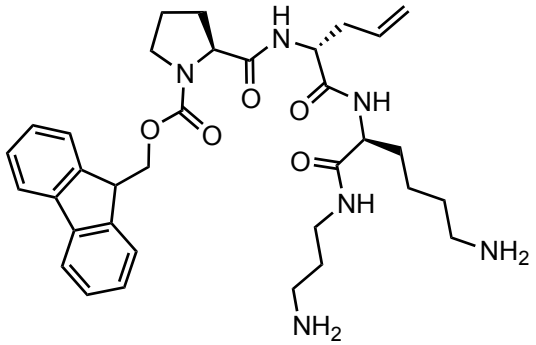

Fmoc-monomer

FT-IR (neat): 3672.21, 3076.73, 2959.56, 2877.6, 2487.04, 2443.64, 2159.16, 2098.41, 2026.08, 1975.45, 1788.37, 1659.15, 1648.54, 1533.79, 1425.3, 1352.97, 1174.09, 1129.73, 986.52, 924.8, 835.6, 797.99, 762.31, 740.13, 718.92

^{1}H NMR (400 MHz, CD_3OD) δ: 7.49 (d, J = 7.4 Hz, 1H), 7.36 – 7.24 (m, 1H), 7.06 (dt, J = 29.8, 7.3 Hz, 2H), 5.48 (qd, J = 16.4, 8.4 Hz, 1H), 4.83 – 4.71 (m, 1H), 4.64 (d, J = 10.0 Hz, 1H), 4.22 – 3.79 (m, 3H), 3.37 – 3.07 (m, 1H), 3.07 – 2.87 (m, 1H), 2.60 (dd, J = 30.9, 6.6 Hz, 2H), 2.22 (tdd, J = 20.6, 14.2, 7.6 Hz, 1H), 2.06 – 1.85 (m, 1H), 1.73 – 1.50 (m, 3H), 1.50 – 1.41 (m, 1H), 1.32 (d, J = 6.6 Hz, 1H), 1.12 (d, J = 6.8 Hz, 1H).

^{13}C NMR (126 MHz, CD_3OD) δ: 175.63, 174.84, 174.02, 157.35, 156.59, 145.49, 145.30, 145.07, 144.91, 142.64, 142.58, 134.83, 134.52, 128.94, 128.25, 126.17, 121.05, 69.01, 62.49, 61.28, 55.22, 54.97, 40.40, 38.14, 36.94, 36.14, 32.68, 32.34, 31.89, 31.34, 28.48, 27.86, 25.47, 23.86.

HRMS *m/z* calculated for $C_{34}H_{47}N_6O_5$ $[M+H]^+$: 619.3602: found: 619.3603.

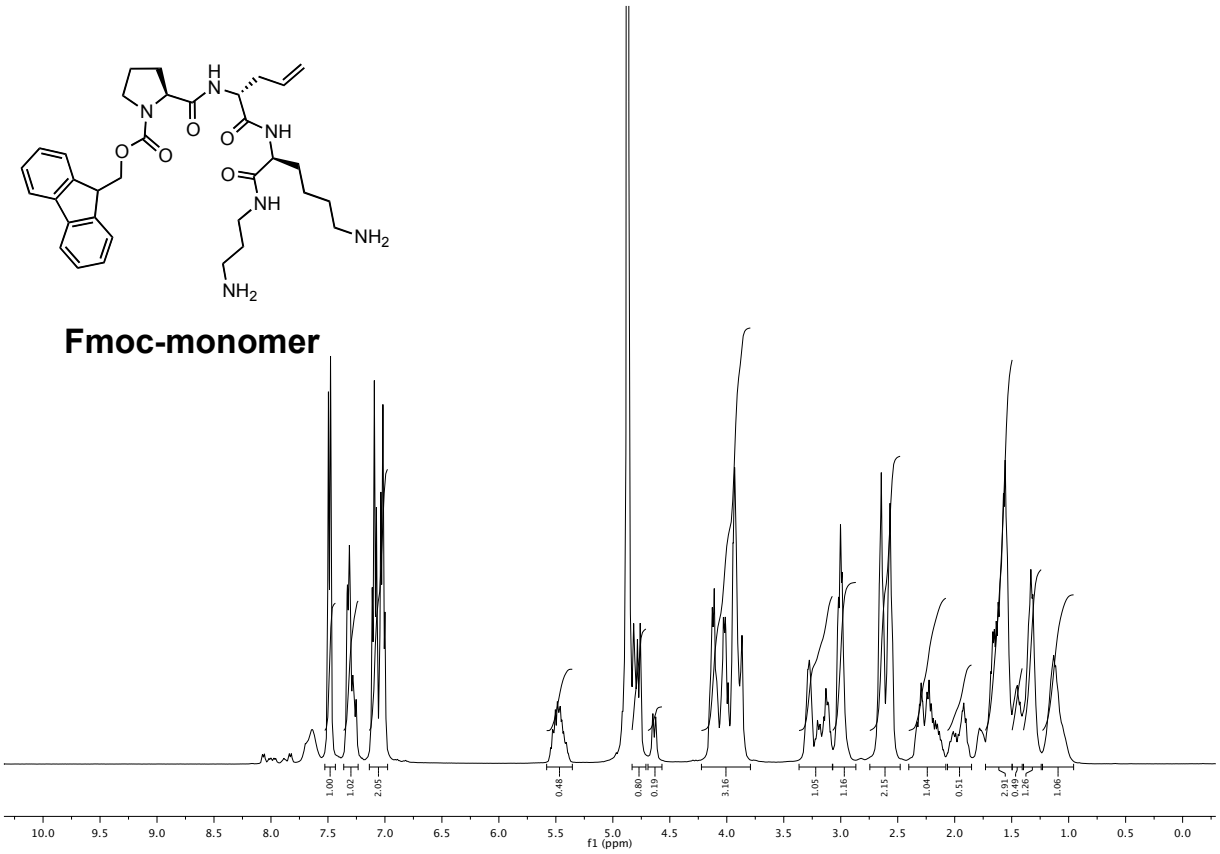
Fmoc-monomer
f1 (ppm)

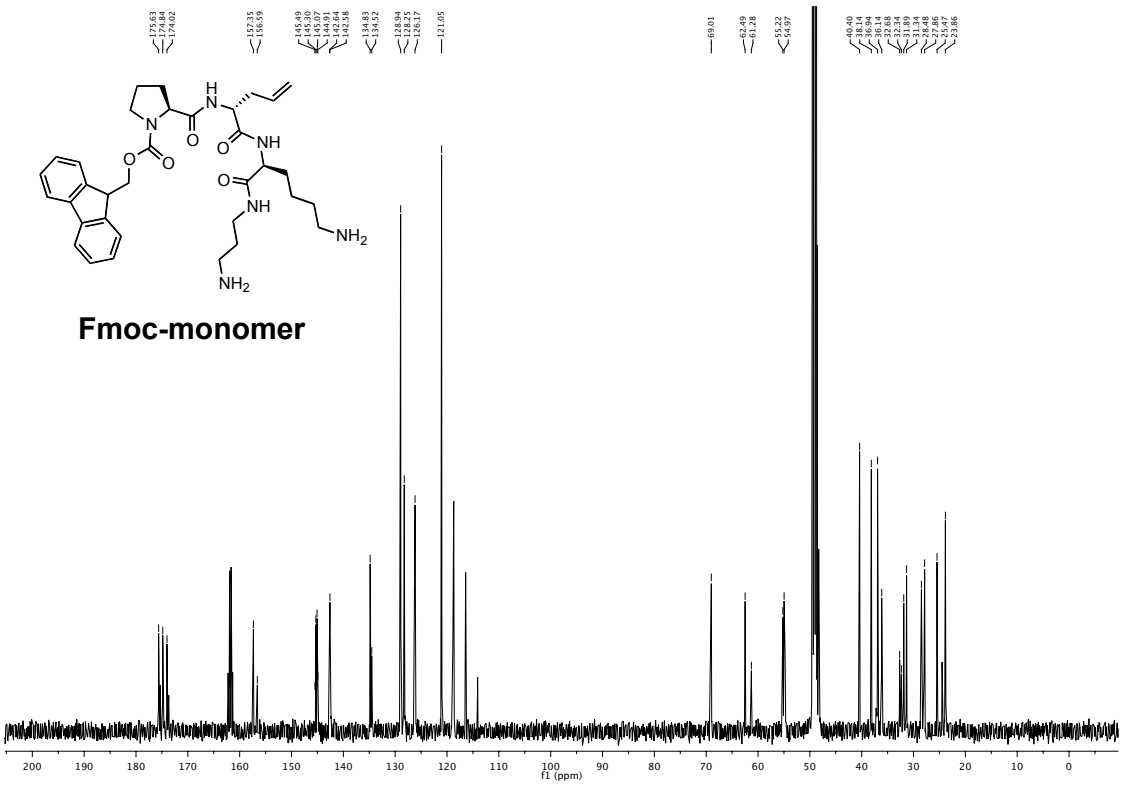
Fmoc-monomer
f1 (ppm)

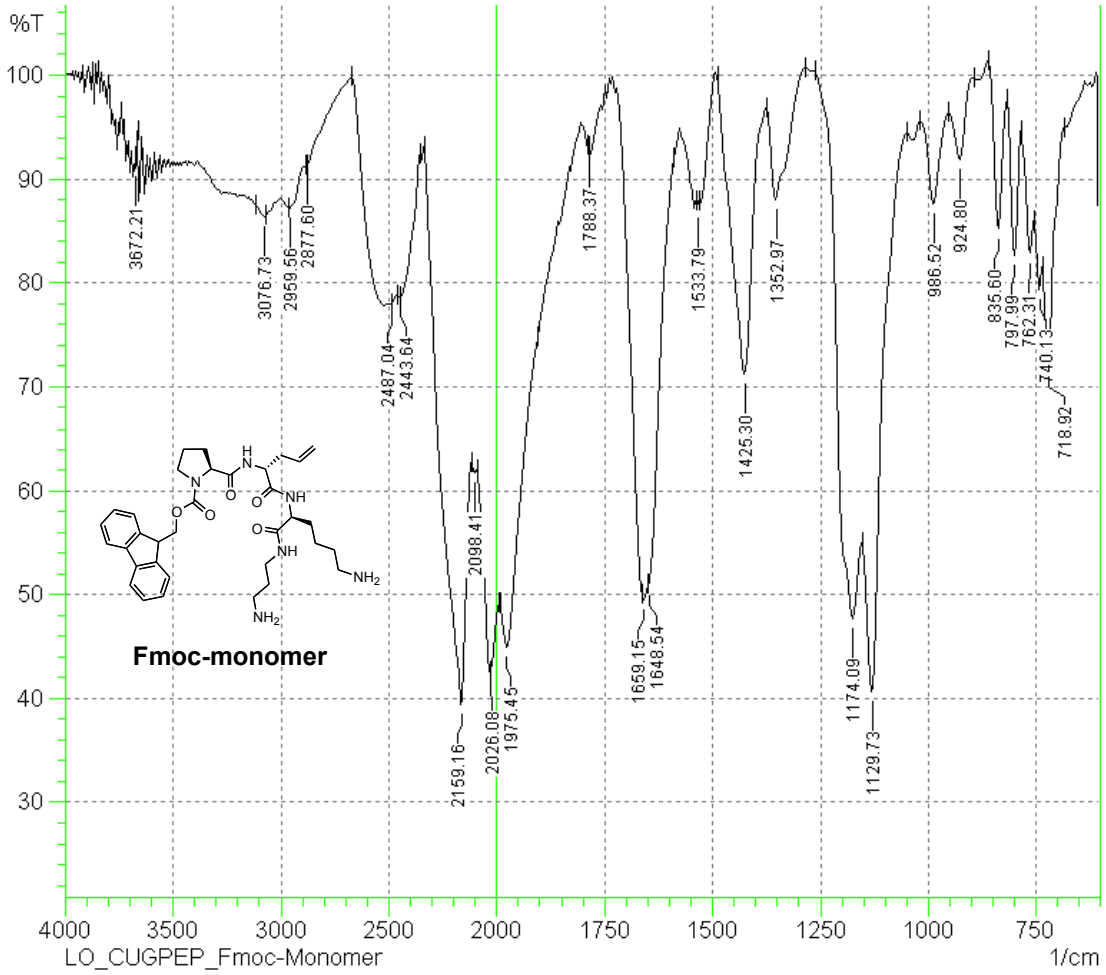
%T
100
90
80
70
60
50
40
30
3672.21
3076.73
2959.56
2877.60
2487.04
2443.64
2159.16
2098.41
2026.08
1975.45
1788.37
1659.15
1648.54
1533.79
1425.30
1352.97
1174.09
1129.73
986.52
924.80
835.60
797.99
762.31
740.13
718.92
Fmoc-monomer
4000
3500
3000
2500
2000
1750
1500
1250
1000
750
LO_CUGPEP_Fmoc-Monomer
1/cm

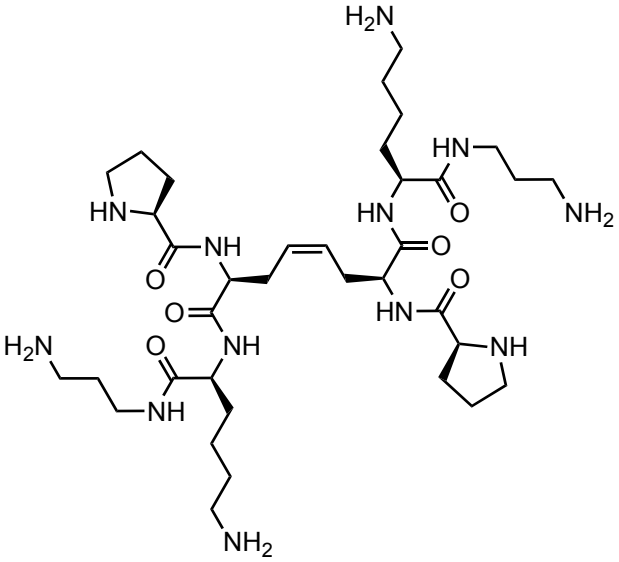

6

FTIR (neat): 3652.93, 3549.26, 3271.53, 3237.78, 3196.31, 3083, 3079.14, 3018.39, 2952.33, 2934.01, 2538.15, 2528.02, 2447.5, 2159.16, 2098.89, 2025.6, 1975.45, 1902.16, 1873.72, 1780.17, 1664.45, 1659.63, 1636.97, 1601.29, 1542.46, 1519.32, 1435.42, 1132.62, 969.16, 838.01, 797.99, 718.92

^{1}H NMR (400 MHz, D_2O) δ: 5.44 (t, J = 3.3 Hz, 2H), 4.46 (t, J = 7.6 Hz, 1H), 4.40 – 4.03 (m, 9H), 3.45 (q, J = 7.1 Hz, 1H), 3.39 – 3.26 (m, 7H), 3.19 (t, J = 6.8 Hz, 7H), 2.89 (dd, J = 14.6, 7.1 Hz, 16H), 2.43 – 2.27 (m, 6H), 1.94 (dd, J = 14.5, 7.4 Hz, 10H), 1.83 – 1.72 (m, 8H), 1.72 – 1.54 (m, 16H), 1.43 – 1.16 (m, 5H).

^{13}C NMR (126 MHz, CD_3OD) δ: 174.80, 173.16, 169.98, 129.80, 80.01, 60.98, 54.85, 54.76, 47.53, 40.41, 38.26, 37.09, 35.78, 32.64, 31.17, 28.64, 28.09, 25.03, 23.85.

HRMS *m/z* calculated for $C_{36}H_{69}N_{12}O_6$ $[M+H]^+$: 765.5458: found: 765.5473.

.

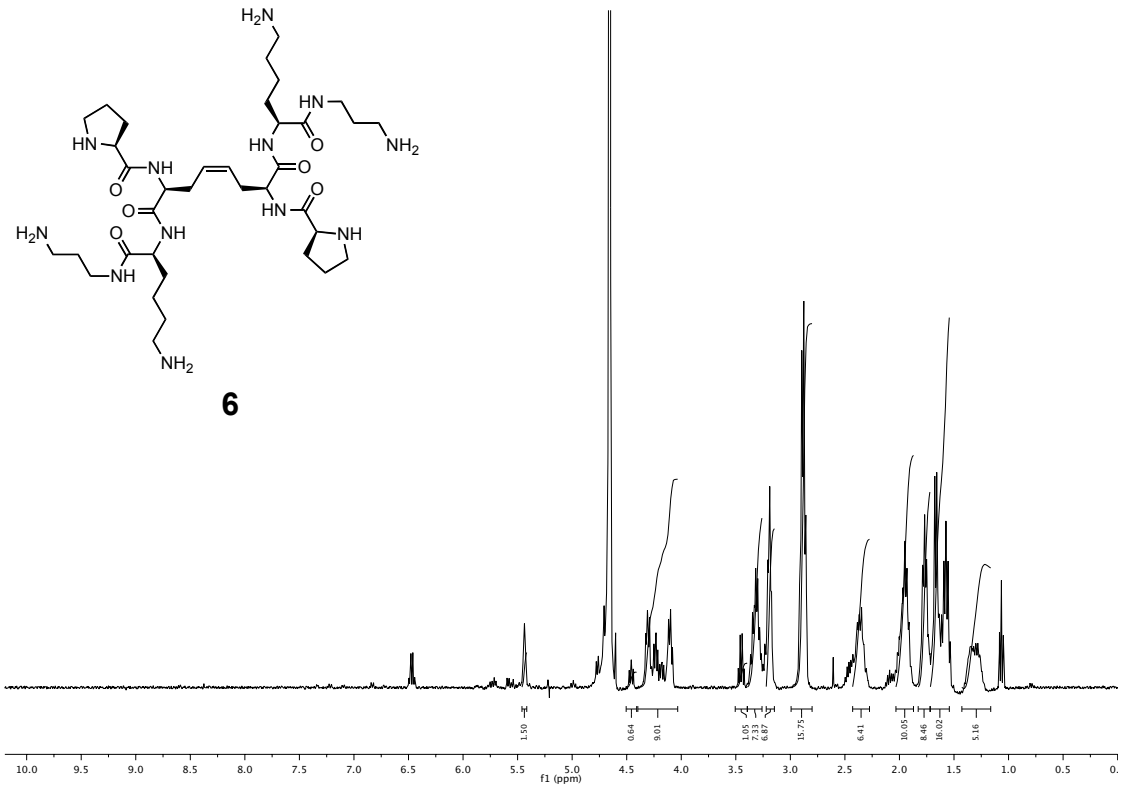
6
f1 (ppm)

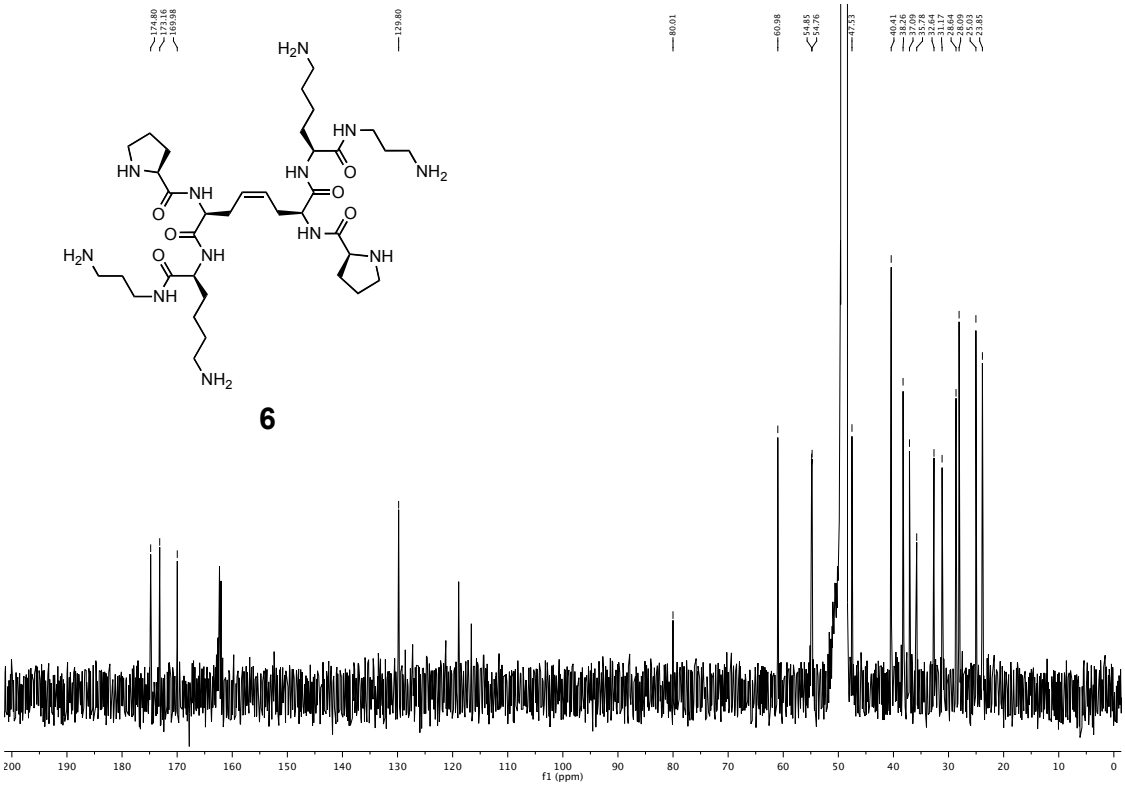
6
f1 (ppm)

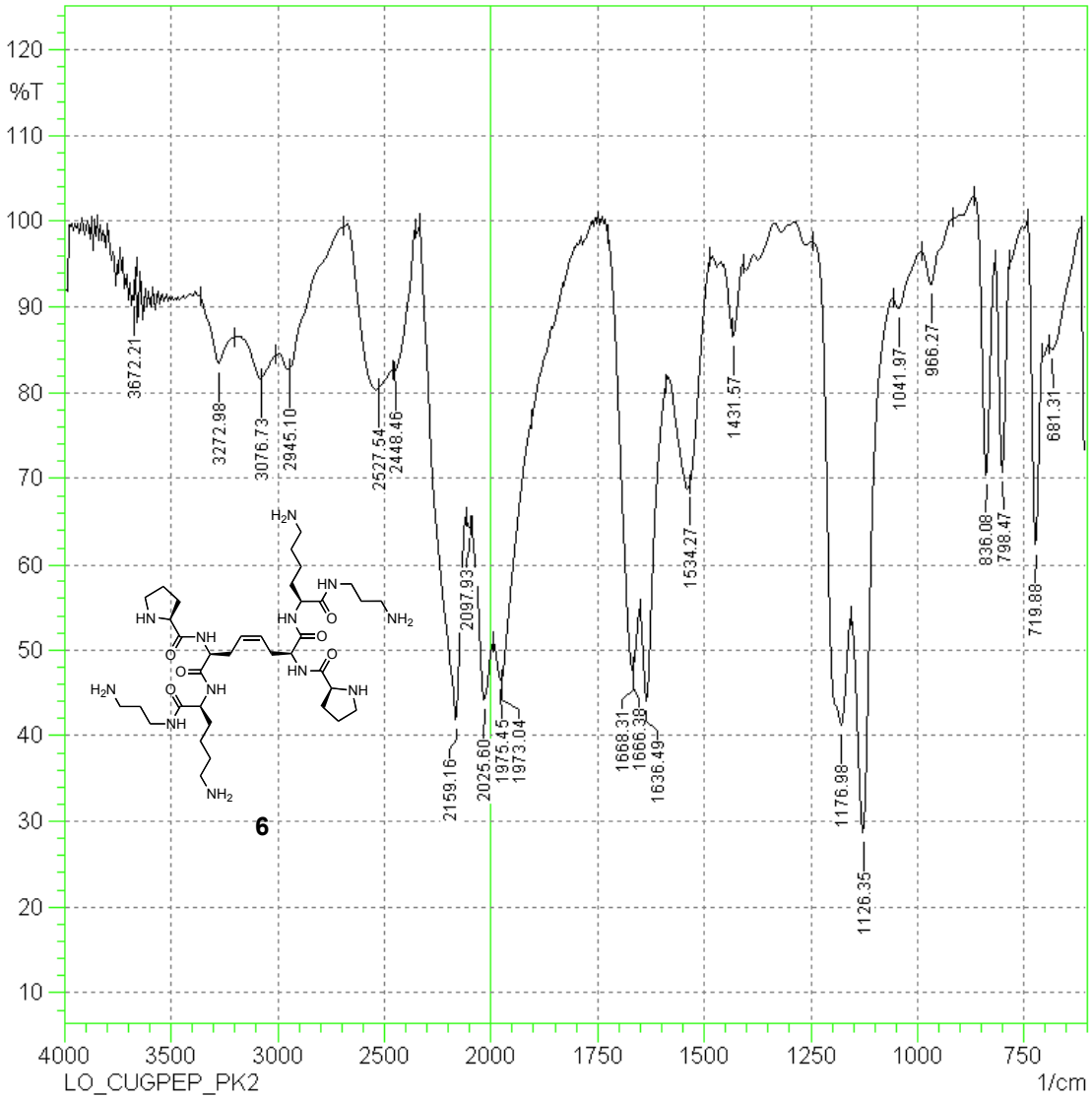
%T
1/cm
LO_CUGPEP_PK2
3672.21
3272.98
3076.73
2945.10
2527.54
2448.46
2159.16
2097.93
2025.60
1975.45
1973.04
1668.31
1666.38
1636.49
1534.27
1431.57
1176.98
1126.35
1041.97
966.27
836.08
798.47
719.88
681.31
6

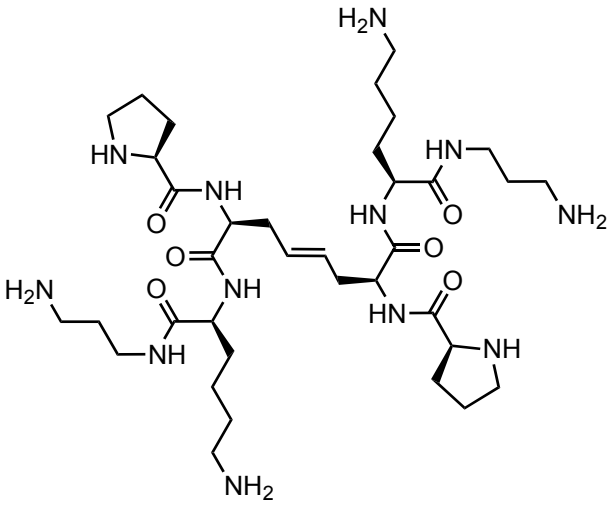

7

FT-IR (neat): 3672.21, 3272.98, 3076.73, 2945.1, 2527.54, 2448.46, 2159.16, 2097.93, 2025.6, 1975.45, 1973.04, 1668.31, 1666.38, 1636.49, 1534.27, 1431.57, 1176.98, 1126.35, 1041.97, 966.27, 836.08, 798.47, 719.88, 681.31

^{1}H NMR (400 MHz, D_2O) δ: 5.45 (t, J = 3.8 Hz, 2H), 4.83 – 4.73 (m, 1H), 4.38 – 4.23 (m, 5H), 4.23 – 4.06 (m, 4H), 3.42 – 3.13 (m, 13H), 2.89 (q, J = 7.6 Hz, 13H), 2.61 – 2.17 (m, 8H), 2.09 – 1.80 (m, 10H), 1.80 – 1.47 (m, 19H), 1.32 (ddd, J = 23.3, 14.4, 7.2 Hz, 6H).

^{13}C NMR (126 MHz, CD_3OD) δ: 174.83, 173.15, 169.97, 129.79, 128.61, 60.99, 54.84, 54.75, 47.52, 45.70, 40.41, 38.26, 37.08, 35.75, 32.63, 31.18, 28.63, 28.58, 28.06, 25.04, 23.83, 23.74.

HRMS *m/z* calculated for $C_{36}H_{69}N_{12}O_6$ $[M+H]^+$: 765.5458: found: 765.5431

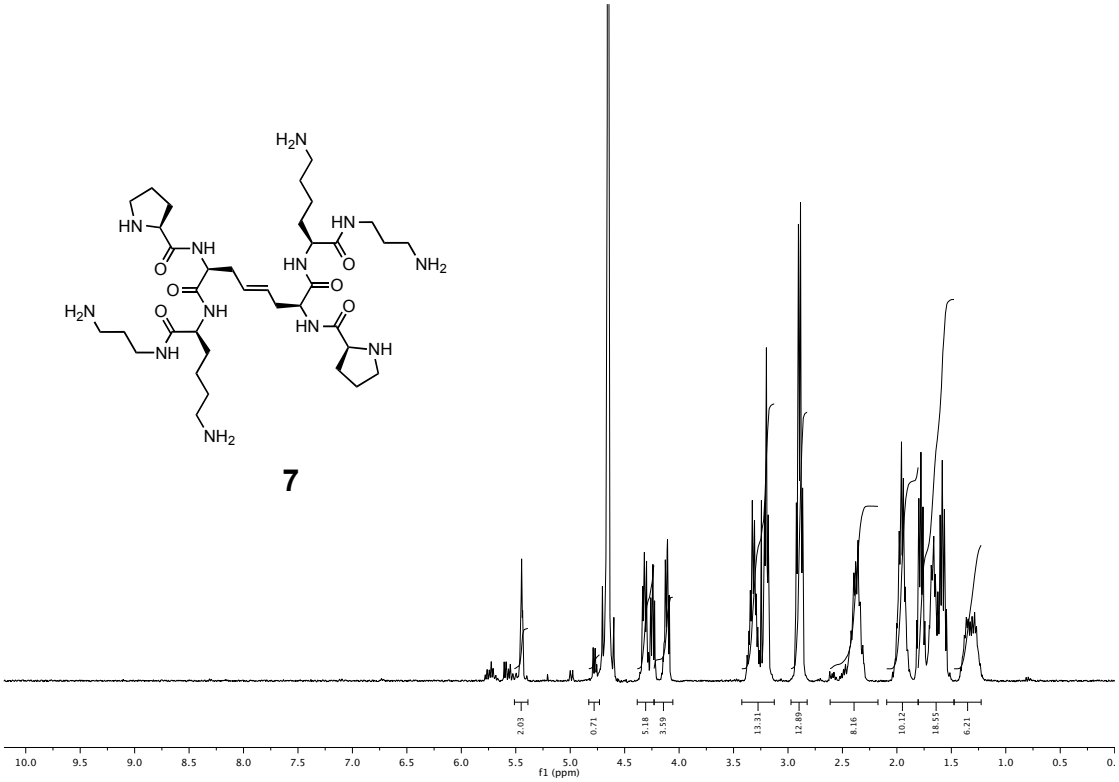
7
2.03
0.71
5.18
3.59
13.31
12.89
8.16
10.12
18.55
6.21
f1 (ppm)

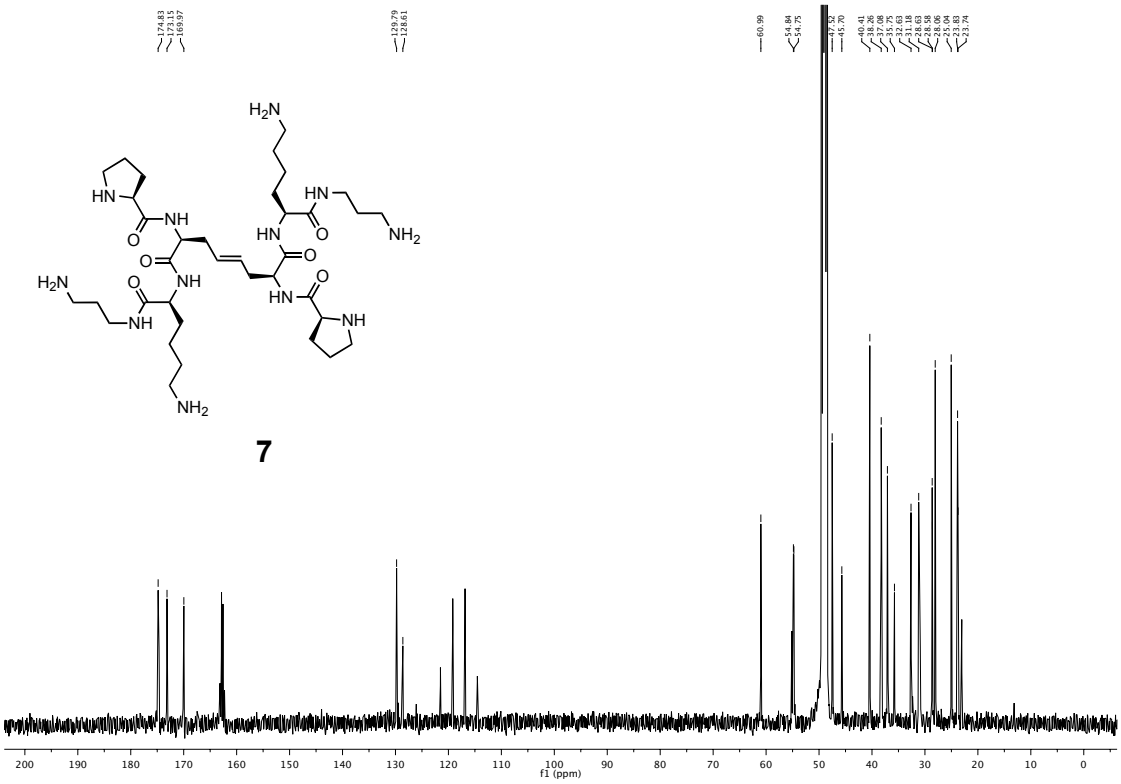
7
174.83
173.15
169.97
129.79
128.61
60.99
54.84
54.75
45.70
40.41
38.26
37.08
35.75
32.63
31.18
28.63
28.58
28.06
25.94
23.83
23.74
f1 (ppm)

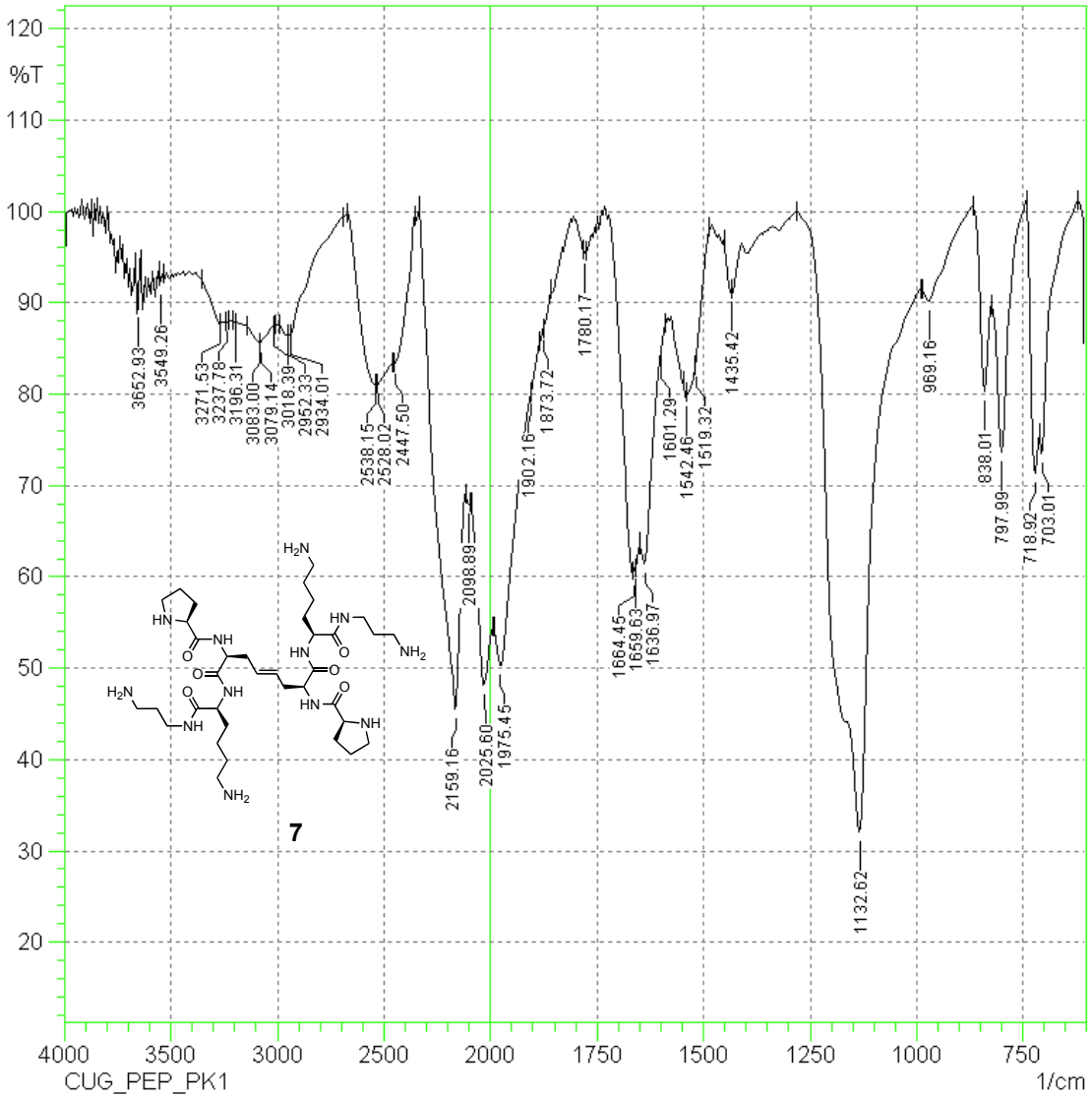
%T
1/cm
CUG_PEP_PK1
3652.93
3549.26
3271.53
3237.78
3196.31
3083.00
3079.14
3018.39
2952.33
2934.01
2538.15
2528.02
2447.50
2159.16
2098.89
2025.60
1975.45
1902.16
1873.72
1780.17
1664.45
1659.63
1636.97
1601.29
1542.46
1519.32
1435.42
1132.62
969.16
838.01
797.99
718.92
703.01
7

Compound **8** and **9**: are constitutional isomers of compounds **4** and **5** in which the amino acid sequence **Lys-Algly-Pro**-Benzo[g]quinoline was re-ordered as **Pro-Algly-Lys**-Benzo[g]quinoline. This was done to verify the importance of the amino acid sequence on CUG repeat RNA binding. The peptide coupling procedure previously describe above was used to synthesize the resin bound scrambled monomer. The resin-bound scrambled monomer was split into two equal parts of 0.5 g each. One part was cleaved and used as solution phase component for olefin metathesis reaction employing Grubbs' second-generation catalyst (**Supplementary Scheme 4**). The products were isolated and purified by reversed phase preparative HPLC, to yield **8** and **9** as a 2:3 ratio of Z- and E isomers respectively. Olefin geometries were assigned as described above.

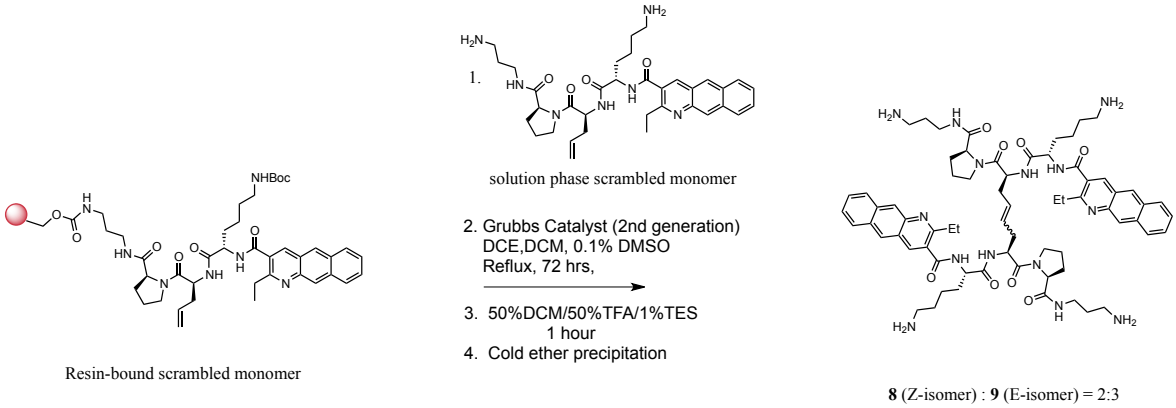

Supplementary Scheme 4. Synthesis of analogs (**8** and **9**) with scrambled amino acid sequence by olefin metathesis.

HPLC trace for compound **8** (minor *Z*-isomer)

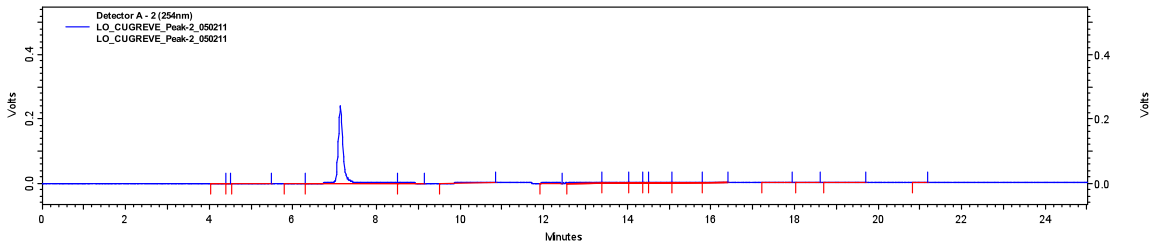

HPLC trace for compound **9** (major E-isomer)

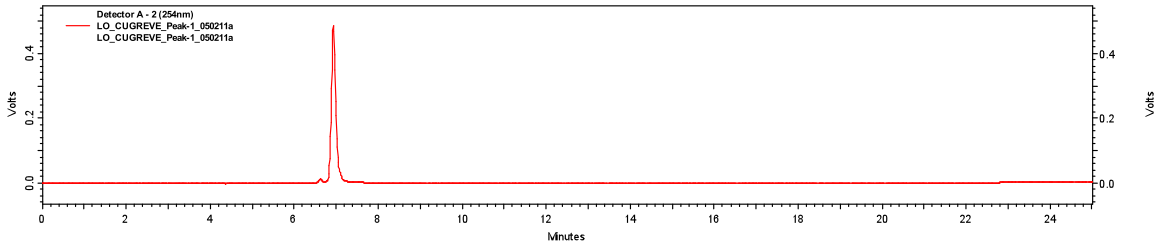

Overlay of HPLC traces for **8** and **9**

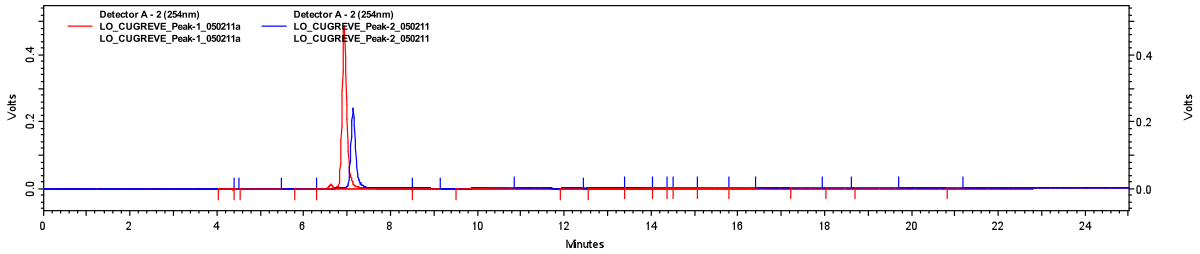

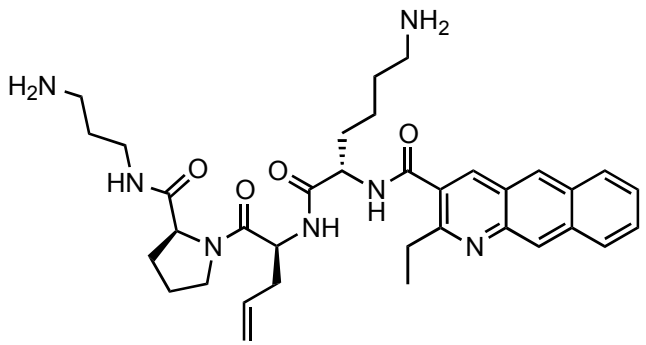

scrambled monomer

FT-IR (neat): 3653.89, 3631.23, 3570.96, 3236.33, 3177.51, 3157.74, 3117.23, 3041.53, 2957.64, 2933.53, 2537.18, 2527.06, 2448.46, 2159.16, 2097.93, 2026.08, 1973.53, 1880.47, 1874.68, 1854.43, 1668.79, 1663.97, 1660.11, 1654.33, 1647.1, 1637.93, 1632.63, 1629.26, 1539.57, 1518.36, 1430.6, 1421.92, 1194.82, 1176.01, 1126.35, 923.84, 880.44, 833.19, 797.51, 718.43.

^{1}H NMR (400 MHz, CD_3OD) δ: 9.12 (s, 1H), 8.74 (s, 1H), 8.55 (s, 1H), 8.02 (t, J = 8.6 Hz, 1H), 7.57 (dd, J = 17.9, 7.2 Hz, 1H), 5.70 (dd, J = 24.5, 14.9 Hz, 2H), 5.12 – 4.88 (m, 15H), 4.50 (s, 1H), 4.41 (s, 1H), 4.15 (s, 1H), 3.67 (s, 1H), 3.50 (d, J = 4.0 Hz, 1H), 3.23 (s, 3H), 3.10 (d, J = 14.3 Hz, 2H), 2.77 (s, 3H), 2.65 (s, 1H), 2.41 (s, 1H), 2.35 – 2.18 (m, 1H), 2.01 (d, J = 6.4 Hz, 2H), 1.95 – 1.33 (m, 8H), 1.29 (s, 1H).

^{13}C NMR (126 MHz, CD_3OD) δ: 175.37, 173.56, 172.25, 167.01, 165.25, 147.00, 137.61, 134.65, 134.46, 131.63, 131.39, 130.11, 129.63, 129.58, 129.38, 125.03, 119.67, 118.85, 61.95, 55.40, 52.71, 40.43, 38.08, 36.81, 36.55, 32.41, 30.83, 28.69, 28.12, 26.06, 23.91, 23.75, 14.50, 14.42, 14.34.

HRMS *m/z* calculated for $C_{35}H_{47}N_7O_4$ $[M+H]^+$: 630.3762: found: 630.3761.

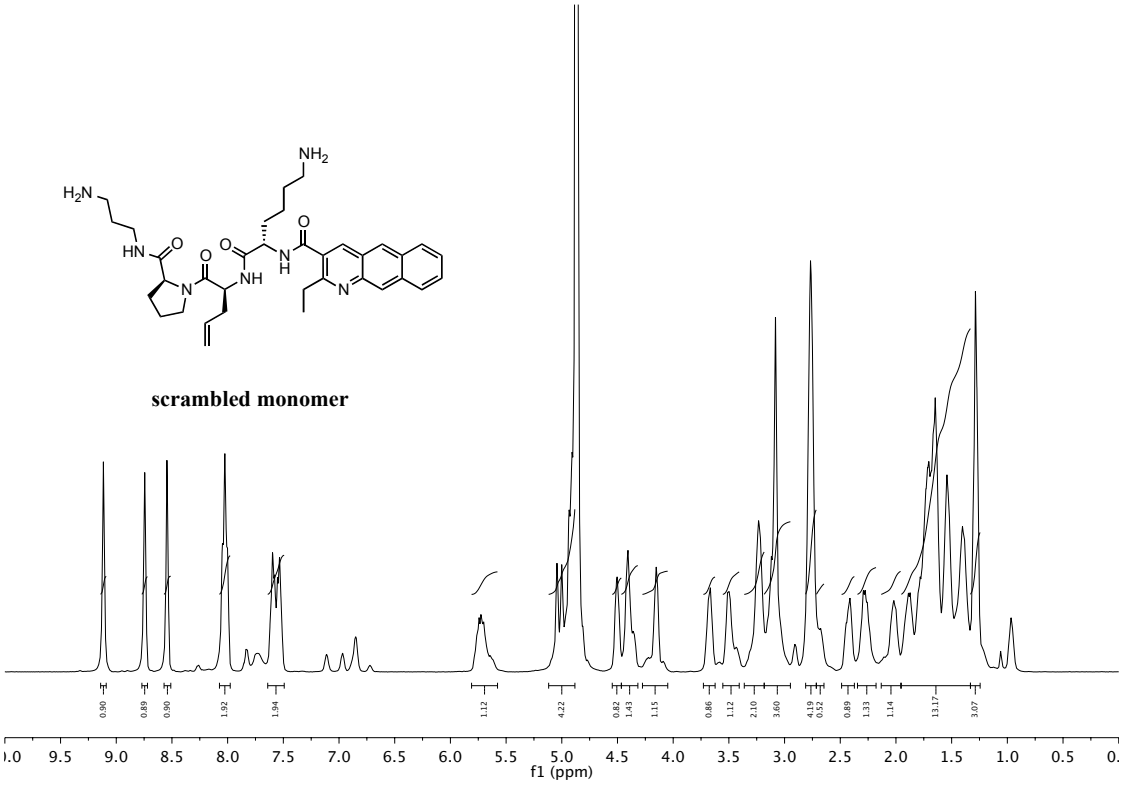
scrambled monomer
f1 (ppm)

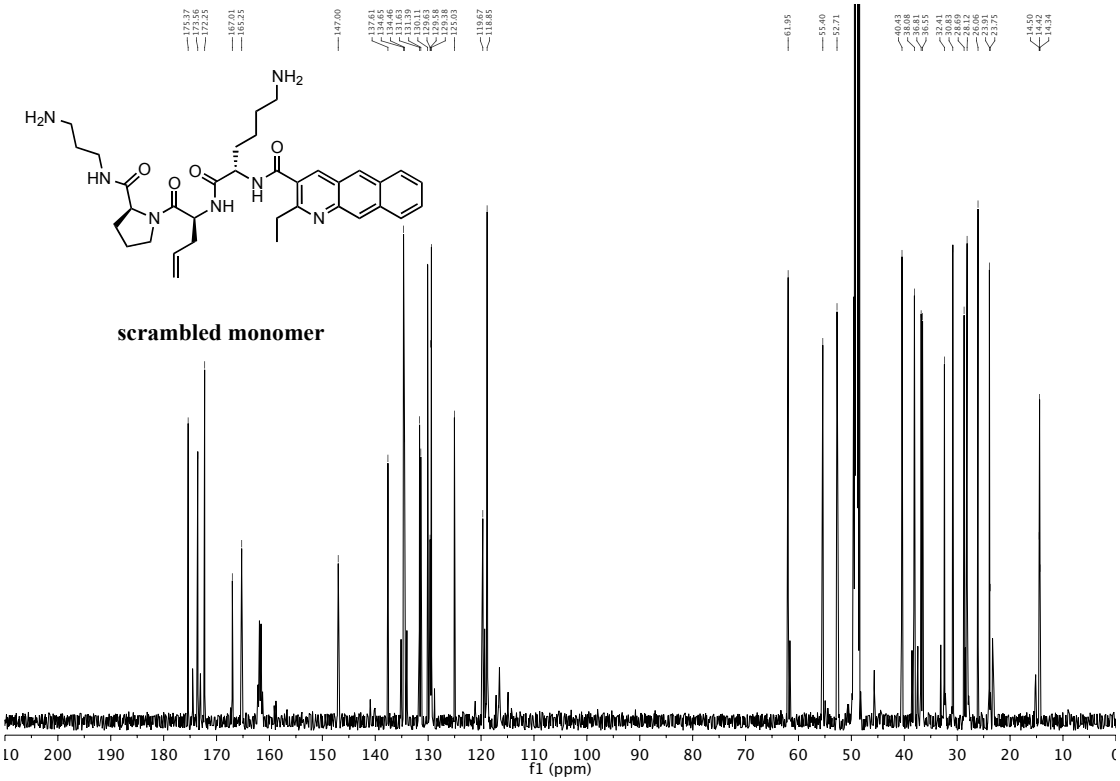
scrambled monomer
f1 (ppm)

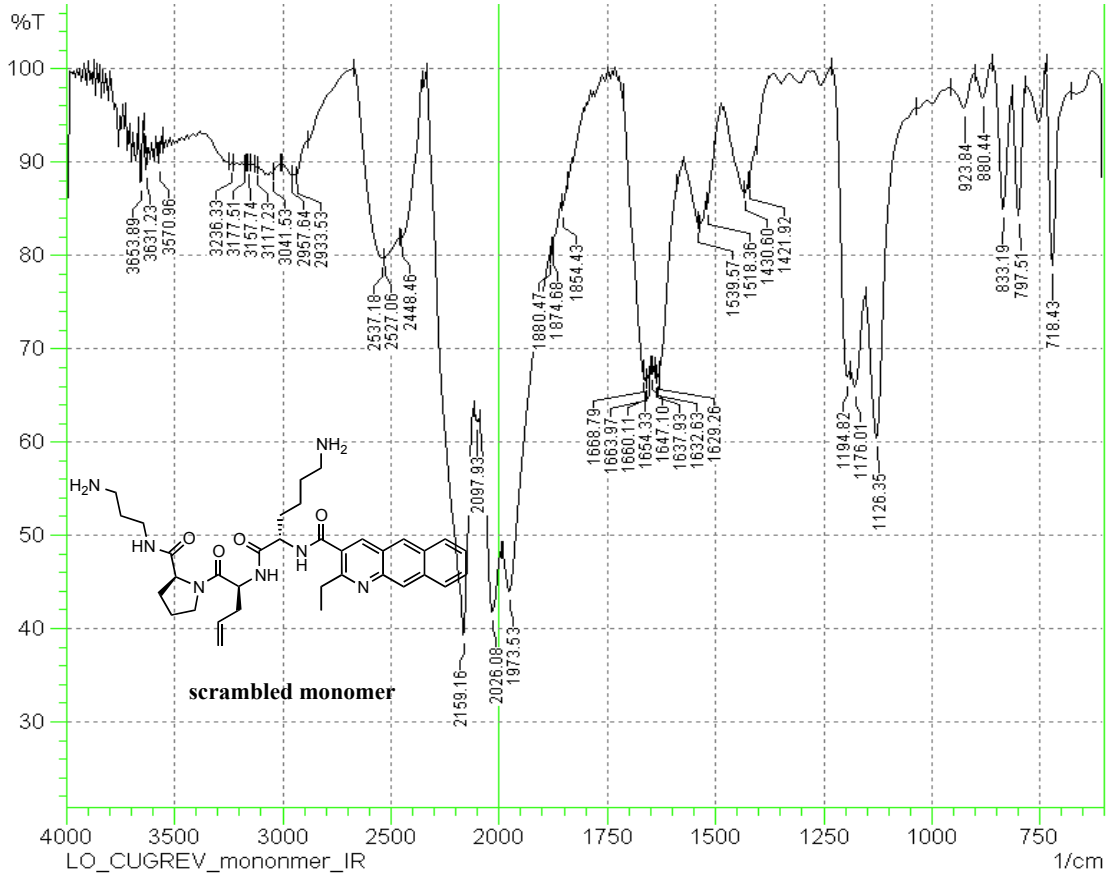
%T
100
90
80
70
60
50
40
30
4000
3500
3000
2500
2000
1750
1500
1250
1000
750
1/cm
LO_CUGREV_mononmer_IR
3653.89
3631.23
3570.96
3236.33
3177.51
3157.74
3117.23
3041.53
2957.64
2933.53
2537.18
2527.06
2448.46
2159.16
2097.93
2026.08
1973.53
1880.47
1874.68
1854.43
1668.79
1663.97
1660.11
1654.33
1647.10
1637.93
1632.63
1629.26
1539.57
1518.36
1430.60
1421.92
1194.82
1176.01
1126.35
923.84
880.44
833.19
797.51
718.43
scrambled monomer

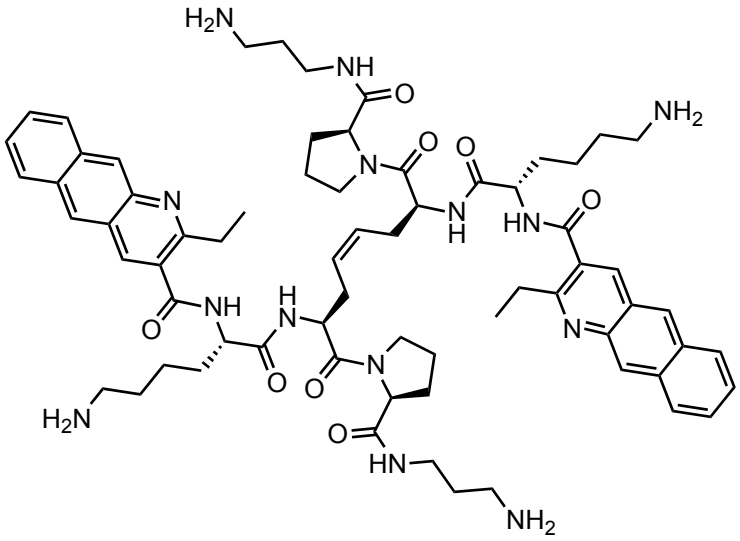

8

FT-IR (neat): 3298.53, 3268.15, 3199.2, 3078.18, 3048.28, 2988.01, 2879.52, 2831.31, 2661.58, 2547.31, 2460.04, 1782.59, 1662.52, 1643.24, 1636.97, 1535.23, 1430.12, 1401.19, 1354.42, 1310.54, 1257.98, 1193.37, 1179.39, 1127.8, 1057.4

^{1}H NMR (500 MHz, D_2O) δ: 8.77 (s, 2H), 8.23 (s, 2H), 7.90 (s, 2H), 7.74 (dd, J = 23.4, 8.7 Hz, 4H), 7.54 (dt, J = 15.2, 7.0 Hz, 4H), 5.75 (t, J = 4.6 Hz, 2H), 4.95 – 4.85 (m, 2H), 4.83 (s, 8H), 4.77 (s, 3H), 4.71 – 4.64 (m, 3H), 4.44 – 4.34 (m, 4H), 3.90 (s, 1H), 3.80 (dd, J = 17.0, 7.0 Hz, 2H), 3.39 – 3.20 (m, 9H), 3.16 (dd, J = 13.7, 7.5 Hz, 2H), 3.03 (dd, J = 18.3, 8.0 Hz, 13H), 2.95 (s, 1H), 2.78 (d, J = 14.4 Hz, 2H), 2.66 (s, 1H), 2.35 (dd, J = 12.9, 8.3 Hz, 3H), 2.09 (ddd, J = 19.6, 12.5, 6.1 Hz, 5H), 1.99 – 1.80 (m, 15H), 1.78 – 1.69 (m, 5H), 1.53 (d, J = 7.8 Hz, 1H), 1.43 – 1.34 (m, 7H).

^{13}C NMR (126 MHz, D_2O) δ: 174.32, 172.91, 171.14, 165.84, 145.12, 135.20, 131.92, 131.59, 130.32, 129.67, 128.33, 127.61, 127.09, 122.18, 117.00, 60.82, 54.05, 51.36, 48.20, 39.08, 37.01, 36.09, 30.60, 29.64, 28.69, 26.63, 26.50, 26.38, 24.71, 22.33, 14.66, 13.25.

HRMS *m/z* calculated for $C_{68}H_{91}N_{14}O_8$ $[M+H]^+$: 1231.7139; found: 1231.7107

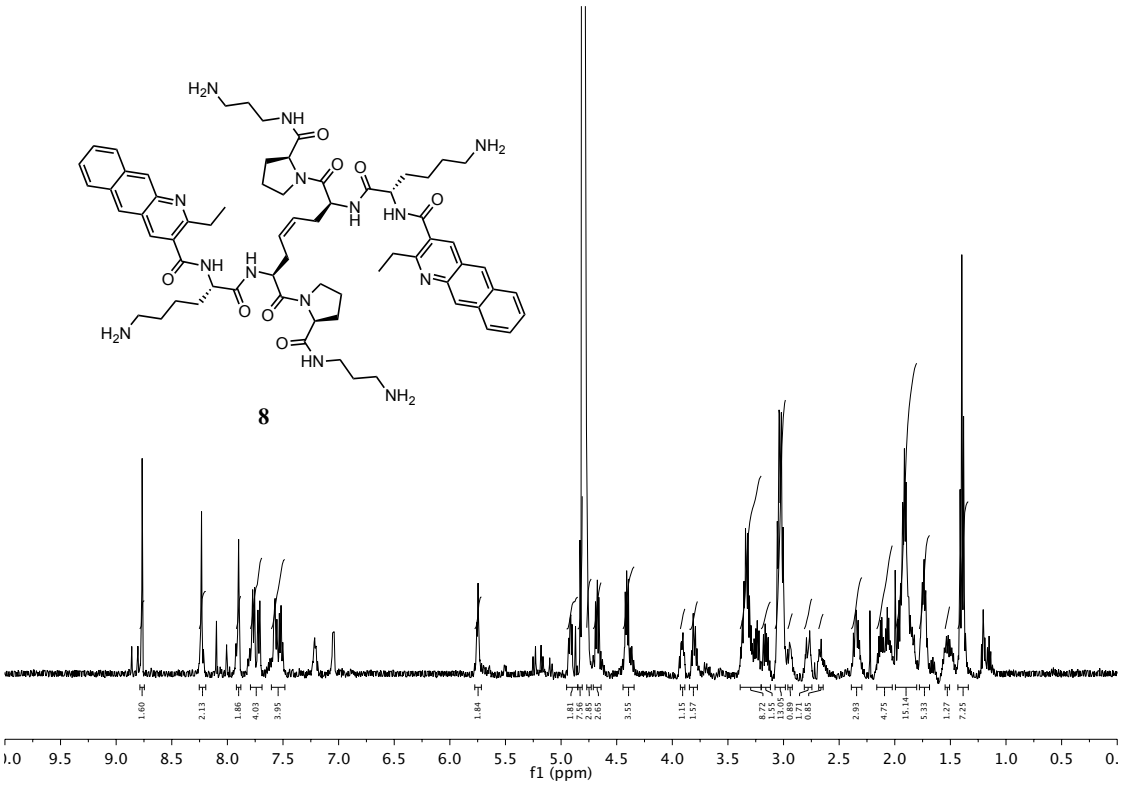
8
f1 (ppm)

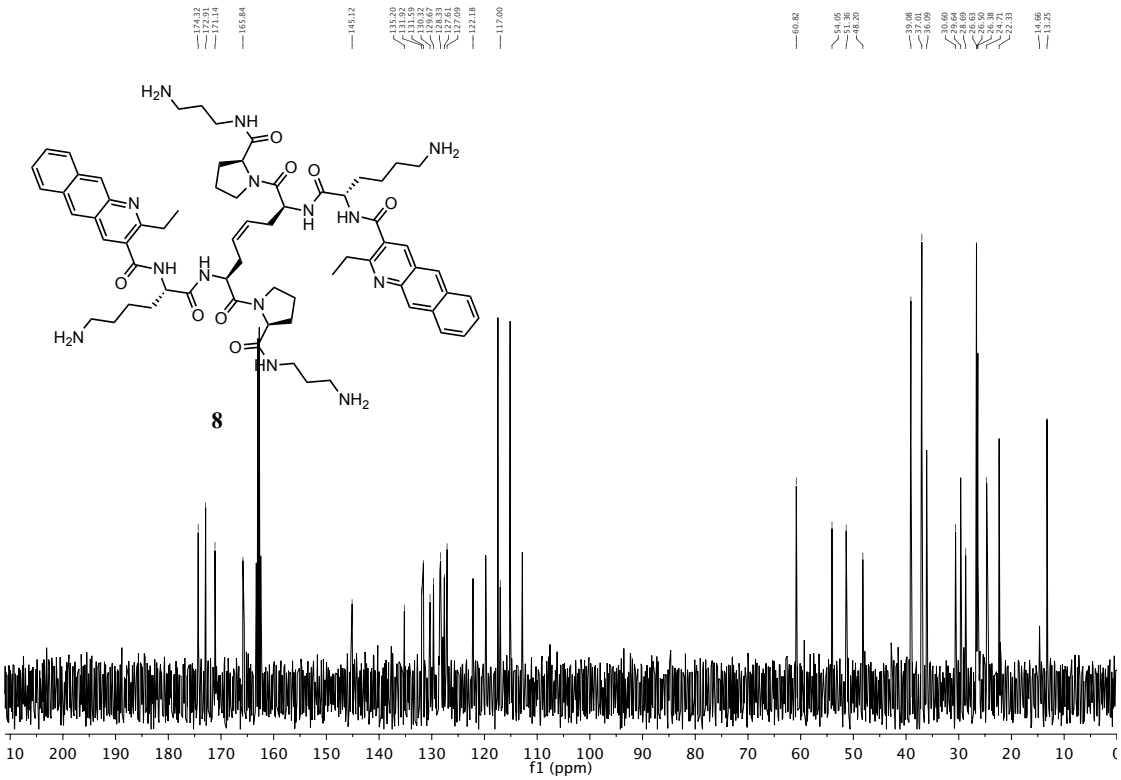
8
f1 (ppm)

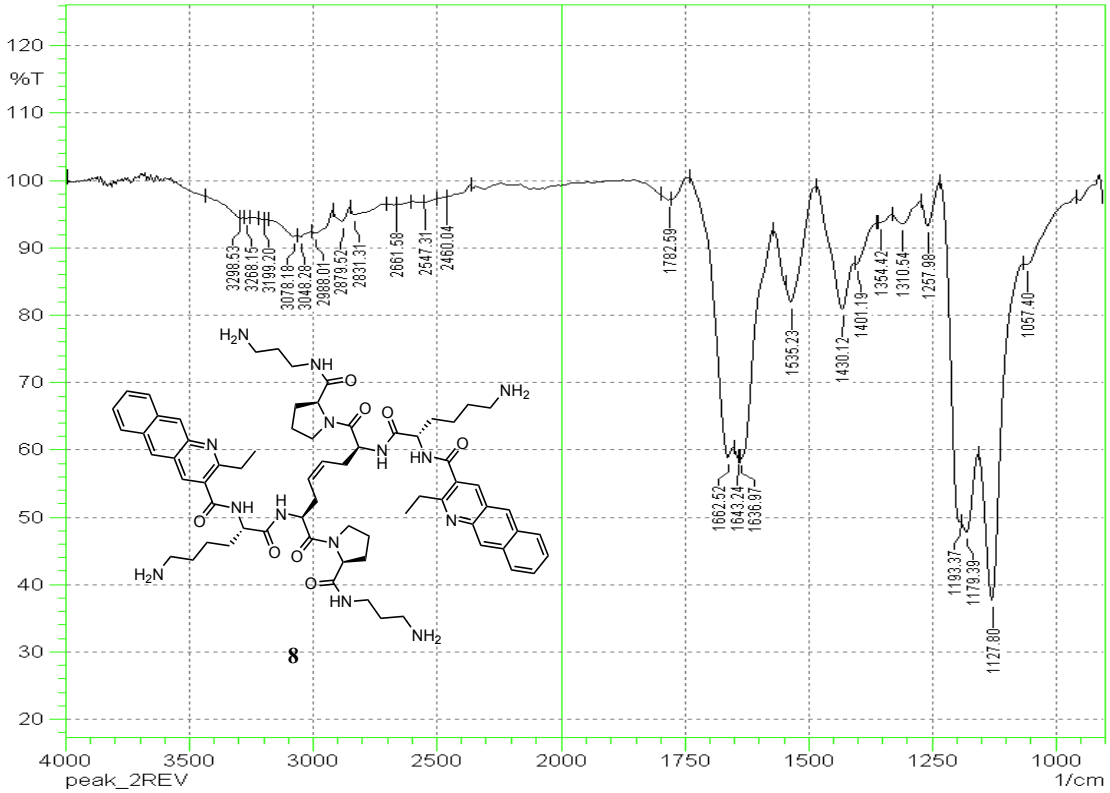
%T
120
110
100
90
80
70
60
50
40
30
20
4000
3500
3000
2500
2000
1750
1500
1250
1000
peak_2REV
1/cm
3298.53
3266.15
3199.20
3078.18
3048.28
2988.01
2879.52
2831.31
2661.58
2547.31
2460.04
1782.59
1662.52
1643.24
1636.97
1535.23
1430.12
1401.19
1354.42
1310.54
1257.98
1193.37
1179.39
1127.80
1057.40
8

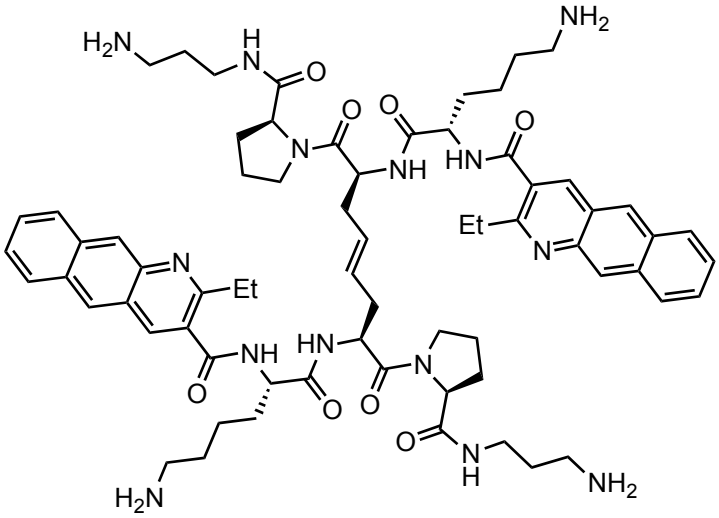

9

FT-IR (neat): 3289.37, 3062.75, 2946.55, 2879.04, 1666.86, 1660.6, 1650.47, 1644.68, 1633.11, 1537.16, 1531.37, 1519.8, 1514.98, 1439.28, 1434.46, 1428.19, 1196.75, 1180.84, 1127.32, 1059.81, 967.72, 881.41, 836.08, 798.47, 749.78, 720.85

^{1}H NMR (500 MHz, D_2O) δ: δ: 8.63 (s, 1H), 8.05 (s, 1H), 7.71 (s, 1H), 7.55 (dd, J = 14.6, 8.4 Hz, 2H), 7.40 (t, J = 7.4 Hz, 1H), 7.33 (t, J = 7.6 Hz, 1H), 5.80 (d, J = 3.5 Hz, 1H), 4.63 – 4.56 (m, 12H), 4.40 (dd, J = 14.0, 6.4 Hz, 7H), 3.97 (s, 3H), 3.82 (dd, J = 17.0, 7.2 Hz, 3H), 3.34 (dt, J = 14.2, 7.1 Hz, 5H), 3.25 – 3.16 (m, 4H), 3.04 (dt, J = 14.3, 5.7 Hz, 12H), 2.69 (d, J = 17.1 Hz, 3H), 2.58 (s, 2H), 2.38 – 2.32 (m, 2H), 2.18 – 2.03 (m, 4H), 2.00 – 1.87 (m, 11H), 1.72 (dd, J = 14.7, 7.4 Hz, 8H), 1.53 (s, 5H), 1.41 (dt, J = 7.6, 6.1 Hz, 11H).

^{13}C NMR (126 MHz, D_2O) δ: 174.36, 172.95, 171.47, 165.73, 145.09, 134.81, 131.56, 131.30, 129.97, 129.56, 128.52, 128.20, 128.10, 127.42, 126.98, 121.99, 116.70, 60.81, 54.10, 51.65, 48.28, 39.09, 37.02, 36.10, 33.91, 30.59, 29.62, 26.66, 26.54, 26.40, 24.73, 22.35, 13.29.

HRMS *m/z* calculated for $C_{68}H_{91}N_{14}O_8$ $[M+H]^+$: 1231.7139; found: 1231.7155

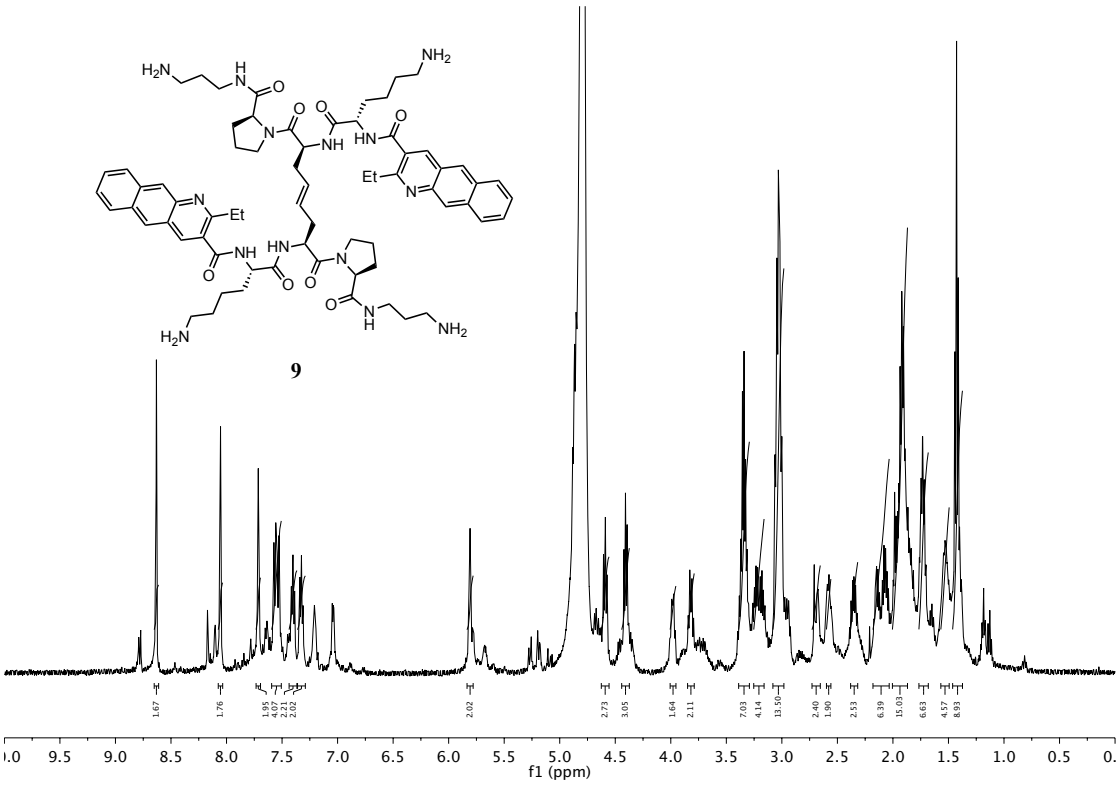
9
f1 (ppm)

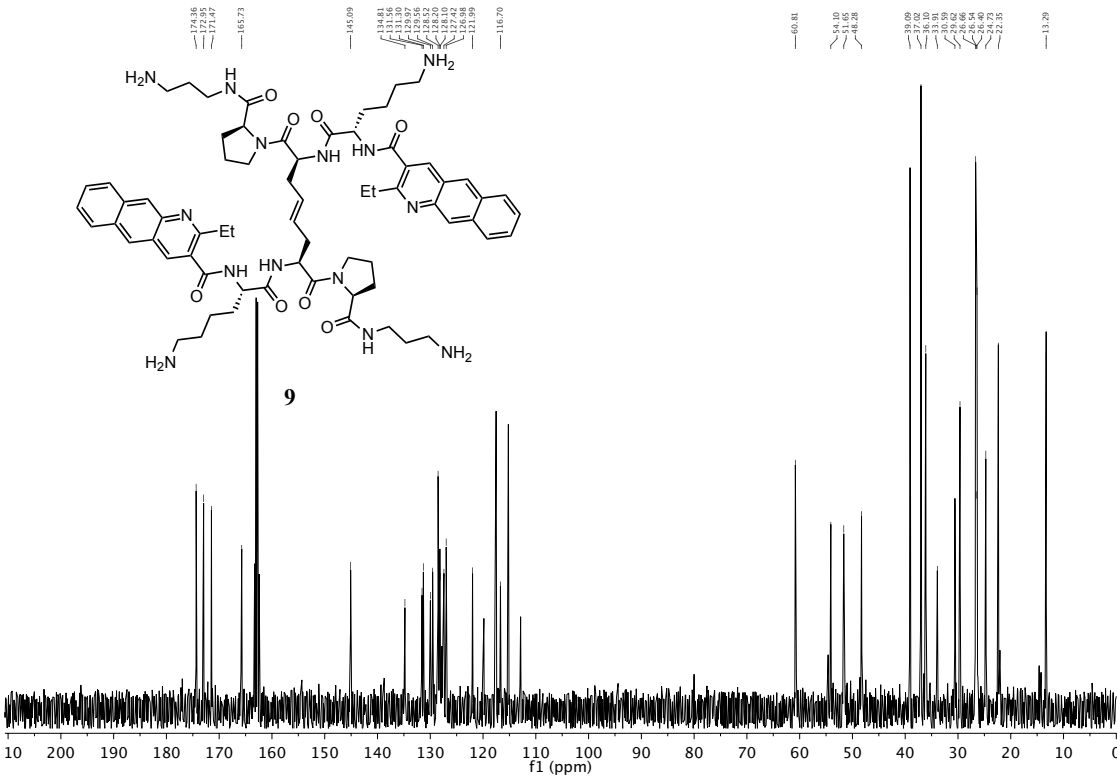
9
f1 (ppm)

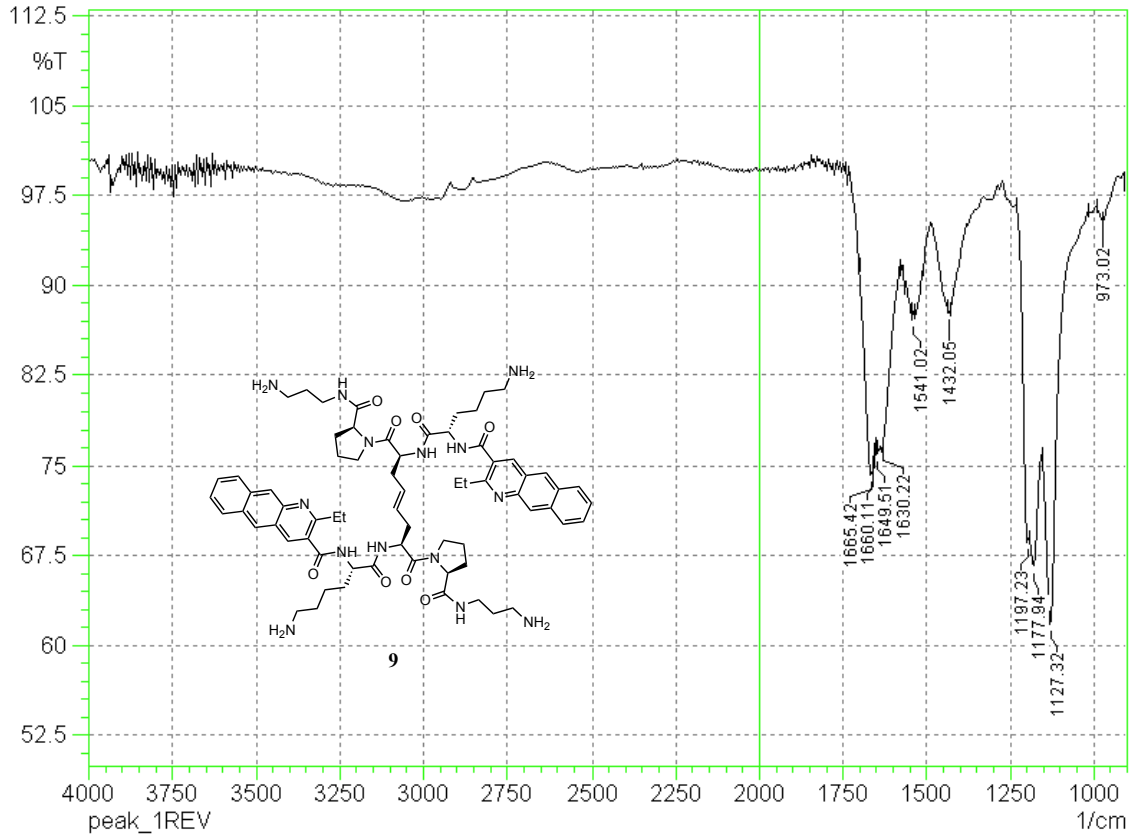
112.5
%T
105
97.5
90
82.5
75
67.5
60
52.5
4000
3750
3500
3250
3000
2750
2500
2250
2000
1750
1500
1250
1000
peak_1REV
1/cm
1665.42
1660.11
1649.51
1630.22
1541.02
1432.05
1197.23
1177.94
1127.32
973.02
9

Compounds **10** and **11** were synthesized by slight modification to the procedures for the synthesis of compounds **4-9.** In order to obtain the required 8-carbon linker spacing, the (L)-Fmoc-Allylglycine was substituted with the unnatural amino acid (L)-Fmoc-pentenylglycine which served as the olefin for the dimerization of the monomer by self metathesis reaction employing Grubbs' second generation catalyst. L-N-Fmoc-pentenylglycine was synthesized using a procedure reported by Meyers *et al.*, in which (*R*, *R*)-(-)-pseudoephedrine is used as a chiral auxiliary for asymmetric alkylation (10). Briefly, (*R*, *R*)-(-)-pseudoephedrine was converted to pseudoephedrine glycinamide hydrate (**supplementary scheme 5** (**a**)) by reaction with glycine methyl ester hydrochloride using methods described in the literature. (*S*)-2-amino-*N*-((1*R*,2*R*)-1-hydroxy-1-phenylpropan-2-yl)-*N*-methylhept-6-enamide (**supplementary scheme 5** (**b**)): Anhydrous lithium chloride (5.29 g, 125.2 mmol, 4.00 equiv) was taken in an oven-dried, 3-necked round-bottom flask equipped with two glass stoppers and an inlet adapter connected to a source of vacuum. Vacuum was applied to the flask and the solid lithium chloride was dried using a low flame. The flask was then cooled to 23 °C and flushed with nitrogen.

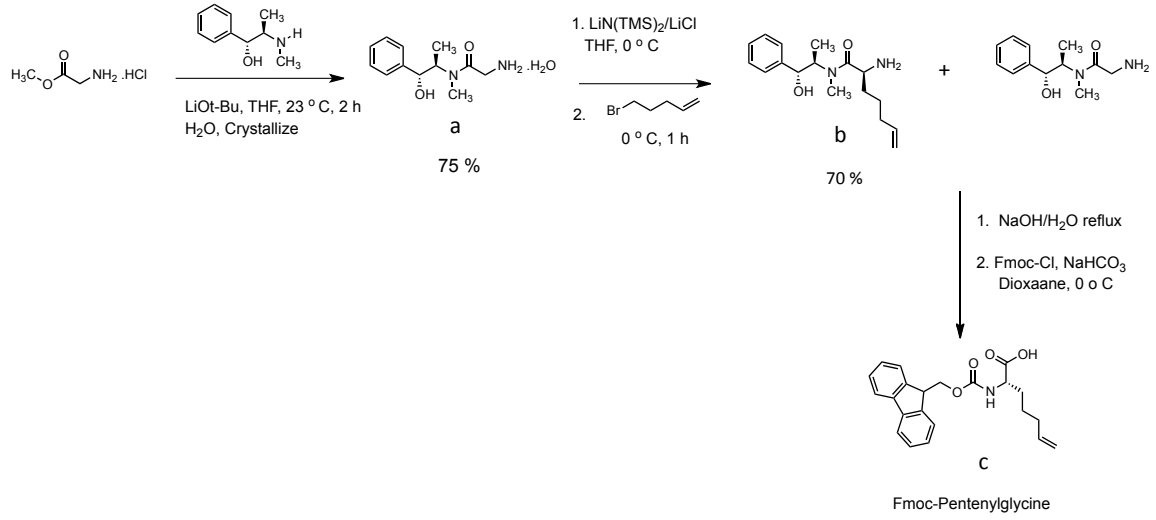

Supplementary Scheme 5: Synthesis of L-Fmoc-pentenylglycine (**c**) by asymmetric alkylation of pseudoephedrine glycinamide hydrate.

Tetrahydrofuran (90 mL) was added to the flask through a pressure equalizing addition funnel and the resulting suspension was stirred at 23 °C for 20 minutes. (*R*, *R*)-(-)-

pseudoephedrine glycinamide hydrate (**a**), (**supplementary Scheme 5**) (7.5 g, 31.3 mmol, 1 equiv) was added to the reaction mixture in portions for 5 minutes resulting in a cloudy solution. The solution was cooled to 0 °C in an ice bath and a 1 M solution of lithium hexamethyldisilazide in tetrahydrofuran (100 mL, 100 mmol, 3.20 equiv) was added dropwise via addition funnel. The speed of the addition was regulated such that the temperature of the reaction did not exceed 3 °C as monitored by a thermometer inserted in the reaction flask via an adapter. After the addition of base was complete, the reaction mixture was stirred at 0 °C for 20 minutes, and 5-bromopentene (4.9 g, 32.8 mmol, 1.05 equiv) was added slowly by syringe. The reaction mixture was stirred at 0 °C for 1 h. Water (75 mL) was added and the resulting biphasic mixture was acidified to pH 0 by the addition of aqueous hydrochloric acid (6 M, 45 mL). The acidified aqueous solution was then extracted with ethyl acetate (100 mL). The ethyl acetate layer was separated and extracted sequentially with single 50 mL portions of 3 M and 1 M aqueous hydrochloric acid solution, respectively. The aqueous layers were combined and cooled to 5 °C by stirring in an ice-water bath. The cold solution was basified to pH 14 by the addition of 50% aqueous sodium hydroxide solution (30 mL). The basified solution was then extracted sequentially with one 120-mL portion and three 40-mL portions of dichloromethane. The combined organic extracts were dried over anhydrous solid potassium carbonate, filtered and concentrated *in vacuo* resulting in a yellow oily product. Attempts to recrystallize the crude product by analogy to (10) were not successful. However, unreacted (*R*, *R*)-(-)-pseudoephedrine glycinamide hydrate did crystallize, allowing its separation from the desired (*S*)-2-amino-*N*-((1*R*,2*R*)-1-hydroxy-1-phenylpropan-2-yl)-*N*-methylhept-6-enamide (**b**) (70 %, HPLC). This crude product was used for the next stage of the reaction without further purification.

Conversion of (**b**) to Fmoc-L-pentenylglycine: to impure (**b**) (8.5 g, 29.3 mmol, 1 equiv) in a 100 mL round bottom flask was added aqueous 1 M sodium hydroxide (58.6 mmol, 2 equiv.) and water (40 mL). The resulting solution was heated to reflux for 2 h and then allowed to cool to RT. Pseudoephedrine was observed to crystallize from the solution upon cooling. The solids were filtered via vacuum filtration and the aqueous solution was extracted with dichloromethane (50 mL and 30 mL) to remove residual pseudoephedrine.

The organic layers were individually back-extracted with water (30 mL); the aqueous extracts were then combined with the original solution and concentrated *in vacuo* to a volume of 45 mL. To this concentrated solution dioxane (45 mL) and sodium bicarbonate (4.92 g, 58.6 mmol, 2 eq) were added, followed by cooling in an ice bath for 20 minutes. 9-flourenylmethoxychloride (8.3 g, 32.2 mmol, 1.1 eq) was added to the cooled solution and the reaction stirred for 3 h (the first 1 h in an ice bath). Water (250 mL) was added, and the solution was washed with 1:1 ethyl acetate:ether (400 mL). The organic layer was washed with a 2% sodium bicarbonate solution (100 mL). The aqueous layers were combined and acidified to pH 1 with 1 N HCl and then extracted with ethyl acetate (2 x 100 mL). The organic layers were dried over sodium sulfate and concentrated *in vacuo*. The residue was dissolved in toluene (20 mL) and concentrated *in vacuo* to remove residual dioxane. The residue was again dissolved in chloroform (2 x 20 mL) and concentrated *in vacuo* yielding an amorphous solid (6.9 g, 67% yield) of impure Fmoc-pentenylglycine. Part of this impure product was purified by preparative HPLC for spectral characterization purposes, and the other part was used in the synthesis of compounds **10** and **11** (**Supplementary Scheme 6**) without purification. First the Fmoc-pentenyglycine was incorporated into the synthesis of the **extended monomer**, which was subjected to olefin self-metathesis in the presence of solution phase extended monomer. The HPLC trace for the monomer showed two major peaks: one resulting from Fmoc-pentenylglycine and the other from a non-alkyated glycine impurity. The final crude reaction product showed the disappearance of the extended monomer, as well as the formation of **10** and **11** as a mixture of isomers. These were separated by prep-HPLC and assigned as described above.

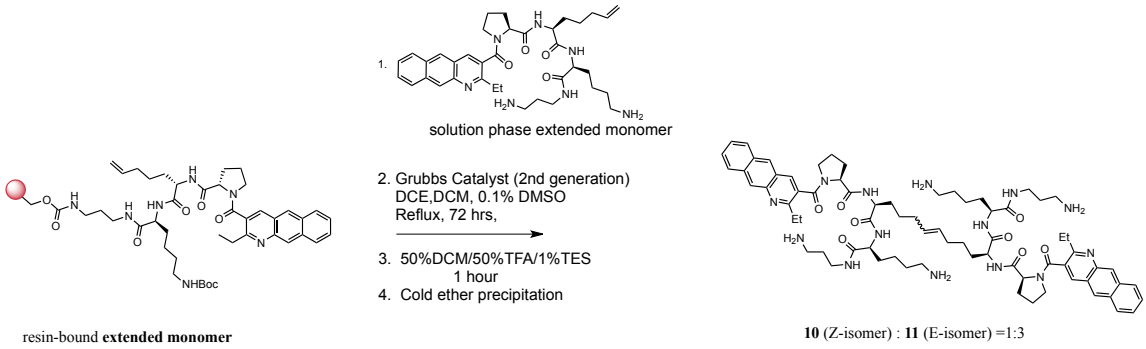

Supplementary Scheme 6: synthesis of compounds with extended linker (**10** and **11)** by olefin metathesis.

HPLC trace for crude **extended monomer**

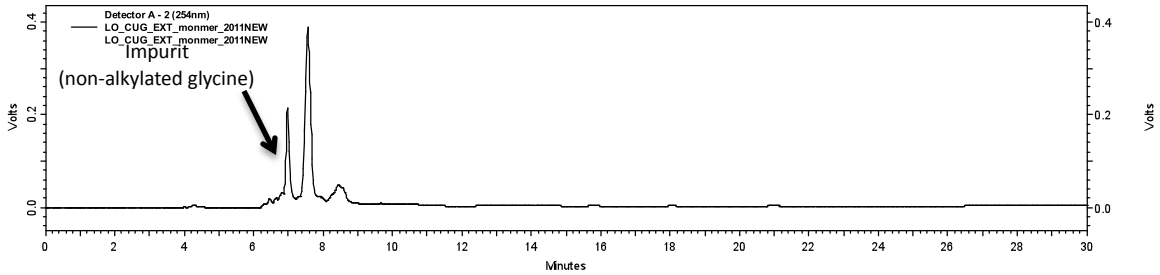

HPLC trace for **extended monomer**

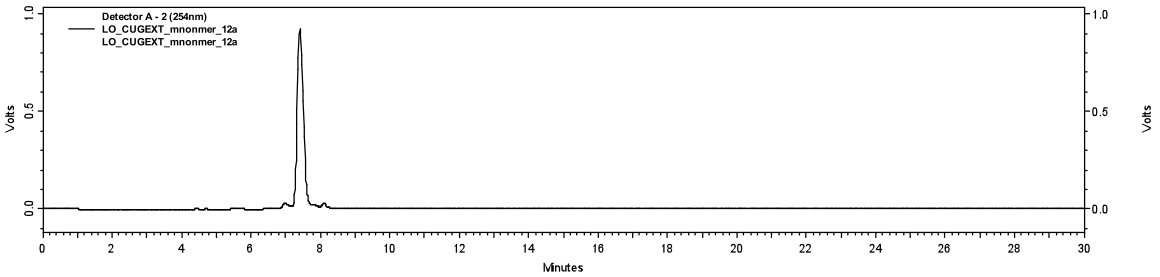

HPLC trace for crude (**10** and **11**) metathesis reaction product

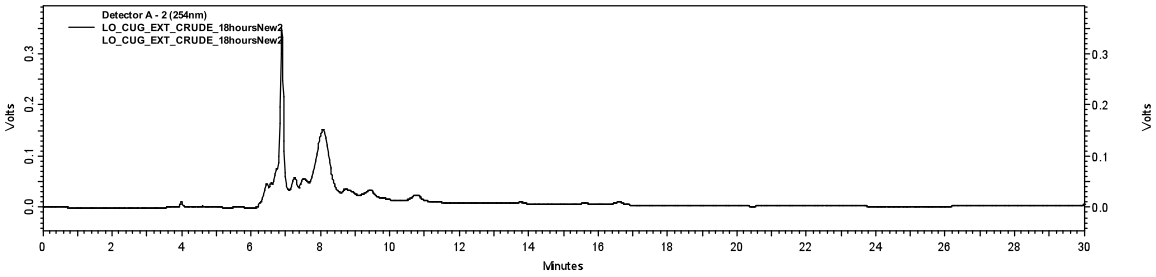

HPLC trace for compound **10** (Z-isomer, minor product)

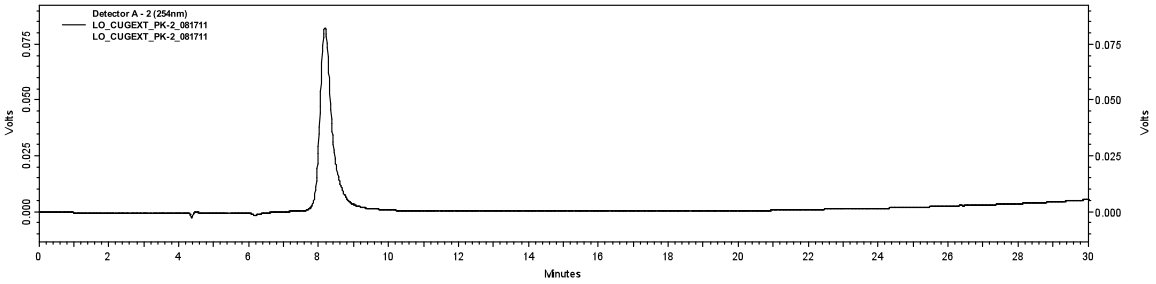

HPLC trace for compound **11** (E-isomer, major product)

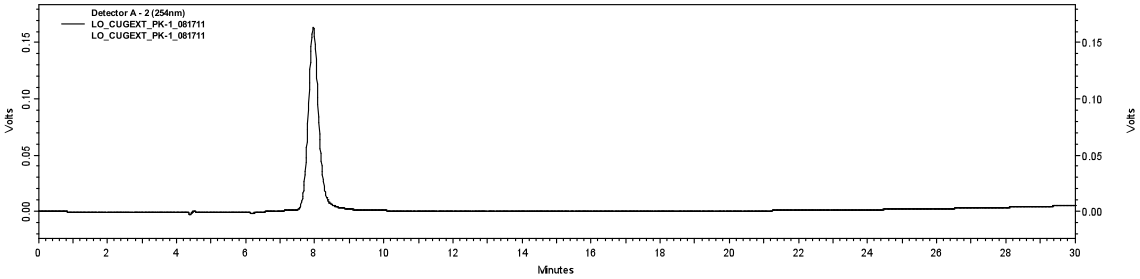

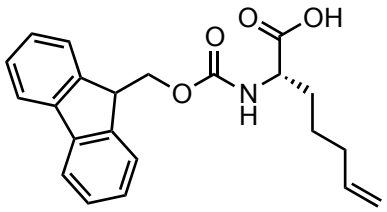

L-Fmoc-Pentenylglycine

FT-IR (neat) 3651.96, 3335.18, 2952.33, 2933.53, 2529.95, 2445.09, 2159.16, 2098.89, 2026.56, 1713.15, 1839.48, 1873.23, 1974.49, 1709.3, 1702.06, 1681.81, 1646.13, 1529.45, 1479.3, 1442.66, 1426.74, 1419.99, 1249.79, 1156.25, 1104.17, 1081.03, 1035.7, 995.68, 969.65, 909.86, 791.24, 758.94, 734.35, 623.45

^{1}H NMR (400 MHz, CD_2Cl_2) δ: 7.77 (t, J = 9.8 Hz, 2H), 7.68 – 7.52 (m, 2H), 7.49 – 7.37 (m, 2H), 7.33 (d, J = 7.0 Hz, 3H), 5.89 – 5.67 (m, 1H), 5.43 – 5.31 (m, 1H), 5.01 (dd, J = 17.7, 11.4 Hz, 2H), 4.52 (d, J = 5.7 Hz, 1H), 4.42 (d, J = 6.4 Hz, 1H), 4.35 (d, J = 4.8 Hz, 1H), 4.24 (t, J = 6.5 Hz, 1H), 3.30 (t, J = 7.0 Hz, 1H), 3.23 – 3.05 (m, 1H), 2.06 (dd, J = 20.4, 6.5 Hz, 2H), 1.89 (d, J = 6.7 Hz, 1H), 1.80 – 1.64 (m, 1H), 1.64 – 1.55 (m, 1H), 1.55 – 1.29 (m, 2H).

^{13}C NMR (126 MHz, CD_2Cl_2) δ: 176.80, 156.10, 143.96, 143.79, 141.29, 137.99, 127.69, 127.06, 125.02, 124.80, 119.94, 114.89, 67.50, 66.94, 47.23, 47.18, 33.08, 31.53, 30.72, 27.27, 24.55.

HRMS *m/z* calculated for $C_{22}H_{24}NO_4$ $[M+H]^+$: 366.1700; found: 366.1703

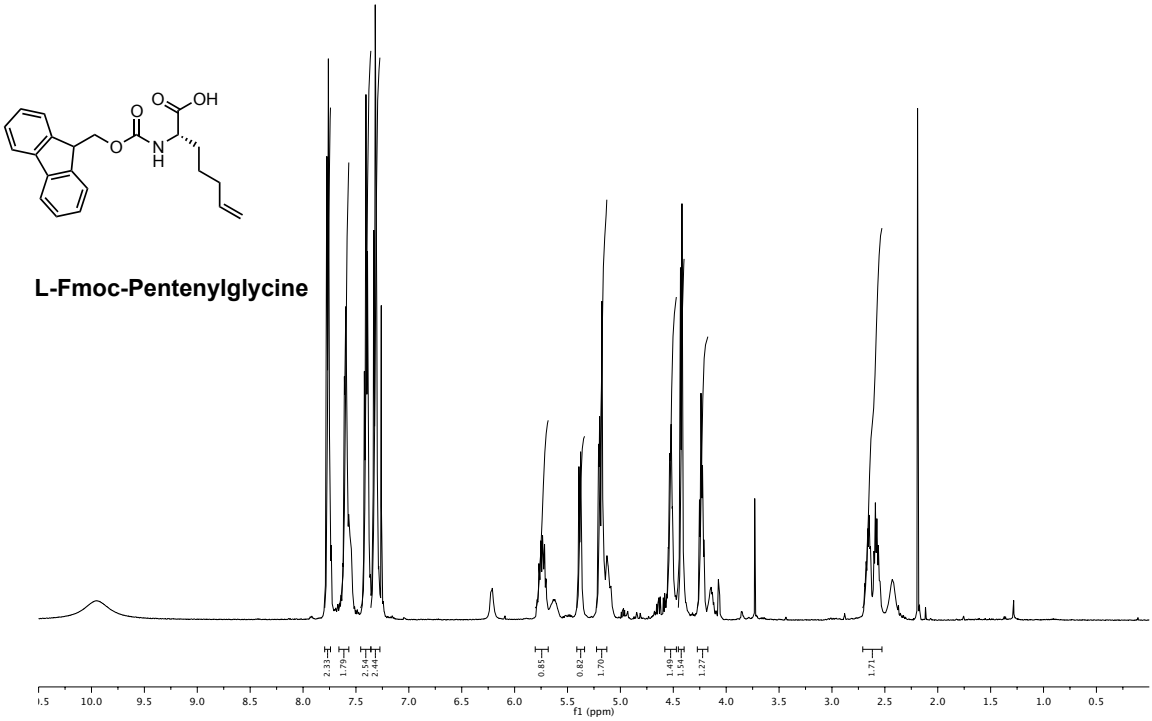
L-Fmoc-Pentenylglycine
f1 (ppm)

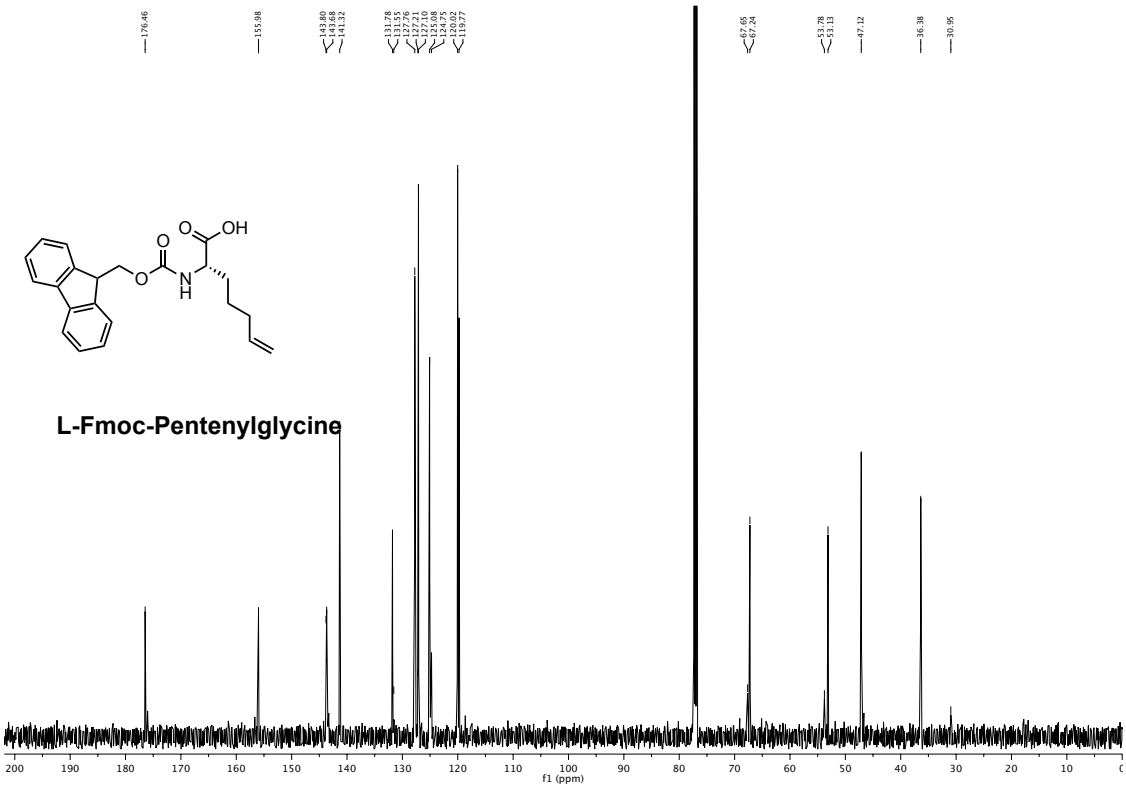
L-Fmoc-Pentenylglycine
f1 (ppm)

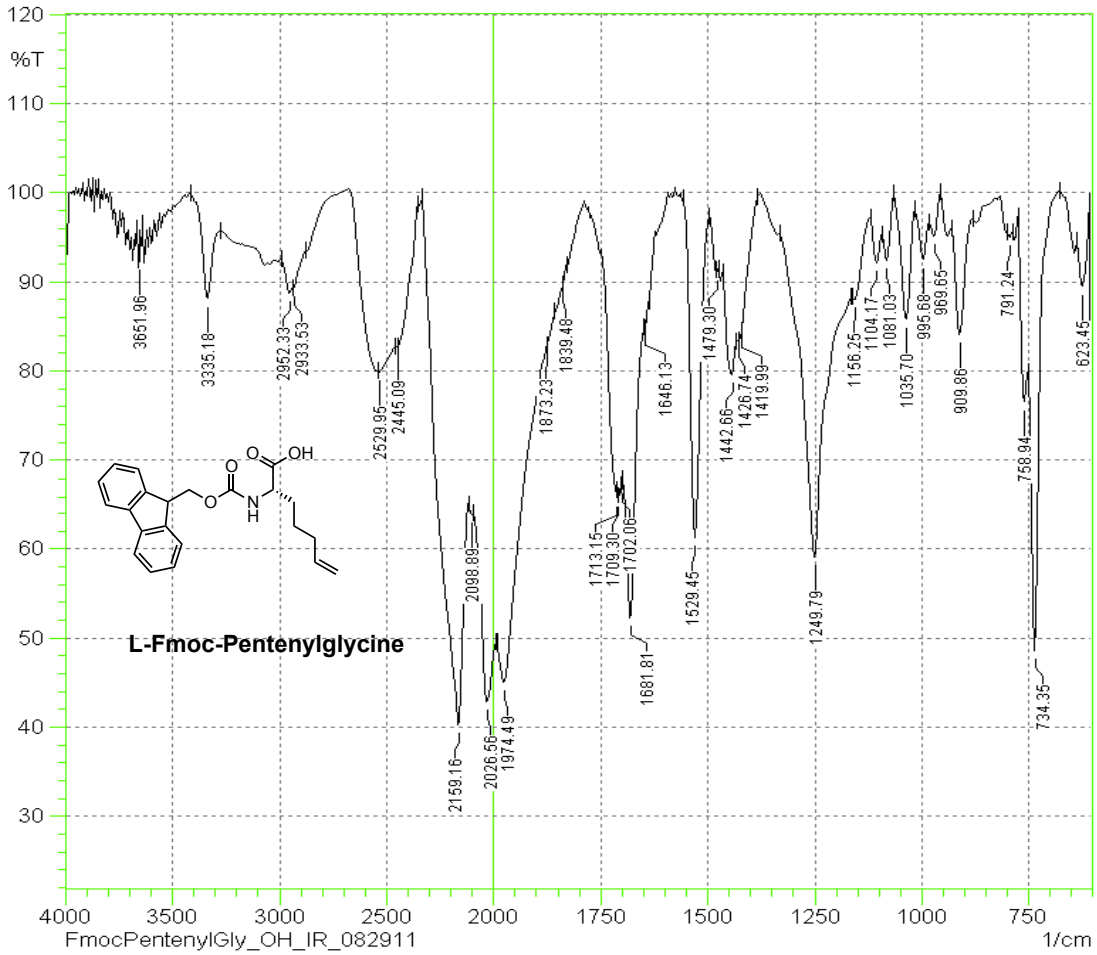
%T
1/cm
FmocPentenylGly_OH_IR_082911
L-Fmoc-Pentenylglycine
3651.96
3335.18
2952.33
2933.53
2529.95
2445.09
2159.16
2098.89
2026.56
1974.49
1873.23
1839.48
1713.15
1709.30
1702.06
1681.81
1646.13
1529.45
1479.30
1442.66
1426.74
1419.99
1249.79
1156.25
1104.17
1081.03
1035.70
995.68
969.65
909.86
791.24
758.94
734.35
623.45

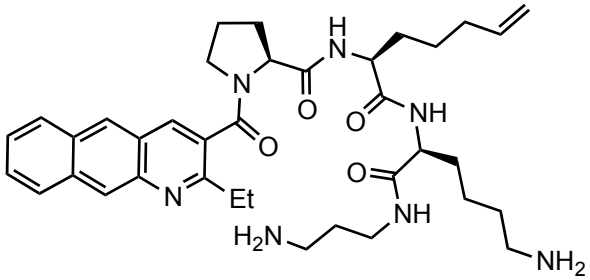

extended monomer

FT-IR (neat): 3655.34, 3272.01, 3073.84, 2940.28, 2880.97, 2538.15, 2448.95, 2159.16, 2027.05, 1974.49, 1666.86, 1662.04, 1655.77, 1649.99, 1645.17, 1639.86, 1536.68, 1434.46, 1404.56, 1195.3, 1176.01, 1128.28, 992.79, 968.68, 913.71, 880.93, 835.12, 798.47, 747.85, 719.88

^{1}H NMR (400 MHz, CD_3OD) δ: 9.16 (s, 1H), 8.83 (s, 1H), 8.69 (s, 1H), 8.20 – 8.11 (m, 2H), 7.76 – 7.61 (m, 2H), 5.75 (tt, J = 10.1, 6.6 Hz, 1H), 5.00 – 4.90 (m, 2H), 4.65 (dd, J = 7.9, 5.4 Hz, 1H), 4.47 – 4.10 (m, 3H), 3.76 (d, J = 5.8 Hz, 1H), 3.53 (dd, J = 16.5, 9.4 Hz, 2H), 3.38 – 3.04 (m, 7H), 2.92 – 2.71 (m, 5H), 2.42 – 2.25 (m, 1H), 2.11 – 1.20 (m, 22H), 1.13 (d, J = 6.4 Hz, 2H).

^{13}C NMR (126 MHz, CD_3OD) δ: 175.01, 174.87, 174.76, 174.42, 174.26, 174.16, 166.92, 164.16, 144.34, 142.78, 139.65, 139.47, 138.62, 137.51, 137.39, 134.49, 134.40, 131.10, 130.98, 130.73, 130.55, 130.26, 130.13, 129.66, 129.56, 129.41, 129.31, 125.46, 125.16, 122.05, 121.21, 120.76, 115.52, 115.30, 110.49, 63.28, 62.05, 61.61, 55.52, 55.43, 54.98, 54.77, 51.52, 49.79, 49.68, 49.56, 49.51, 49.41, 49.34, 49.17, 49.00, 48.83, 48.66, 40.61, 38.36, 38.29, 37.16, 37.09, 34.60, 34.44, 34.08, 33.34, 32.58, 32.53, 32.49, 31.76, 31.39, 28.81, 28.76, 28.20, 28.14, 26.55, 26.30, 26.19, 24.39, 24.05, 23.93, 14.34, 14.27, 14.19, 14.06.

LRMS (APCI$^+$) *m/z* calculated for $C_{22}H_{24}NO_4$ $[M+H]^+$: 658; found: 658, $[M+Na]^+$680

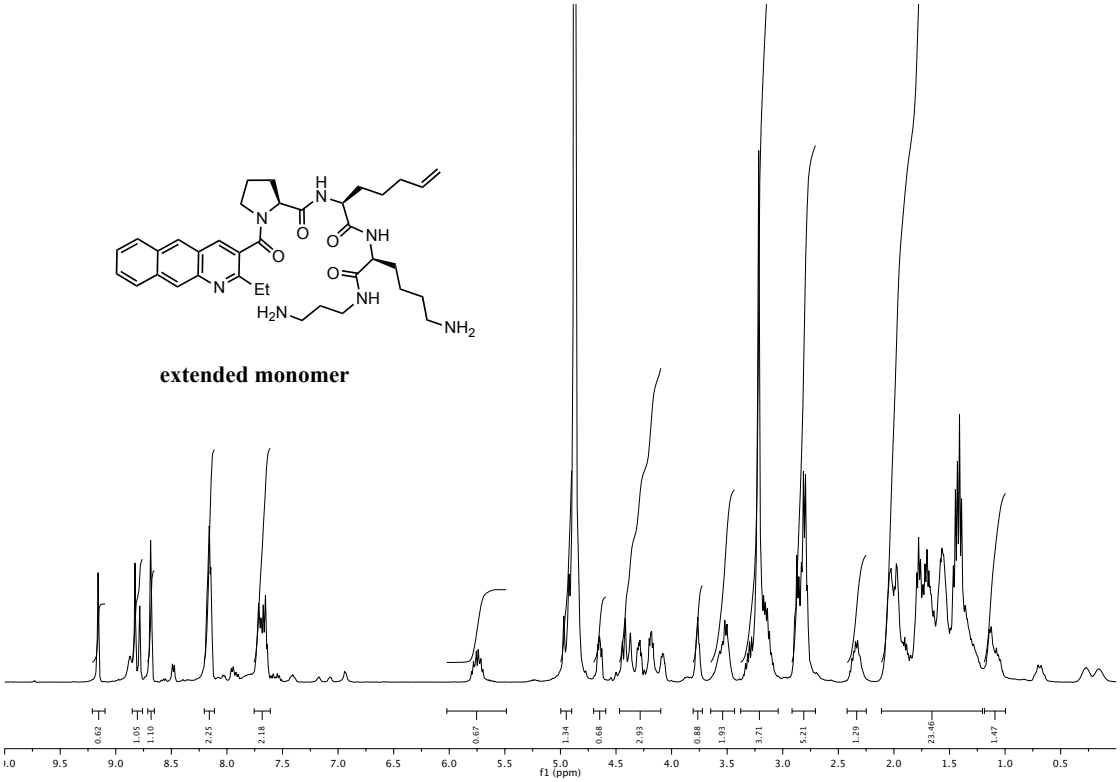
extended monomer
f1 (ppm)

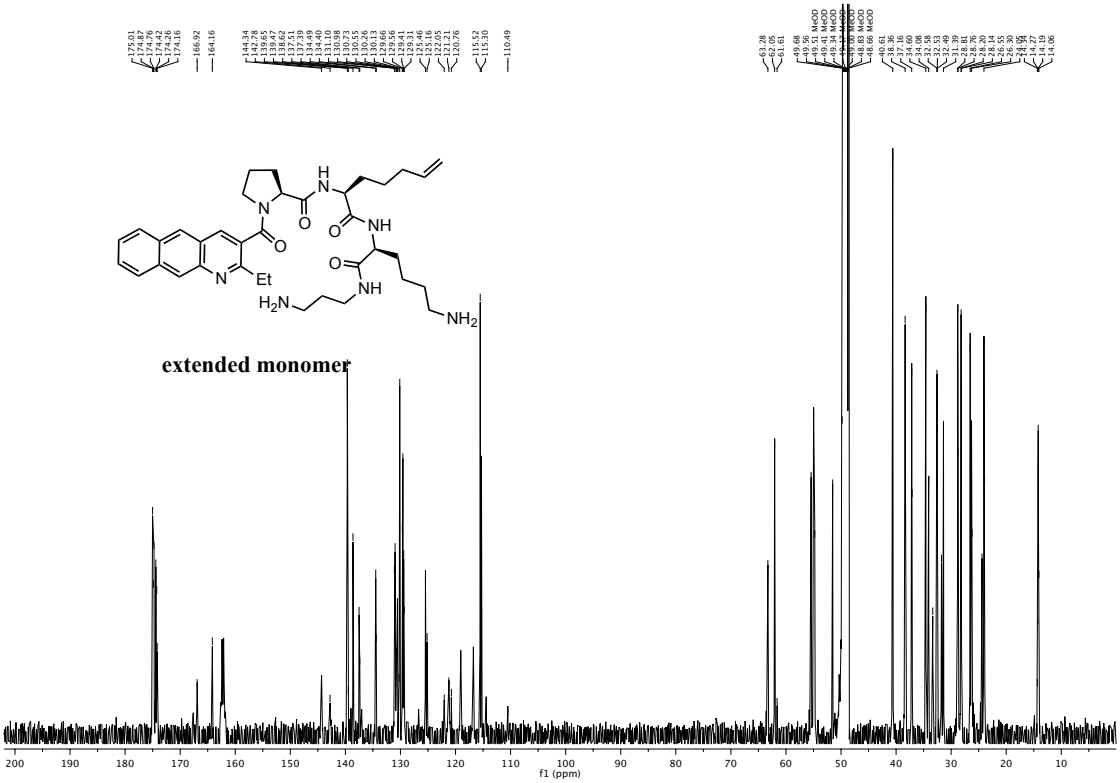
extended monomer
f1 (ppm)

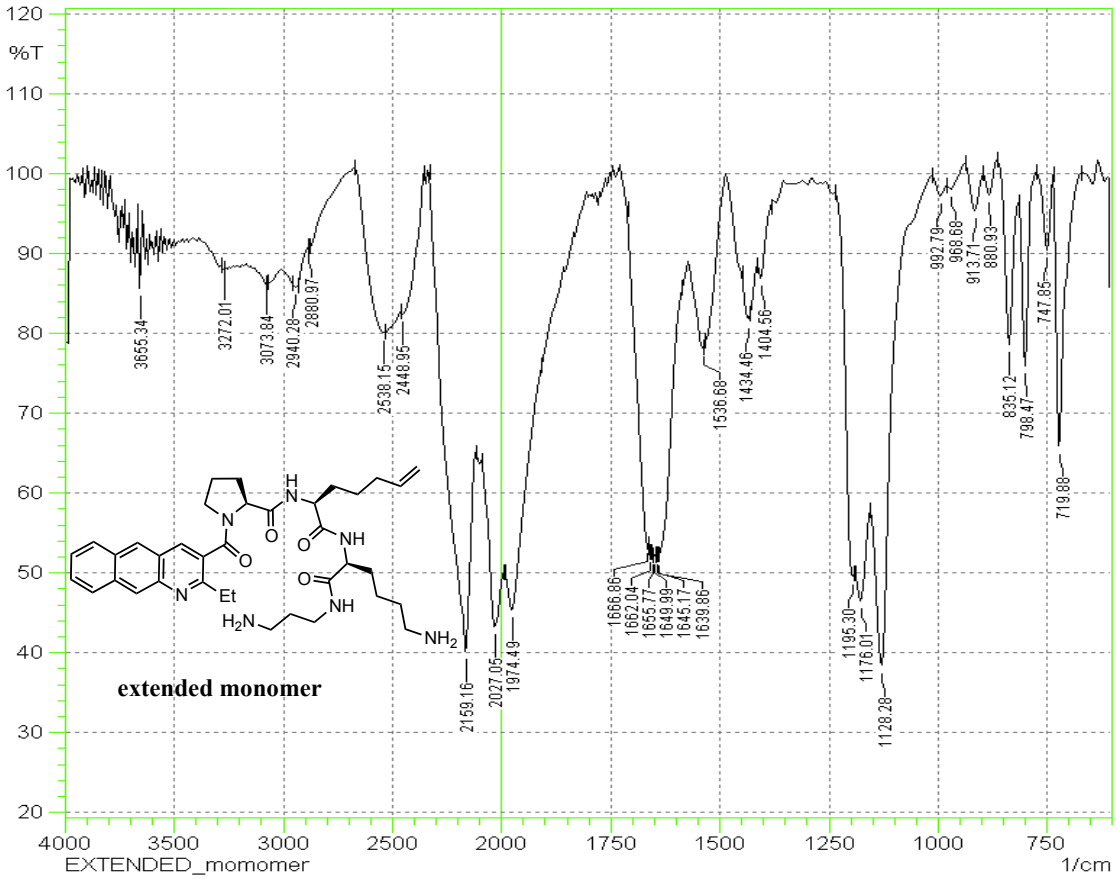
%T
1/cm
EXTENDED_momomer
extended monomer
3655.34
3272.01
3073.84
2940.28
2880.97
2538.15
2448.95
2159.16
2027.05
1974.49
1666.86
1662.04
1655.77
1649.99
1645.17
1639.86
1536.68
1434.46
1404.56
1195.30
1176.01
1128.28
992.79
968.68
913.71
880.93
835.12
798.47
747.85
719.88

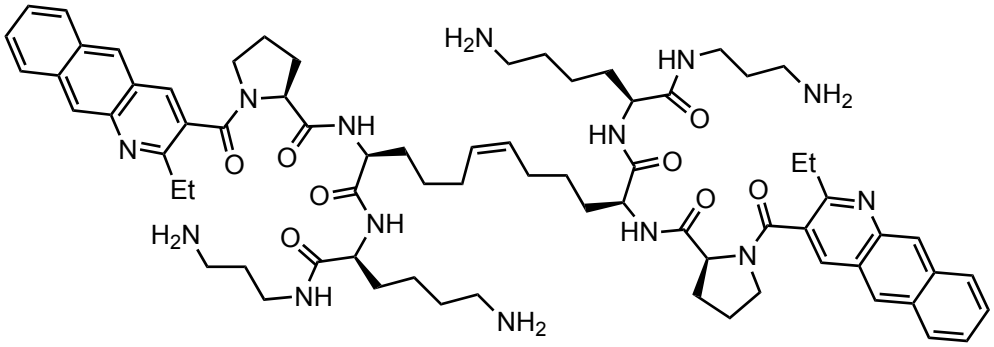

10

FT-IR (neat): 3652.93, 3591.21, 3549.26, 3271.53, 3236.81, 3138.93, 3116.27, 3095.54, 3079.14, 3067.57, 3043.46, 2937.38, 2535.25, 2528.02, 2445.57, 2159.16, 2097.44, 2025.6, 1974.97, 1902.16, 1874.2, 1853.46, 1665.9, 1659.63, 1649.02, 1636.97, 1582.48, 1541.98, 1518.36, 1436.39, 1432.53, 1193.85, 1179.87, 1126.83, 969.16, 837.53, 798.96, 750.26, 720.36

^{1}H NMR (400 MHz, D_2O) δ: 8.65 (s, 2H), 8.56 (s, 4H), 8.01 (s, 2H), 7.94 – 7.89 (m, 4H), 7.64 – 7.39 (m, 4H), 7.18 – 6.98 (m, 4H), 5.45 – 5.33 (m, 2H), 5.06 – 4.85 (m, 1H), 4.35 – 3.91 (m, 2H), 3.96 – 3.17 (m, 3H), 3.18 (d, J = 5.9 Hz, 1H), 3.11 (ddd, J = 19.6, 12.5, 6.1 Hz, 9H), 2.85 – 2.73 (m, 9H), 2.70 (s, 1H), 2.47 (d, J = 73.1 Hz, 3H), 1.72 – 1.71 (m, 1H), 1.69 – 1.60 (m, 6H), 1.51 (ddd, J = 34.8, 19.6, 6.2 Hz, 12H), 1.35 – 1.10 (m, 12H).

^{13}C NMR (126 MHz, D_2O) δ: 173.61, 173.55, 173.36, 170.64, 166.22, 148.35, 138.23, 137.35, 135.41, 132.95, 131.99, 131.95, 128.62, 128.55, 128.08, 128.00, 127.77, 127.74, 127.58, 127.55, 127.40, 127.25, 126.74, 125.12, 111.86, 81.46, 68.61, 58.07, 53.91, 53.70, 48.09, 45.14, 39.10, 36.99, 36.91, 36.13, 36.05, 30.45, 30.33, 29.69, 26.63, 26.53, 26.30, 26.25, 26.19, 25.17, 25.01, 22.09, 22.02, 13.22.

HRMS *m/z* calculated for $C_{72}H_{99}N_{14}O_8$ $[M+H]^+$: 1287.7765; found: 1287.7796.

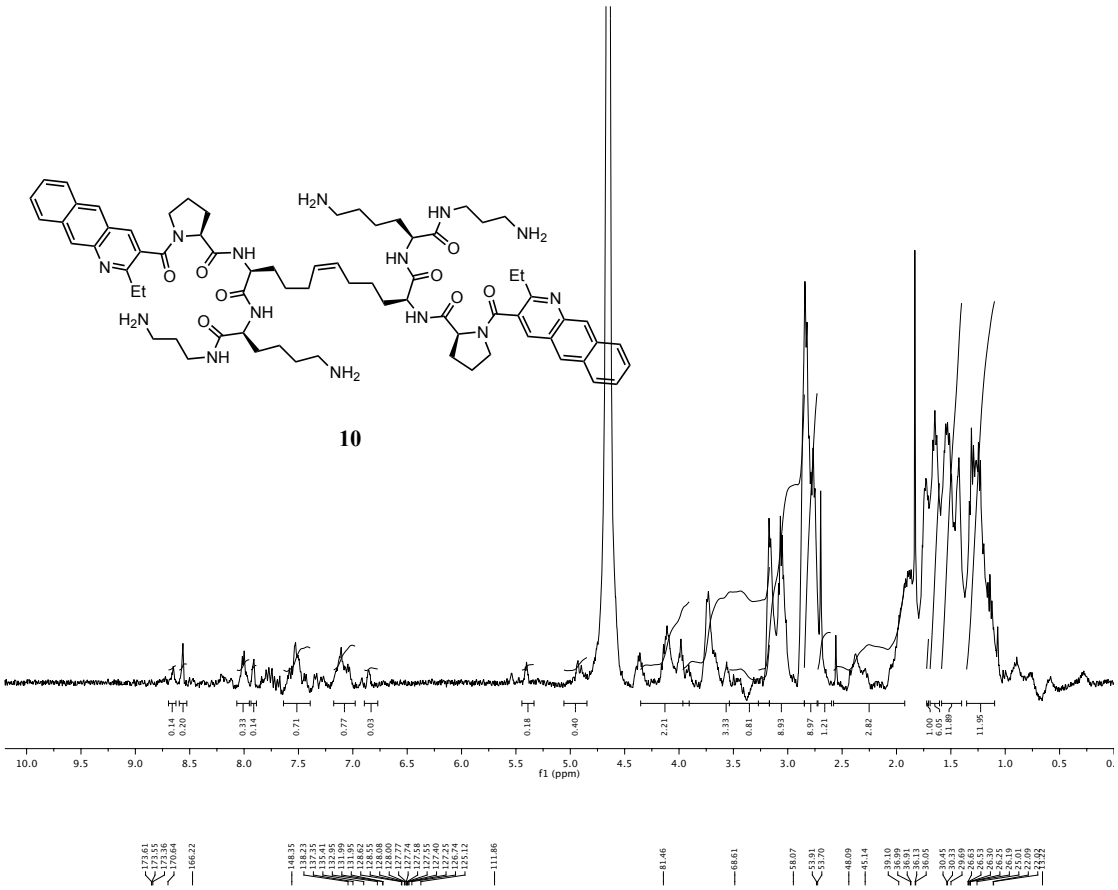
10
f1 (ppm)

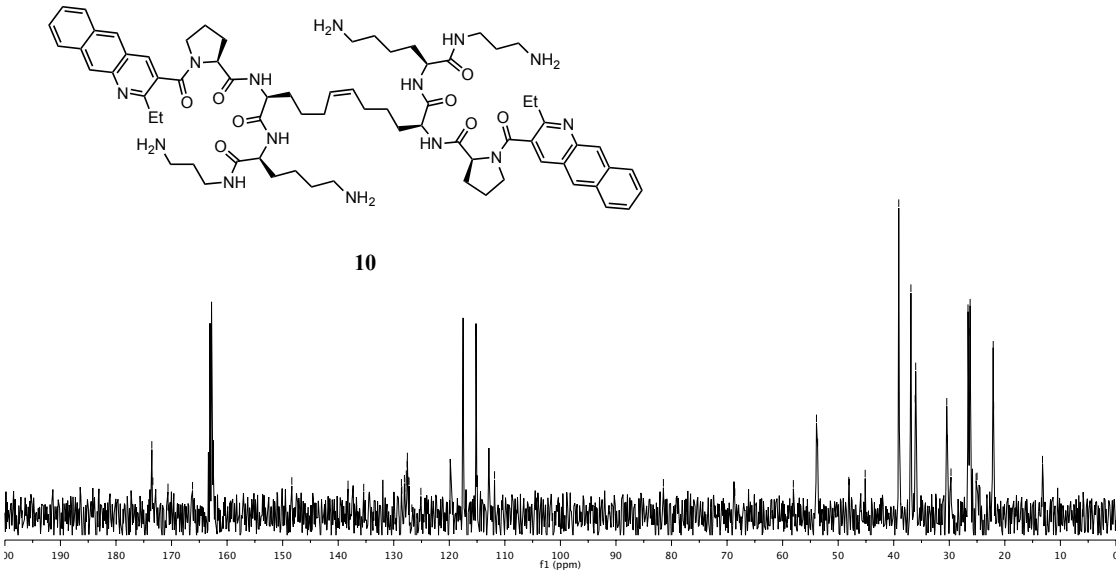
10
f1 (ppm)

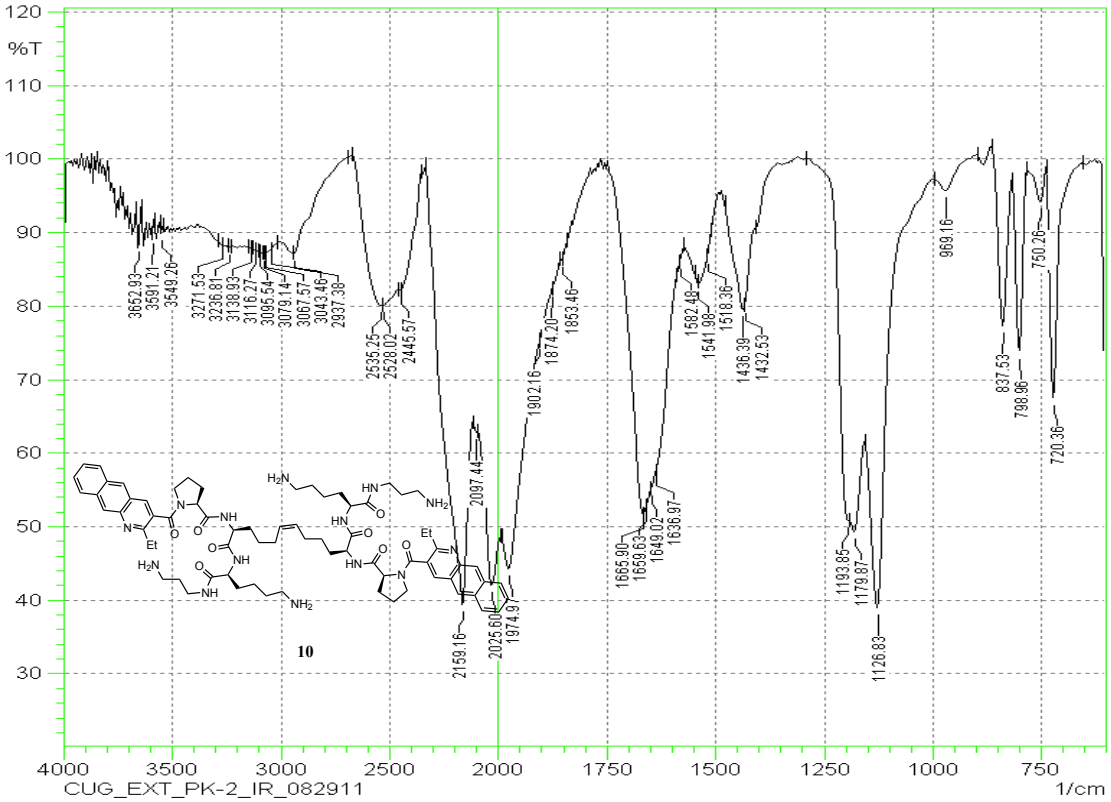
%T
1/cm
CUG_EXT_PK-2_IR_082911
3652.93
3591.21
3549.26
3271.53
3236.81
3138.93
3116.27
3095.54
3079.14
3067.57
3043.46
2937.38
2535.25
2528.02
2445.57
2159.16
2097.44
2025.60
1974.91
1902.16
1874.20
1853.46
1665.90
1659.63
1649.02
1636.97
1582.48
1541.98
1518.36
1436.39
1432.53
1193.85
1179.87
1126.83
969.16
837.53
798.96
750.26
720.36
10

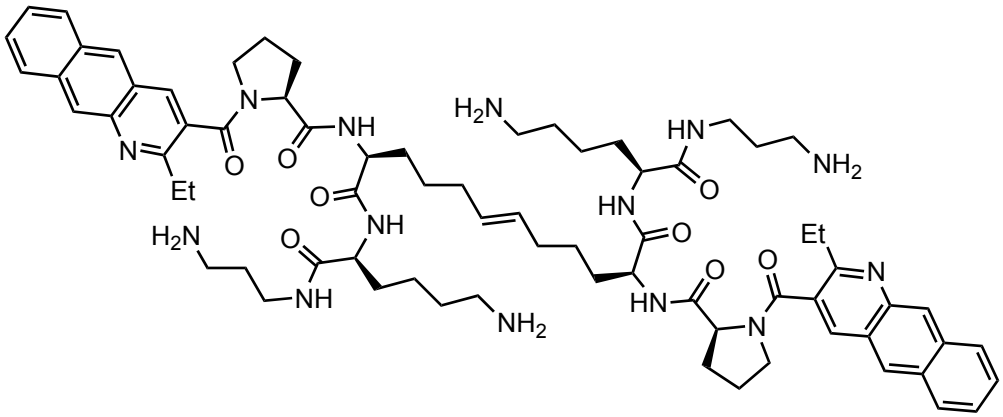

11

FTIR (neat): 3686.2, 3229.1, 2936.9, 2530.91, 2517.41, 2161.09, 2023.19, 1974.49, 1661.08, 1545.84, 1435.42, 1187.1, 1128.28, 968.68, 835.6, 798.47, 752.19, 716.99, and 535.21.

^{1}H NMR (500 MHz, D_2O) 8.74 (s, 1H), 8.16 (s, 1H), 8.07 (s, 1H), 7.85 – 7.68 (m, 3H), 7.61 (d, J = 6.3 Hz, 1H), 7.53 (s, 1H), 7.49 (s, 1H), 7.42 (s, 1H), 7.22 (s, 1H), 7.16 (s, 1H), 5.62 – 5.52 (m, 1H), 4.42 (d, J = 9.4 Hz, 1H), 4.28 – 4.17 (m, 2H), 4.09 (s, 1H), 4.01 (s, 1H), 3.83 (s, 3H), 3.59 (d, J = 11.8 Hz, 2H), 3.34 – 3.23 (m, 4H), 3.17 (dd, J = 15.6, 8.7 Hz, 6H), 3.01 – 2.81 (m, 14H), 2.49 (s, 1H), 2.43 – 2.35 (m, 1H), 2.04 (dd, J = 28.9, 23.3 Hz, 9H), 1.84 (d, J = 7.7 Hz, 7H), 1.80 – 1.70 (m, 9H), 1.70 – 1.50 (m, 16H), 1.49 – 1.41 (m, 6H), 1.39 – 1.32 (m, 5H).

^{13}C NMR (126 MHz, D_2O) δ: 173.95, 173.88, 173.65, 173.35, 165.63, 161.90, 144.57, 143.46, 139.15, 135.95, 135.09, 134.57, 131.81, 130.55, 129.34, 128.98, 128.19, 127.66, 125.74, 122.35, 76.32, 60.70, 60.32, 53.92, 53.72, 53.59, 53.23, 50.31, 48.02, 39.10, 39.04, 36.99, 36.90, 36.13, 36.03, 31.03, 30.44, 30.30, 29.90, 29.78, 26.63, 26.54, 26.29, 26.25, 26.17, 25.05, 24.54, 22.62, 22.11, 22.00, 13.57, 13.27, 13.11.

HRMS *m/z* calculated for $C_{72}H_{99}N_{14}O_8$ $[M+H]^+$: 1287.7765; found $[M+Na]^+$: 1309.7548.

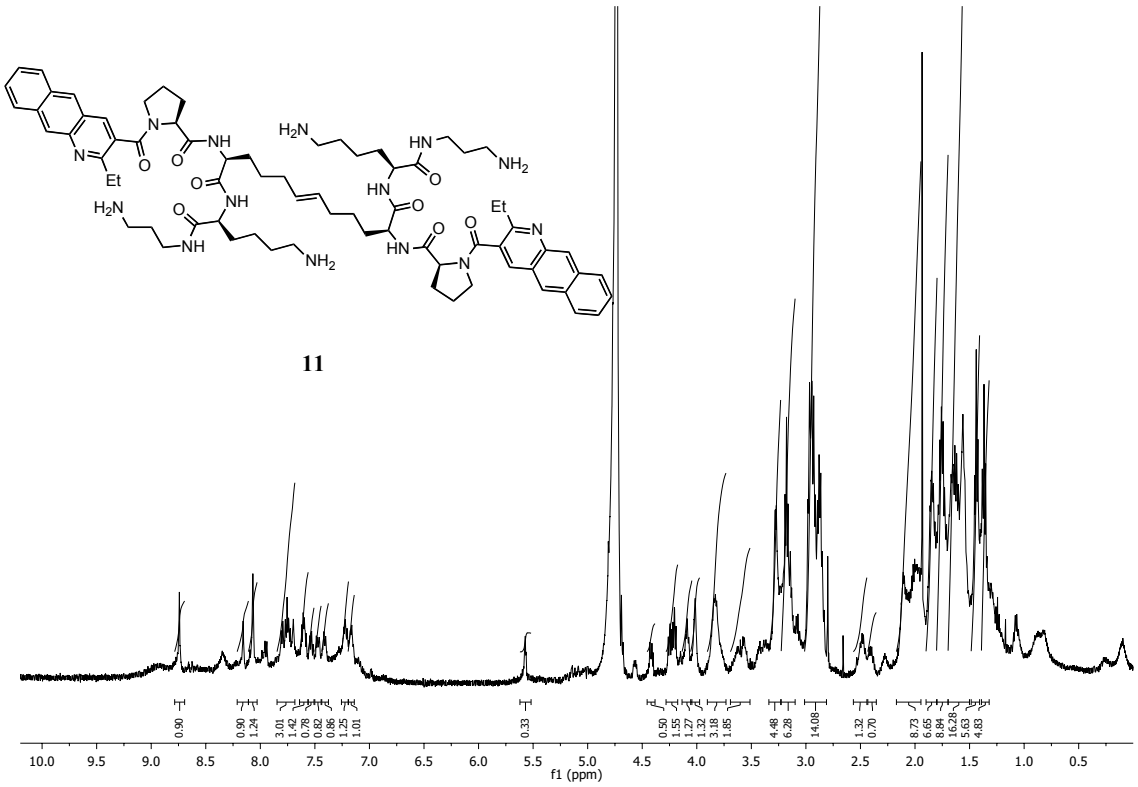
11
f1 (ppm)

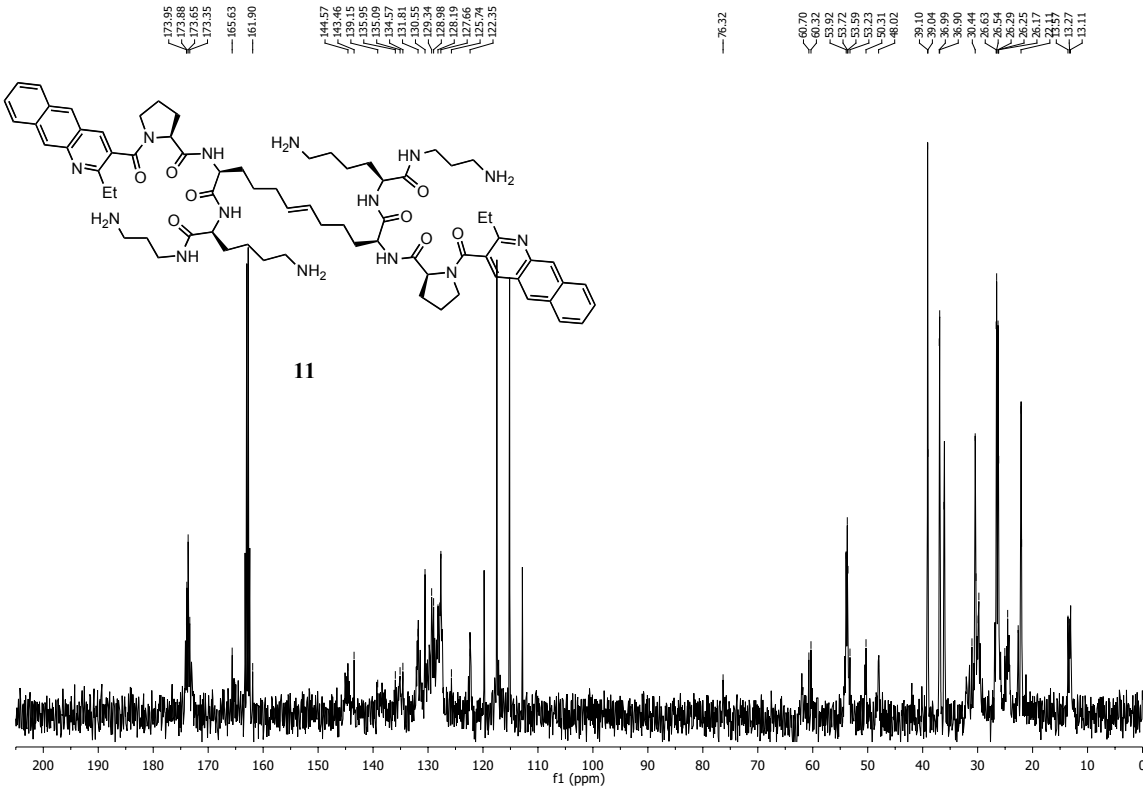
11
f1 (ppm)

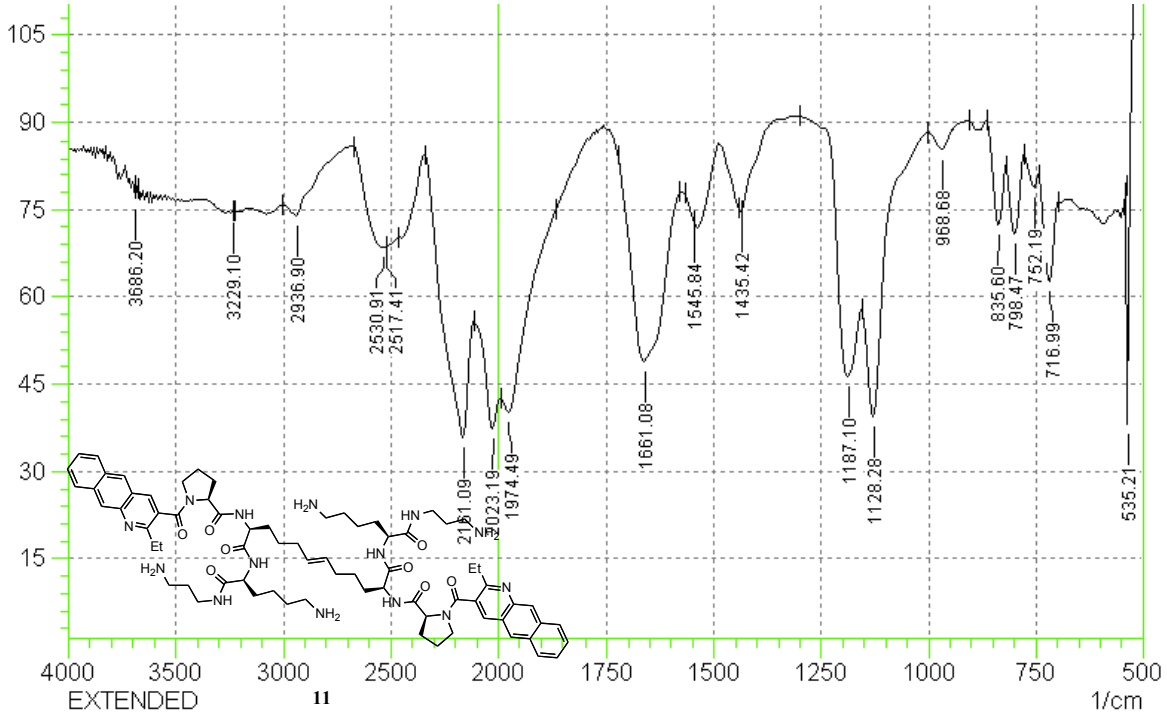
105
90
75
60
45
30
15
3686.20
3229.10
2936.90
2530.91
2517.41
2181.09
2023.19
1974.49
1661.08
1545.84
1435.42
1187.10
1128.28
968.68
835.60
798.47
752.19
716.99
535.21
4000
3500
3000
2500
2000
1750
1500
1250
1000
750
500
EXTENDED
1/cm
11

Binding Analyses by Surface Plasmon Resonance (SPR)

SPR binding measurements were performed on a Biacore-X instrument (Biacore, Inc., Uppsala, Sweden) with two flow channels (FC1 and FC2). 5'-Biotinylated-RNA sequences, with a C_6 linker separating the biotin label from the RNA (Integrated DNA Technologies Inc.), were immobilized on streptavidin (Rockland Immunochemicals) functionalized carboxyl methyl dextran coated sensor chips (CM5, G.E. Healthcare) using EDC/NHS (Advanced ChemTech) coupling chemistry. Filtered (0.2 μ), degassed and autoclaved HBS-N buffer (0.01M Hepes, pH=7.4, 0.15 M NaCl) was employed as sample and as running buffer for all SPR experiments. A typical protocol for an experiment is as follows: a CM5 sensor chip was allowed to equilibrate to room temperature and then docked into the instrument. Following priming with running buffer, FC1 and FC2 were conditioned by manual injection of 20 μL aqueous NaOH (50 mM) at a flow rate of 30 μL/min. This was repeated 3 times followed by a wash command. Next the carboxyl groups on the sensor chip surface in both flow cells were activated separately by injecting 60 μL of freshly prepared 1:1 mixture of EDC (0.4 M) and NHS (0.1 M) at a 5 μL/min flow rate followed by a wash. Streptavidin (100 μg/mL in 10 mM sodium acetate buffer, pH=5.0) was immediately injected in pulses until approximately between 2500-3000 RU was achieved in both flow cells. After washing, the surface was deactivated with 60 μL injection of ethanolamine (1M, pH=8.5) at 5 μL/min. The flow cells were primed, and the streptavidin surface in FC1 alone was blocked with 30 μL of biotin (20 μM in HBS-N) at 5 μL/min. The RNA (200 nM in running buffer, HBS-N) to be immobilized was unfolded by heating above its predicted melting temperature in a heated block for 2 min and then allowed to refold by cooling gradually to room temperature. The RNA was then immobilized in FC2 alone to response units ranging from 200-1000 RU using a 5 μL/min flow rate. A representative sensorgram for the immobilization procedure is shown in **supplementary Fig. 1**. Two 20 μL aliquots of NaCl (0.5 M) were injected at a 30 μL/min flow rate to remove non-specifically bound RNA. The level of RNA immobilized was noted when the baseline was stable, usually after repeated buffer injection followed by a "prime" command. Binding measurements were performed by flowing various concentrations of the compounds to be analyzed over the immobilized RNA and recording the reference-subtracted (FC2-FC1) sensorgrams.

For kinetic analysis, at least five sensorgrams corresponding to different concentrations of compound (usually ranging from 0.05-1 μM in HBS-N) were obtained using flow rates of either 60 μL/min or 30 μL/min. The experimental sensorgrams were globally fitted to a 1:1 binding equation (Biaevaluation software) to obtain association rates (k_a) and dissociation rates (k_d) as well as equilibrium binding constants (K_D). To measure the binding stoichiometry (n), the relations in equations (1-3) below were used:

$$RU_{\max} = \frac{MW_{compound}}{MW_{RNA}} \times RU_{RNA} \times Stoichiometry(n) \qquad (1)$$

$$RU_{(\max)predict} = n \times RU_{(\max)observed} \qquad (2)$$

$$r = \frac{RU_{eq}}{RU_{\max}} \qquad (3)$$

where $RU_{\max}$ is the maximum resonance response unit at saturation, RU_{RNA} is the amount RU of RNA immobilized, n is the stoichiometry, $MW_{compound}$ and MW_{RNA} are molecular weights of compound and RNA respectively, and RU_{eq} represents the resonance response at steady-state (equilibrium). The response units at equilibrium were subjected to Scatchard binding plots of (r/C_{free} vs. r).

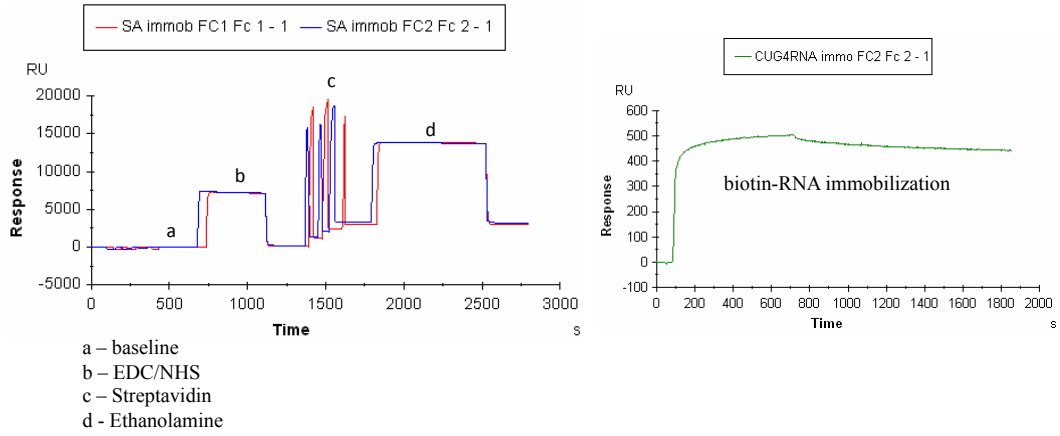

Supplementary Fig. 1. Left: representative sensorgrams for streptavidin immobilization on CM5 sensor chip. Right: sensorgram for non-covalent biotin-RNA capture on a streptavidin coated CM5 sensor surface.

Supplementary Table 1

compound **3**	RNA SEQUENCE
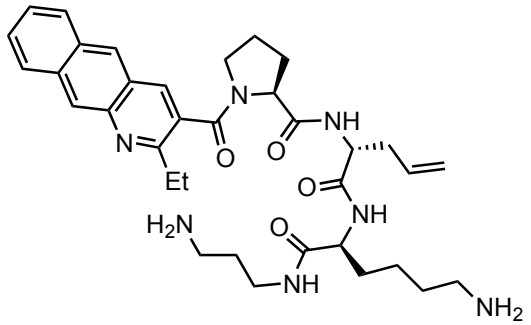	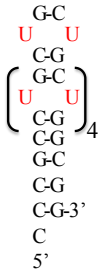 **(CUG)10**
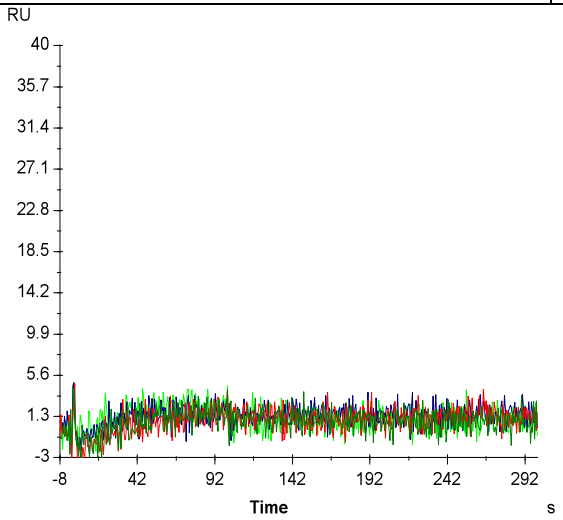	
K_a ($M^{-1}s^{-1}$)	-
k_d (s^{-1})	-
K_D (nM)	No Binding observed
Chi^2	-

Supplementary Table 2

compound **4**	RNA SEQUENCE
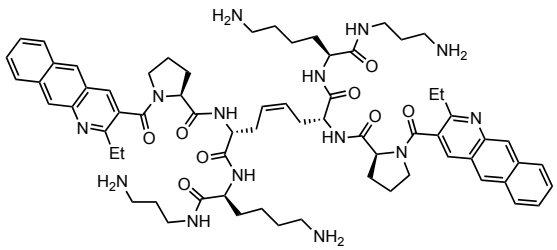	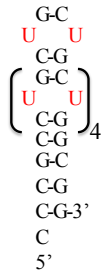 **(CUG)10**
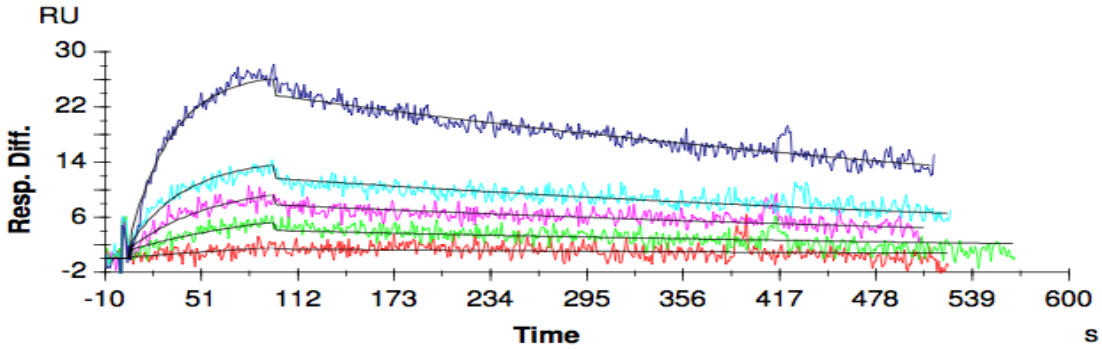	
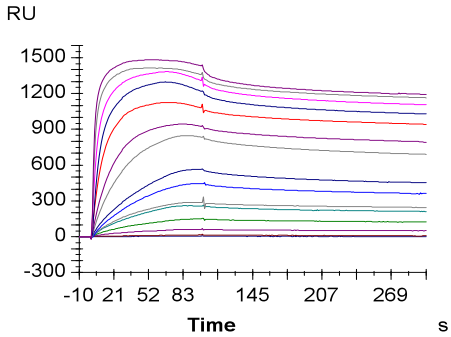 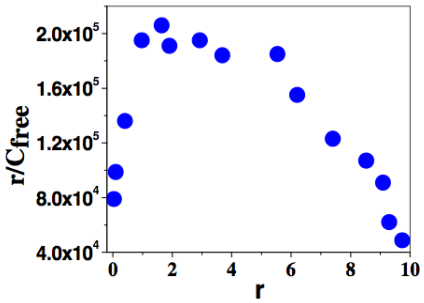	

	Trial-1	Trial-2
k_a ($M^{-1}s^{-1}$)	$(3.6 \pm 0.7) \times 10^4$	$(2.6 \pm 0.3) \times 10^4$
k_d (s^{-1})	$(1.4 \pm 0.1) \times 10^{-3}$	$(1.0 \pm 0.6) \times 10^{-3}$
K_D (nM)	38	40
Chi^2	0.9	1.0
n	10	

Supplementary Table 3

compound **4**	RNA SEQUENCE
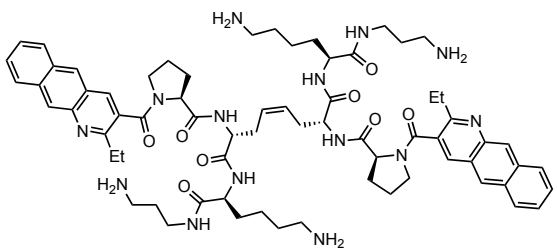	G-C U U C-G G-C U U C-G C-G G-C C-G C-G-3' C 5' **(CUG)4**

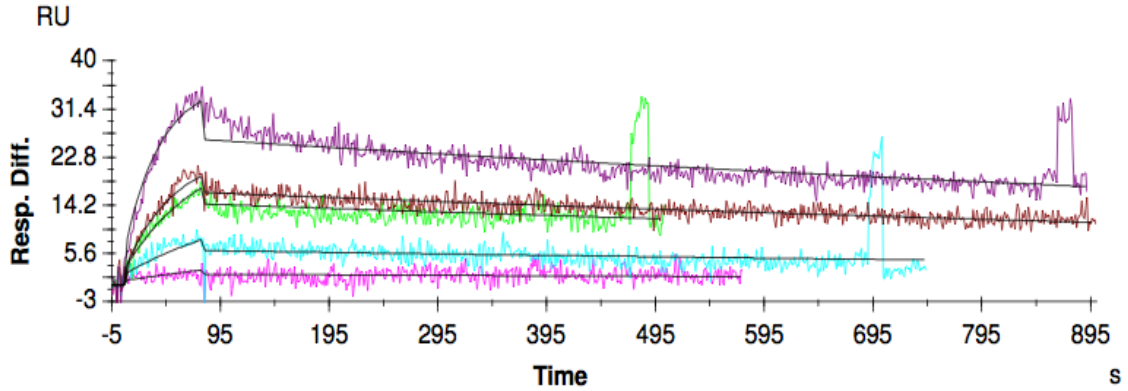

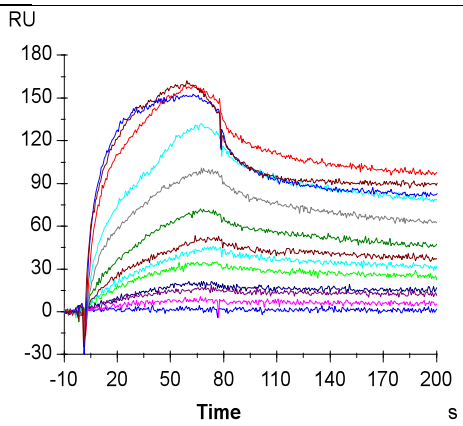

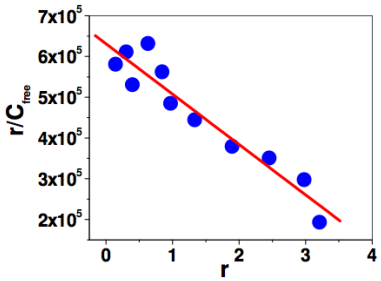

	Trial-1	Trial-2
k_a ($M^{-1}s^{-1}$)	$(2.5 \pm 0.7) \times 10^{4}$	$(1.4 \pm 0.2) \times 10^{4}$
k_d (s^{-1})	$(4.8 \pm 0.6) \times 10^{-4}$	$(3.6 \pm 0.1) \times 10^{-4}$
K_D (nM)	19	26
Chi^2	5.1	6.1
n	4	

Supplementary Table 4

compound **4**	RNA SEQUENCE
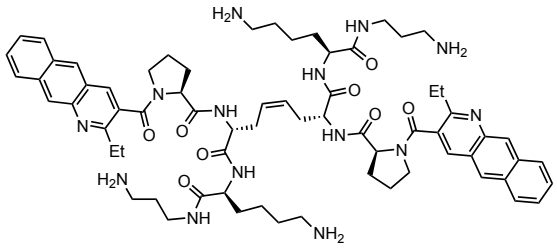	G-C U U C-G G-C C-G C-G-3' C 5' **(CUG)2**
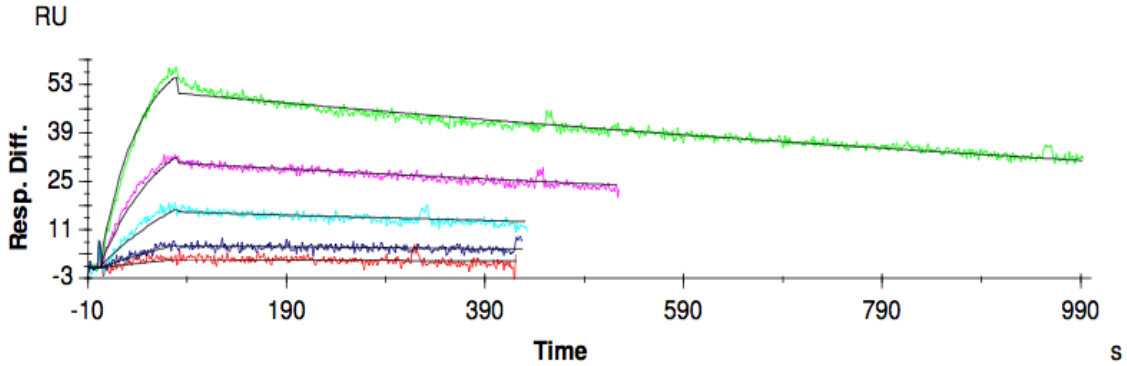	
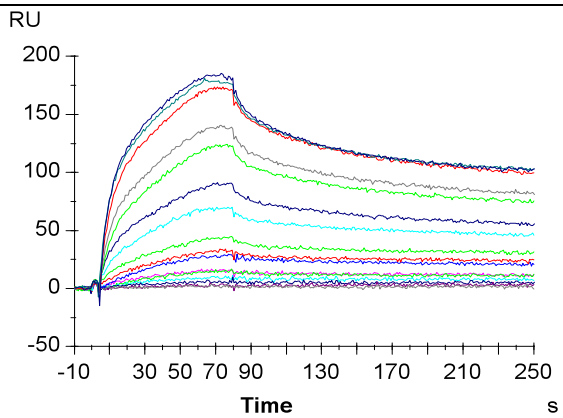 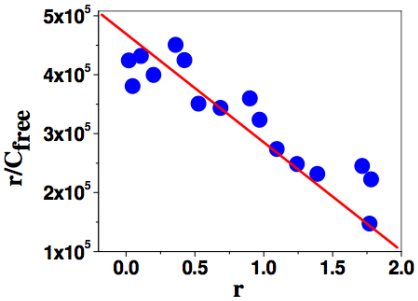	

	Trial-1	Trial-2
k_a ($M^{-1}s^{-1}$)	$(3.1 \pm 0.4) \times 10^{4}$	$(2.5 \pm 0.6) \times 10^{4}$
k_d (s^{-1})	$(1.3 \pm 0.8) \times 10^{-3}$	$(5.3 \pm 0.2) \times 10^{-4}$
K_D (nM)	43	21
Chi^2	1.9	1.2
n	2	

Supplementary Table 5

compound 4	RNA SEQUENCE
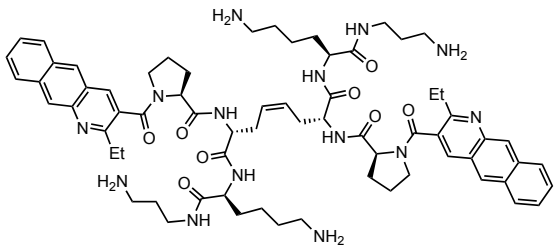	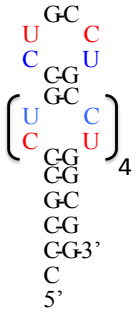 **(CCUG)10**
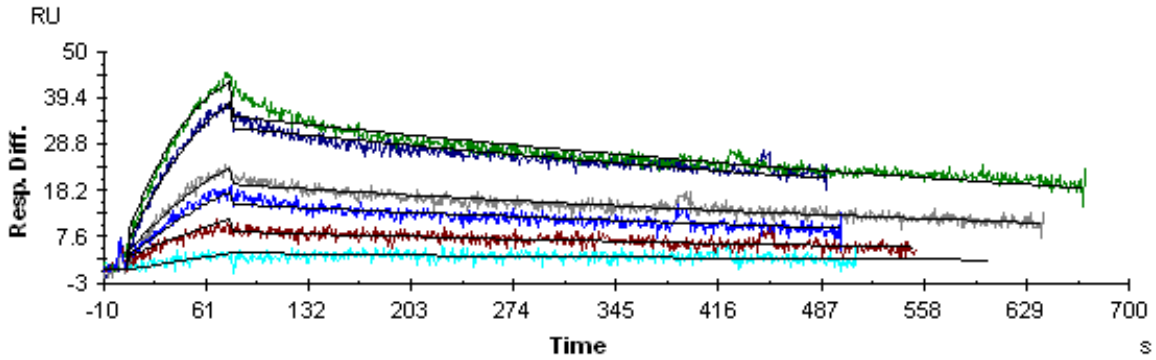	
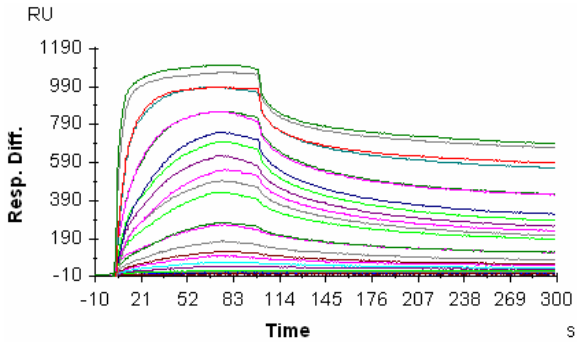 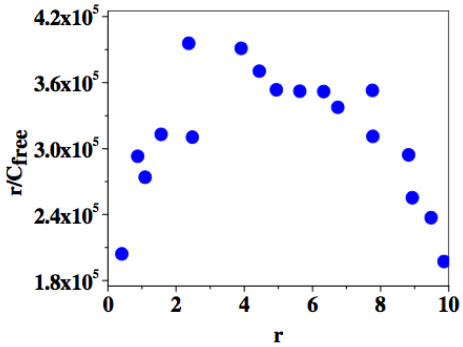	
Trial-1	Trial-2
k_a ($M^{-1}s^{-1}$) $(2.0 \pm 0.2) \times 10^{4}$	$(2.8 \pm 0.4) \times 10^{4}$
k_d (s^{-1}) $(7.6 \pm 0.8) \times 10^{-4}$	$(1.1 \pm 0.4) \times 10^{-3}$
K_D (nM) 38	38
Chi^2 2.5	1.4
n	10

Supplementary Table 6

compound **4**	RNA SEQUENCE
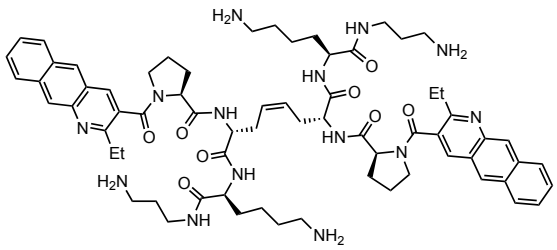	G-C A A C-G G-C A A C-G C-G 4 G-C C-G C-G-3' C 5' **(CAG)10**
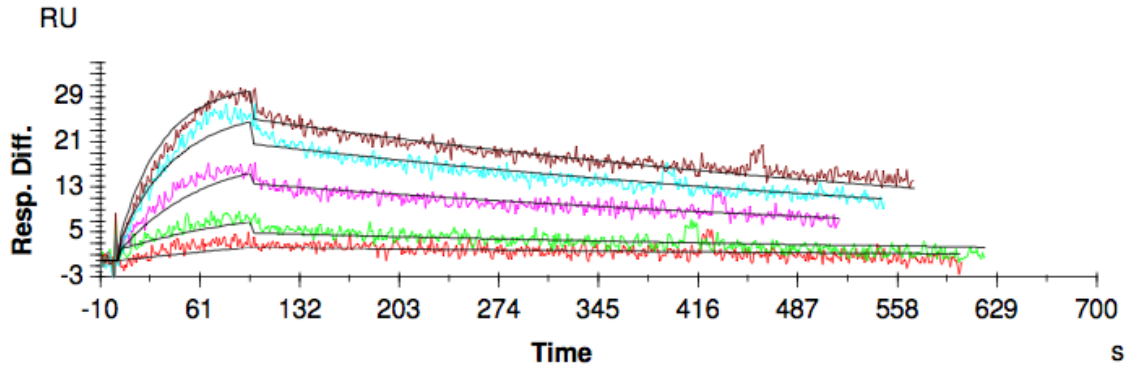	
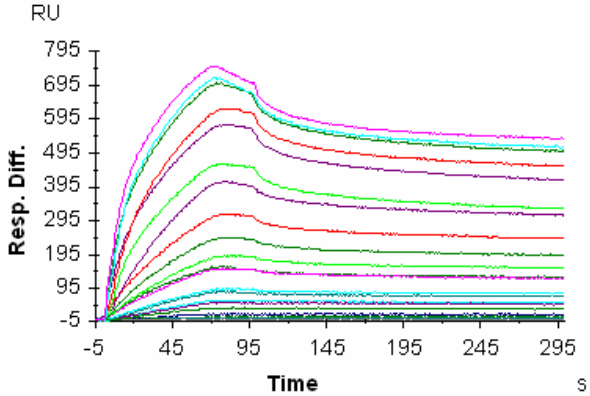 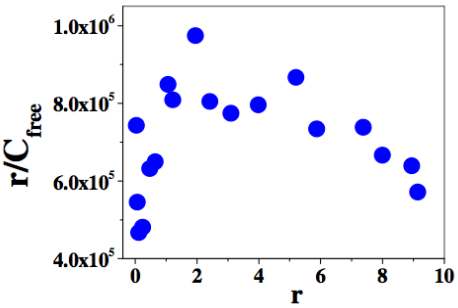	

	Trial-1	Trial-2
k_a ($M^{-1}s^{-1}$)	$(3.1 \pm 0.5) \times 10^{4}$	$(3.1 \pm 0.3) \times 10^{4}$
k_d (s^{-1})	$(1.6 \pm 0.1) \times 10^{-3}$	$(1.4 \pm 0.1) \times 10^{-3}$
K_D (nM)	46	52
Chi^2	1.4	1.3
n	10	

Supplementary Table 7

compound **4**	RNA SEQUENCE
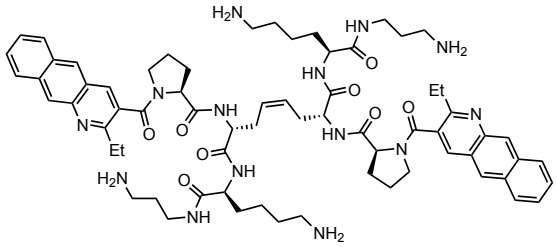	G-C U A C-G (G-C U-A C-G)$_4$ C-G G-C C-G C-G-3' C 5' **Duplex**

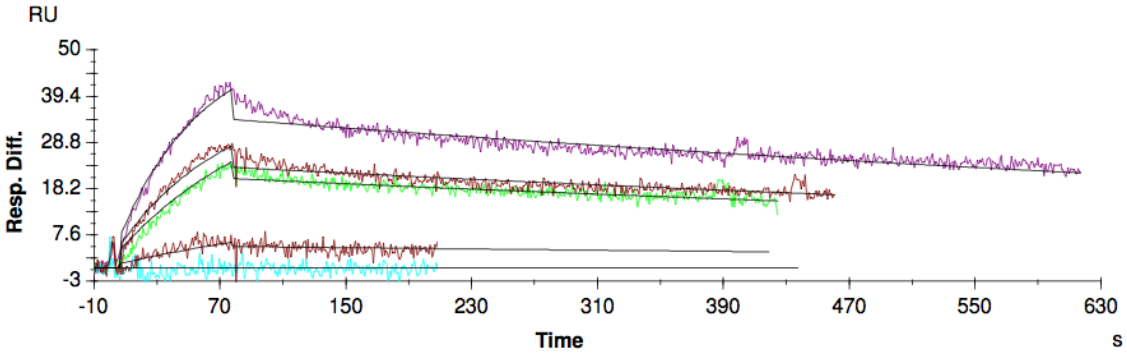

	Trial-1	Trial-2
k_a ($M^{-1}s^{-1}$)	$(1.5 \pm 0.3) \times 10^{4}$	$(1.4 \pm 0.1) \times 10^{4}$
k_d (s^{-1})	$(8.3 \pm 0.5) \times 10^{-4}$	$(9.0. \pm 0.0) \times 10^{-4}$
K_D (nM)	56	78
Chi^2	1.8	1.2
n	ND	

Supplementary Table 8

compound **4**	RNA SEQUENCE
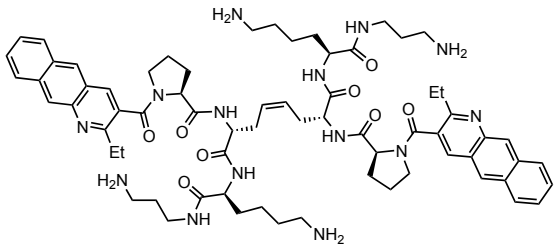	C-A A A C-G C-G C-G U-A U-A C-G C-G G-C G-C 3' 5' **HIV-1FSS**
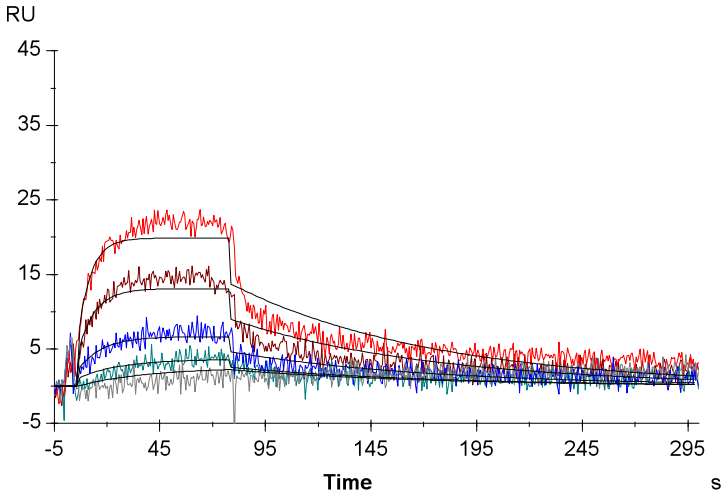	
	Trial-1 / Trial-2
k_a ($M^{-1}s^{-1}$)	$(1.3 \pm 0.2) \times 10^{4}$ / $(4.2 \pm 0.1) \times 10^{3}$
k_d (s^{-1})	$(1.5 \pm 0.1) \times 10^{-2}$ / $(5.60 \pm 0.09) \times 10^{-3}$
K_D (nM)	1140 / 1340
Chi^2	3.5 / 1.6
n	ND

Supplementary Table 9

COMPOUND 5	RNA SEQUENCE
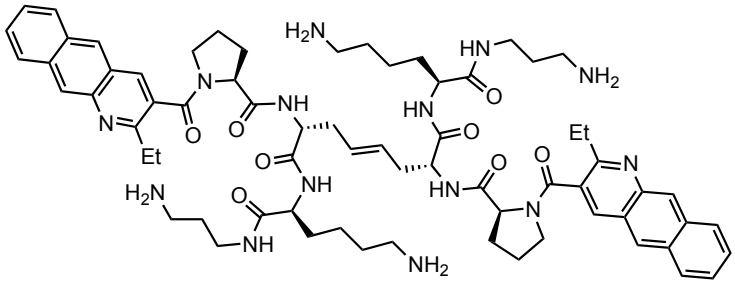	G-C U U C-G G-C U U C-G C-G G-C C-G C-G-3' C 5' $(CUG)_4$ **(CUG)10**
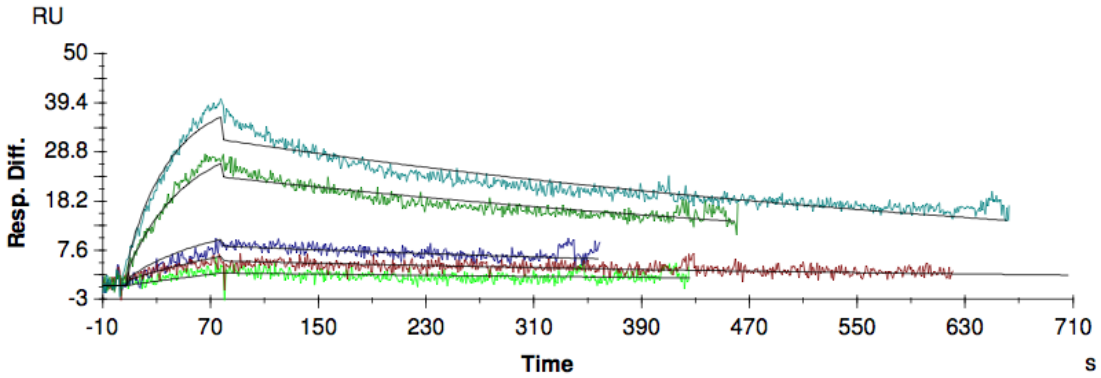	
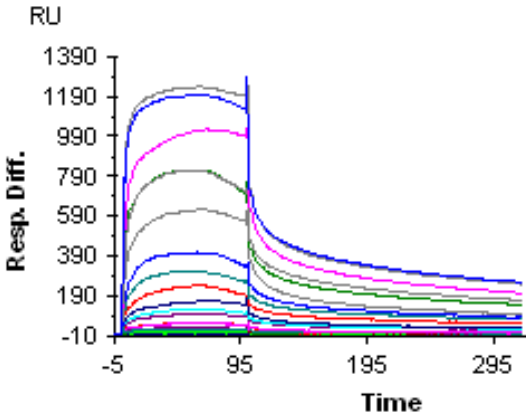 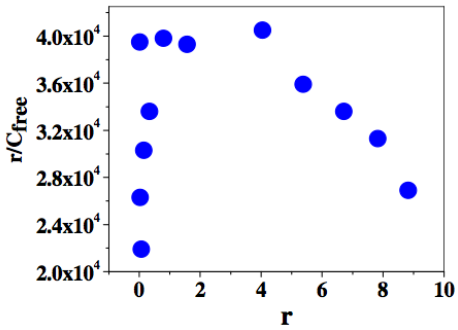	

	Trial-1	Trial-2
k_a ($M^{-1}s^{-1}$)	$(2.9 \pm 0.4) \times 10^{4}$	$(2.80 \pm 0.03) \times 10^{4}$
k_d (s^{-1})	$(1.4 \pm 0.3) \times 10^{-3}$	$(1.47 \pm 0.01) \times 10^{-3}$
K_D (nM)	48	88
Chi^2	1.7	1.1
n	10	

Supplementary Table 10

compound **5**	RNA SEQUENCE
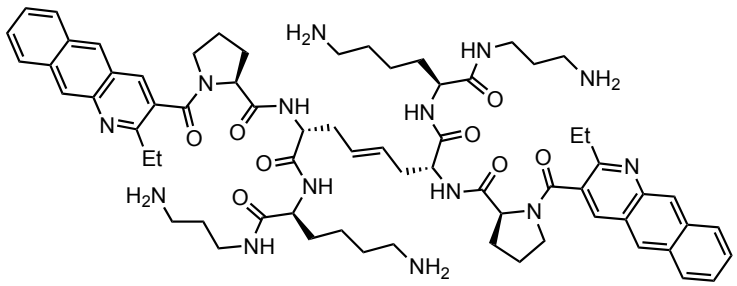	G-C U U C-G G-C U U C-G C-G G-C C-G C-G-3' C 5' **(CUG)4**

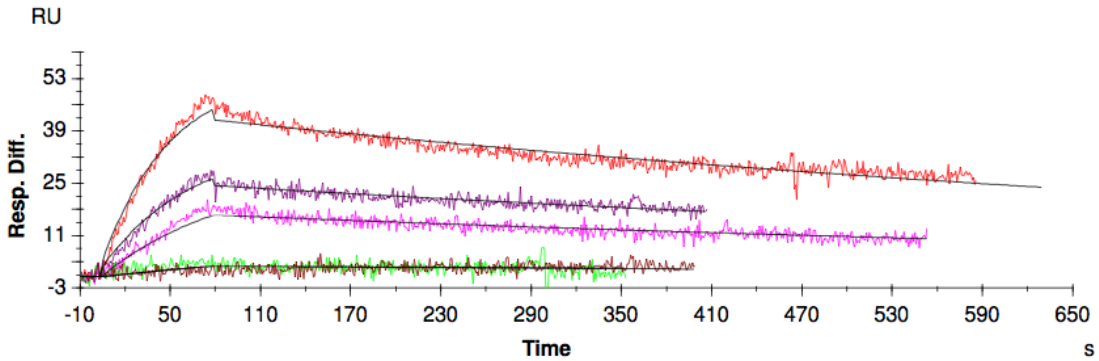

	Trial-1	Trial-2
k_a ($M^{-1}s^{-1}$)	$(3.5 \pm 0.4) \times 10^{4}$	$(2.2 \pm 0.3) \times 10^{4}$
k_d (s^{-1})	$(9.7 \pm 0.7) \times 10^{-4}$	$(1.0 \pm 0.5) \times 10^{-3}$
K_D (nM)	28	48
Chi^2	2	2
n	ND	

Supplementary Table 11

compound **5**	RNA SEQUENCE
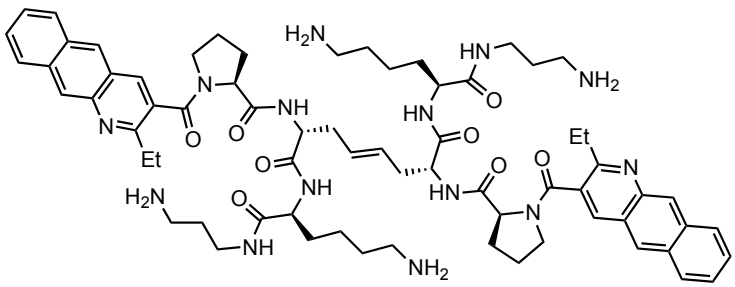	G-C U U C-G G-C C-G C-G-3' C 5' **(CUG)2**
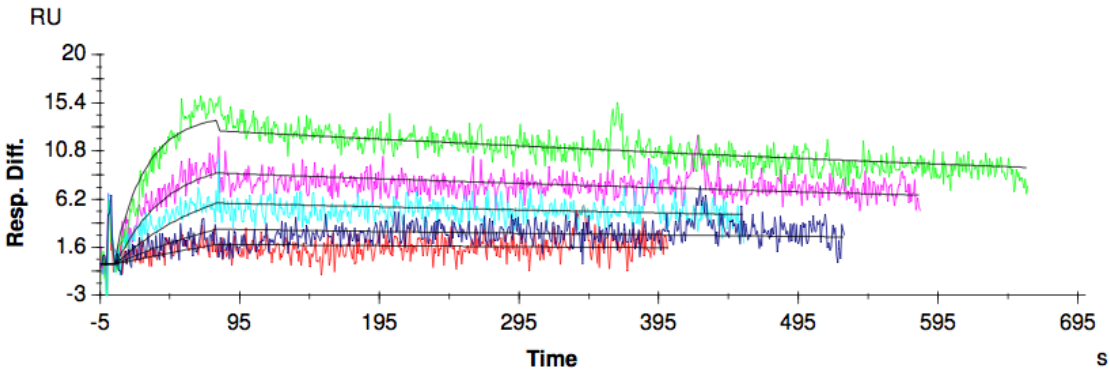	
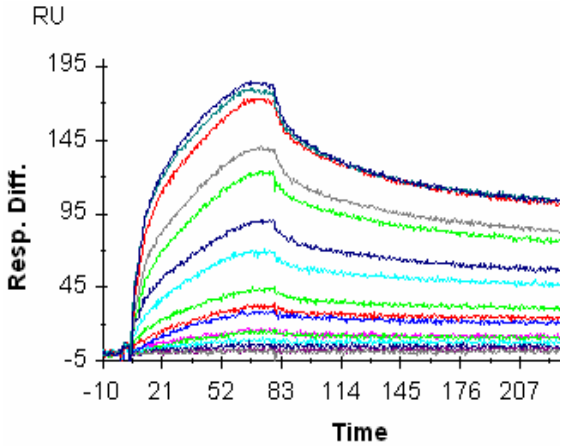 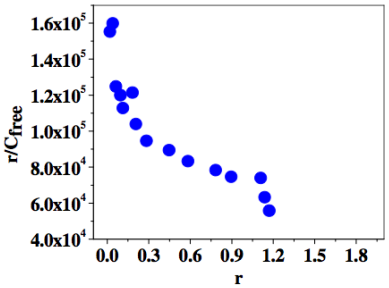	

	Trial-1	Trial-2
k_a ($M^{-1}s^{-1}$)	$(3.1 \pm 0.6) \times 10^{4}$	$(5.4 \pm 0.1) \times 10^{4}$
k_d (s^{-1})	$(1.0 \pm 0.1) \times 10^{-3}$	$(5.6 \pm 0.9) \times 10^{-4}$
K_D (nM)	33	10
Chi^2	1.3	1.0
n	≥ 1.2	

Supplementary Table 12

compoud **5**		RNA SEQUENCE
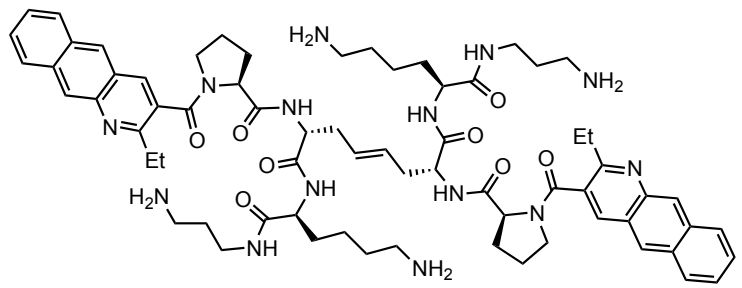		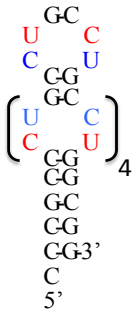 **(CCUG)10**
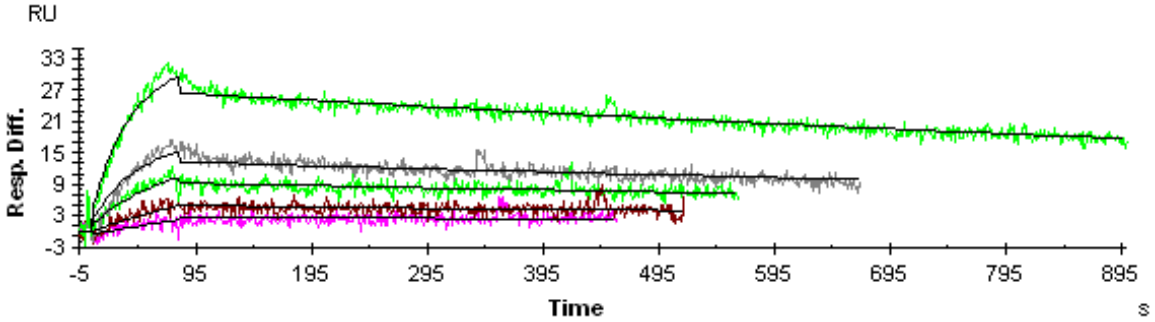		
	Trial-1	Trial-2
k_a ($M^{-1}s^{-1}$)	$(2.9 \pm 0.4) \times 10^{4}$	$(4.1 \pm 0.6) \times 10^{4}$
k_d (s^{-1})	$(4.9 \pm 0.2) \times 10^{-4}$	$(5.5 \pm 0.7) \times 10^{-3}$
K_D (nM)	17	13
Chi^2	1.5	1.1
n	ND	

Supplementary Table 13

compound **5**	RNA SEQUENCE
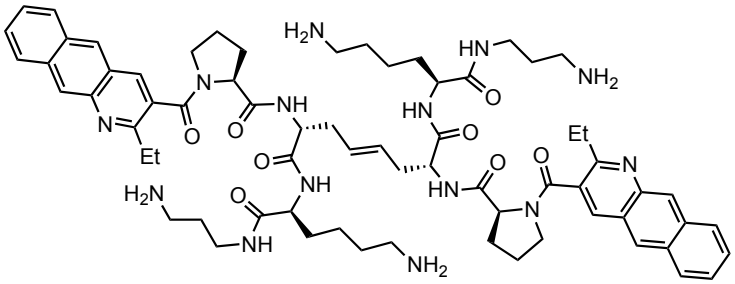	G-C A A C-G G-C A A C-G C-G 4 G-C C-G C-G-3' C 5' **(CAG)10**
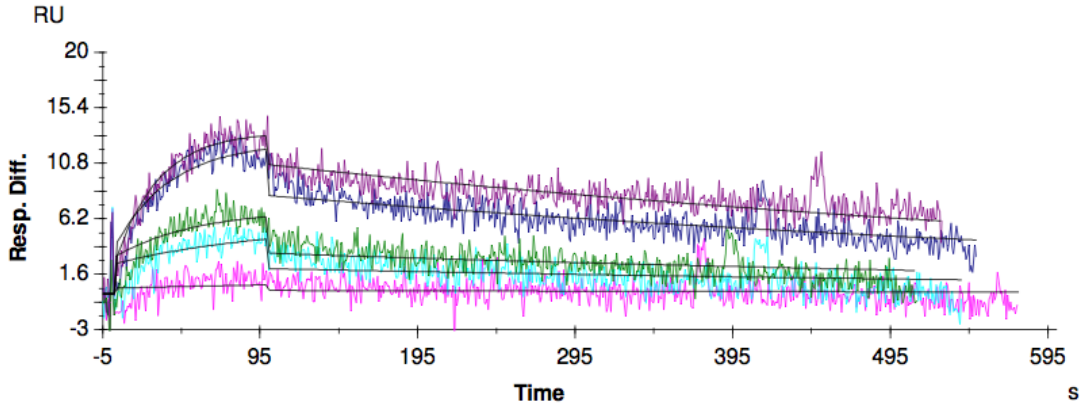	

	Trial-1	Trial-2
k_a ($M^{-1}s^{-1}$)	4.4 ± 0.7) × 10^{4}	(3.0 ± 0.7) × 10^{4}
k_d (s^{-1})	(2.8 ± 0.3) × 10^{-3}	(1.4 ± 0.2) × 10^{-3}
K_D (nM)	66	45
Chi^2	0.9	1.2
n	ND	

Supplementary Table 14

compound **5**	RNA SEQUENCE
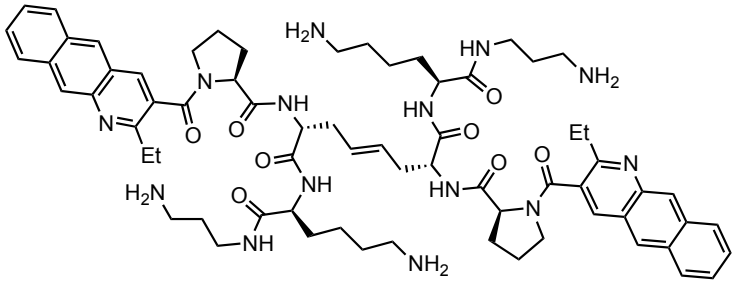	G-C U A C-G (G-C U-A C-G)$_4$ C-G G-C C-G C-G-3' C 5' **Duplex**
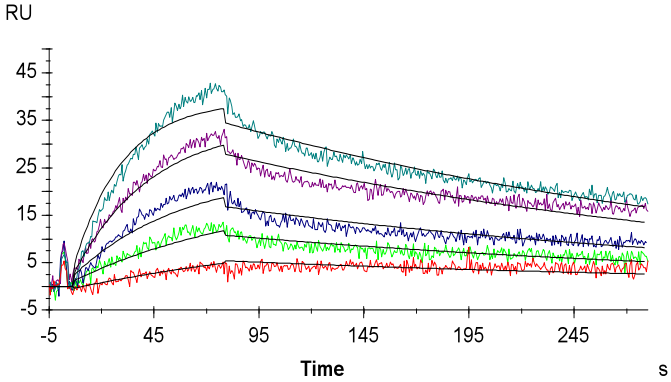	

	Trial-1	Trial-2
k_a ($M^{-1}s^{-1}$)	$(8.62 \pm 0.01) \times 10^{3}$	$(2.13 \pm 0.03) \times 10^{4}$
k_d (s^{-1})	$3.68 \pm 0.02) \times 10^{-3}$	$(4.00 \pm 0.06) \times 10^{-3}$
K_D (nM)	427	188
Chi^2	2.5	1.8
n	ND	

Supplementary Table 15

compond **5**	RNA SEQUENCE
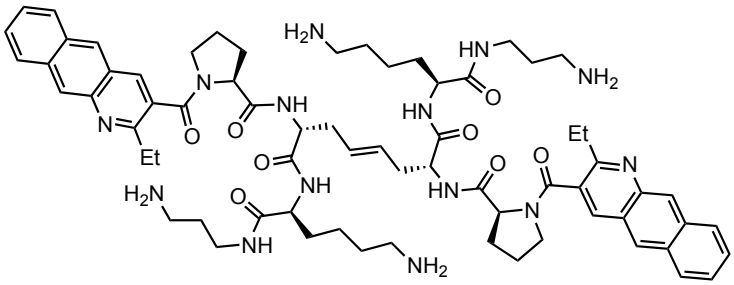	C-A A A C-G C-G C-G U-A U-A C-G C-G G-C G-C 3' 5' **HIV-1FSS**

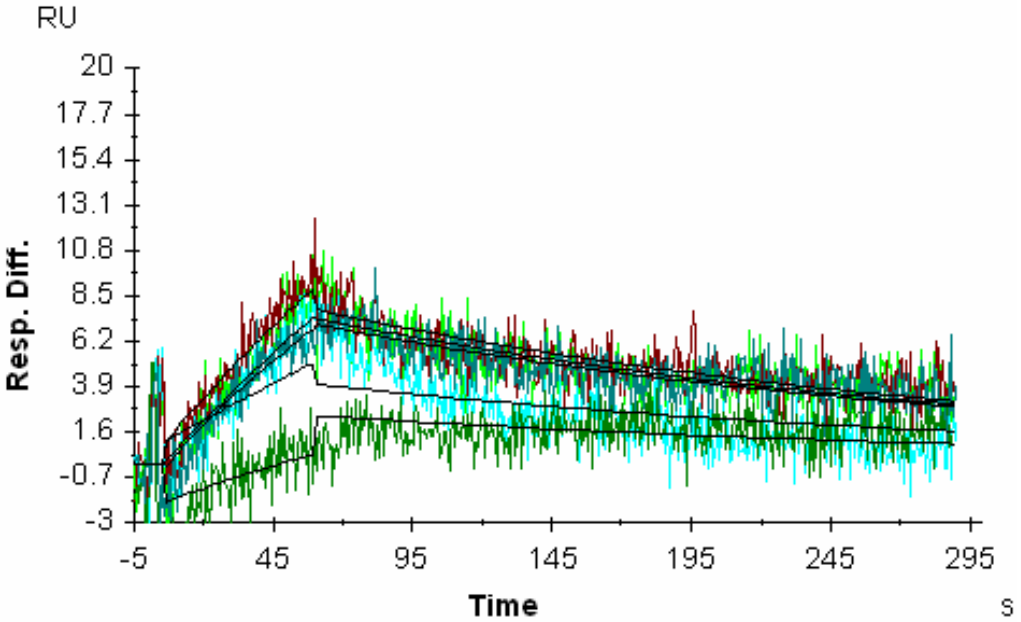

	Trial-1	Trial-2
k_a ($M^{-1}s^{-1}$)	$(5.44 \pm 0.04) \times 10^{3}$	$(4.9 \pm 0.9) \times 10^{3}$
k_d (s^{-1})	$3.93 \pm 0.06) \times 10^{-3}$	$(3.92 \pm 0.06) \times 10^{-3}$
K_D (nM)	723	795
Chi^2	1.8	1.4
n	ND	

Supplementary Table 16

compound **6**	RNA SEQUENCE
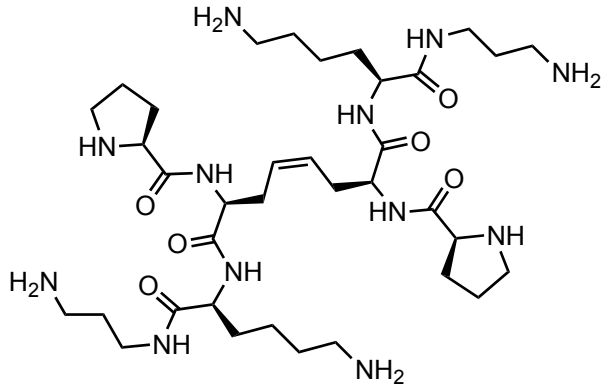	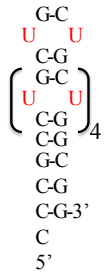 **(CUG)10**
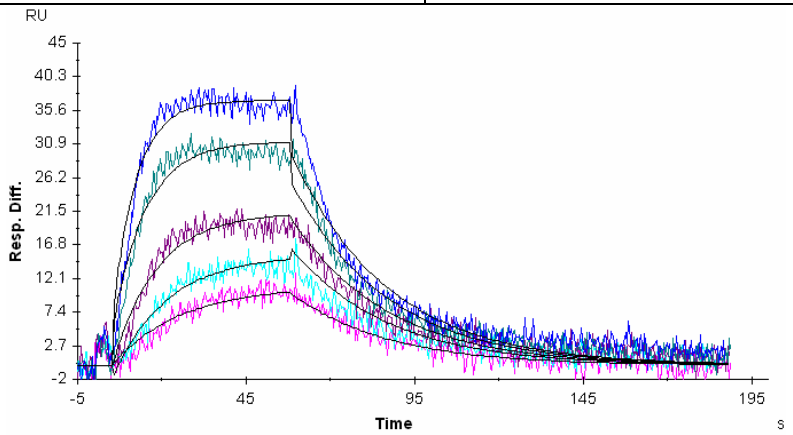	
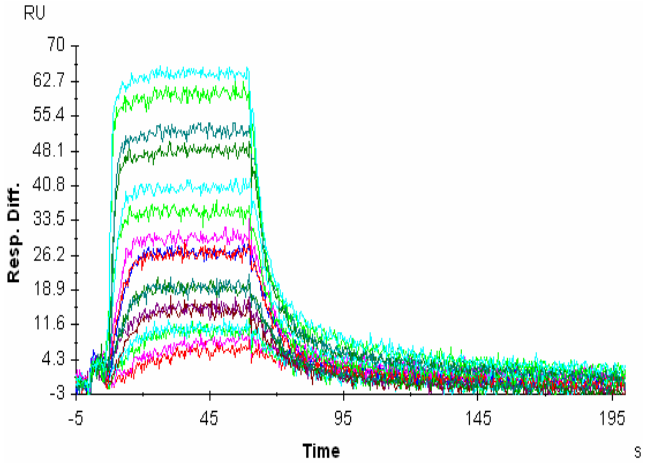 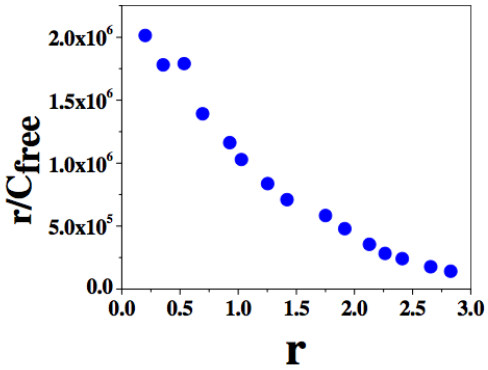	

	Trial-1	Trial-2
k_a ($M^{-1}s^{-1}$)	$(1.35 \pm 0.03) \times 10^{5}$	$(1.29 \pm 0.03) \times 10^{5}$
k_d (s^{-1})	$(3.54 \pm 0.03) \times 10^{-2}$	$(3.41 \pm 0.03) \times 10^{-2}$
K_D (nM)	263	263
Chi^2	2.2	2.3
n	≥ 3	

Supplementary Table 17

compound **6**	RNA SEQUENCE
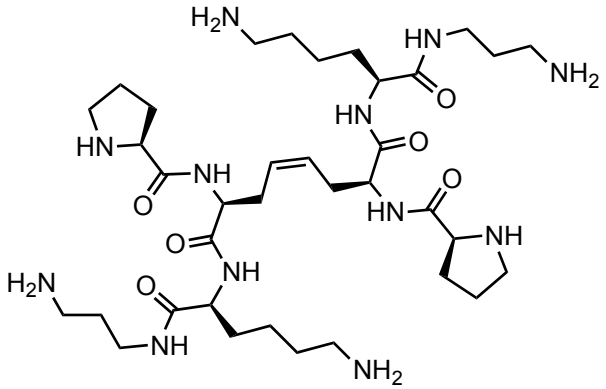	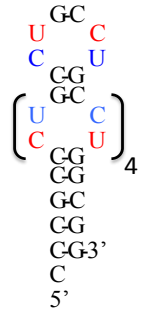 **(CCUG)10**

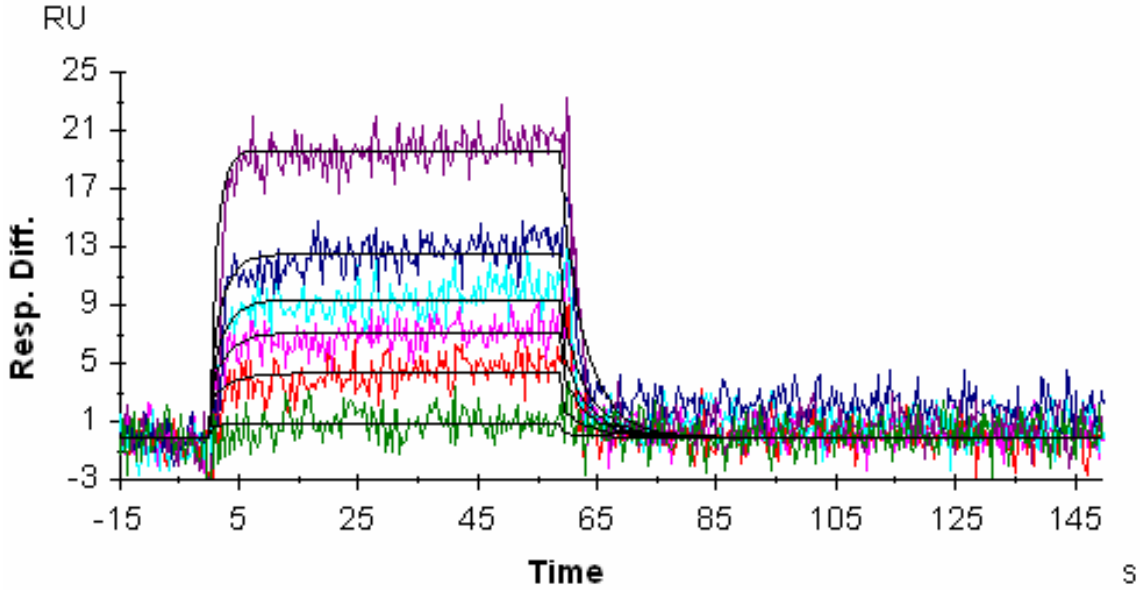

	Trial-1	Trial-2
k_a ($M^{-1}s^{-1}$)	$(1.6 \pm 0.2) \times 10^{4}$	$(1.2 \pm 0.1) \times 10^{4}$
k_d (s^{-1})	$(3.5 \pm 0.1) \times 10^{-1}$	$(2.4 \pm 0.8) \times 10^{-1}$
K_D (nM)	22600	21200
Chi^2	1.5	1.5
n	ND	

Supplementary Table 18

compound **6**	RNA SEQUENCE
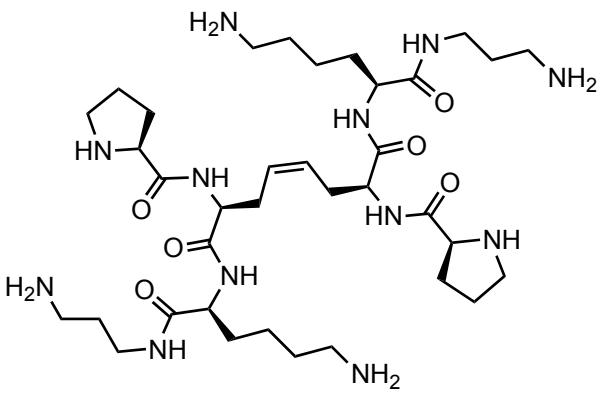	G-C A A C-G G-C (A A C-G) C-G 4 G-C C-G C-G-3' C 5' **(CAG)10**

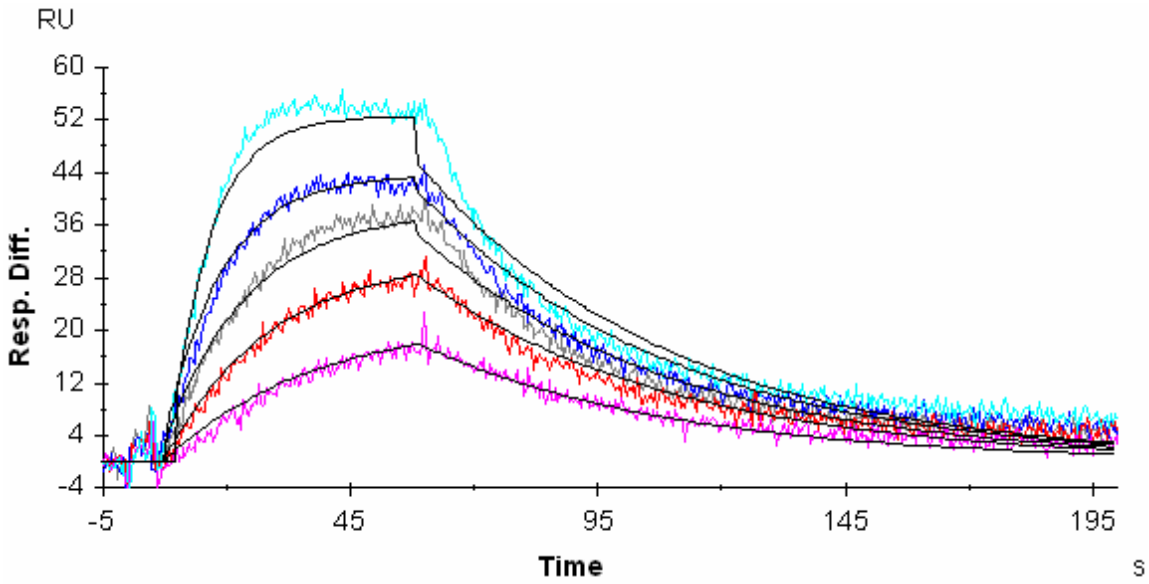

	Trial-1	Trial-2
k_a ($M^{-1}s^{-1}$)	$(1.35 \pm 0.01) \times 10^{5}$	$(1.0 \pm 0.1) \times 10^{5}$
k_d (s^{-1})	$(1.96 \pm 0.07) \times 10^{-2}$	$(1.84 \pm 0.01) \times 10^{-2}$
K_D (nM)	145	176
Chi^2	4.1	4.6
n	ND	

Supplementary Table 19

compound **6**	RNA SEQUENCE
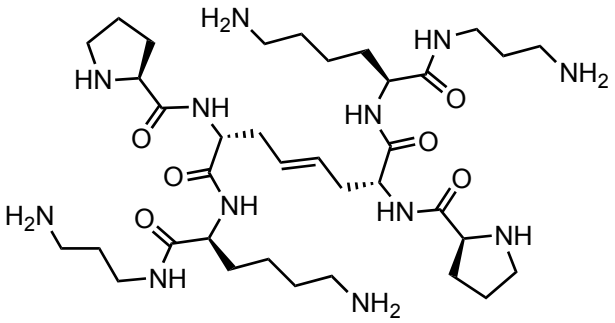	G-C U A C-G (G-C U-A C-G)$_4$ C-G G-C C-G C-G-3' C 5' **Duplex**
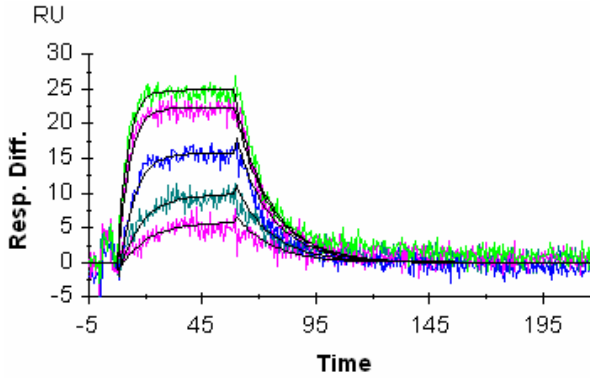	
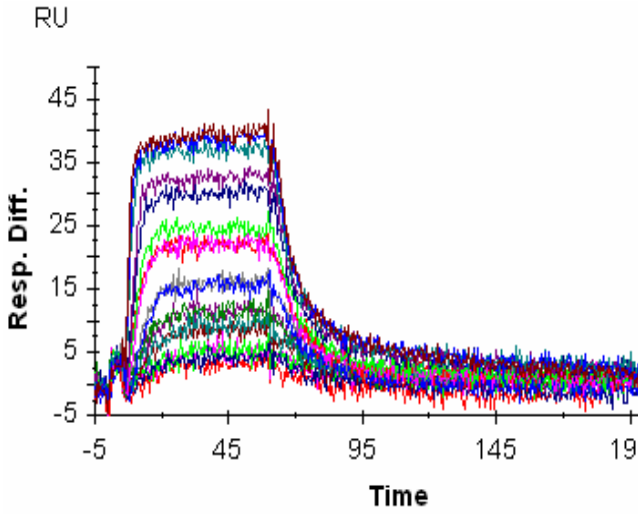 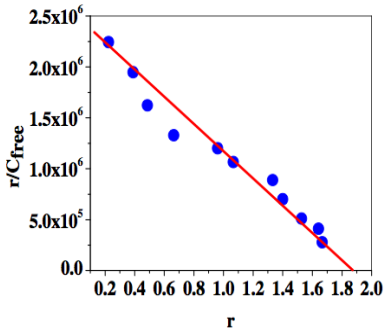	

	Trial-1	Trial-2
k_a ($M^{-1}s^{-1}$)	$(1.54 \pm 0.05) \times 10^{5}$	$(1.82 \pm 0.04) \times 10^{5}$
k_d (s^{-1})	$(5.01 \pm 0.06) \times 10^{-2}$	$(6.32 \pm 0.07) \times 10^{-2}$
K_D (nM)	325	348
Chi^2	1.4	1.5
n	2	

Supplementary Table 20

compound **6**	RNA SEQUENCE
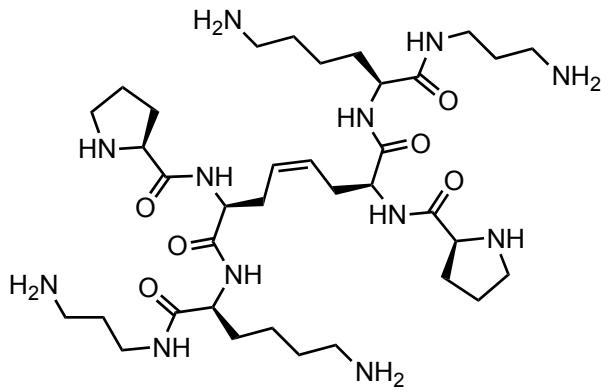	C-A A A C-G C-G C-G U-A U-A C-G C-G G-C G-C 3' 5' **HIV-1FSS**

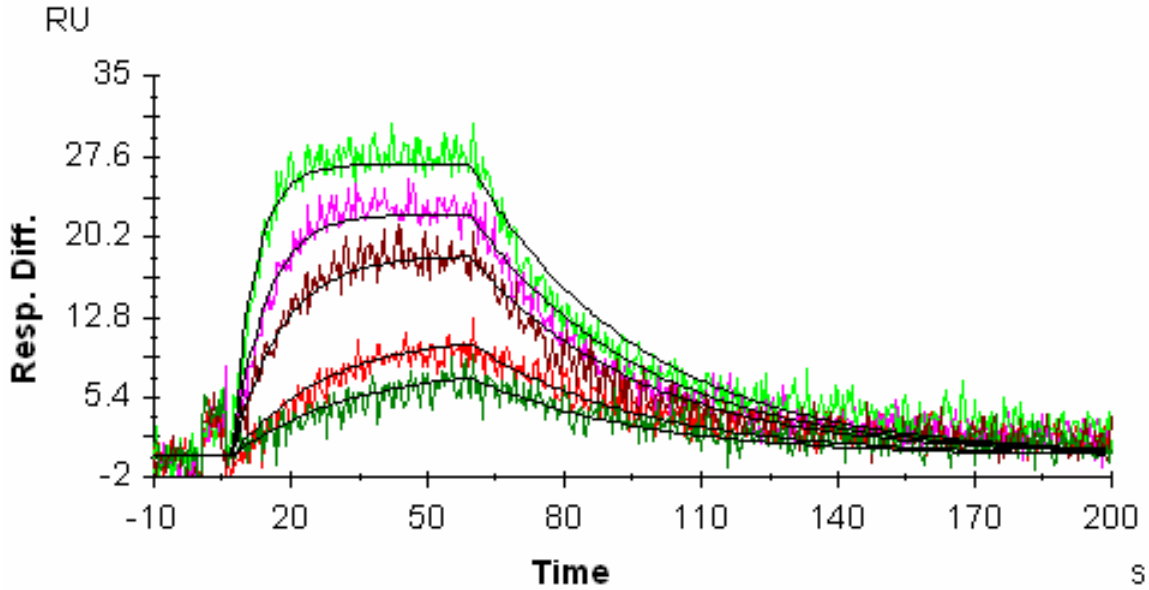

	Trial-1	Trial-2
k_a ($M^{-1}s^{-1}$)	$(2.29 \pm 0.05) \times 10^{5}$	$(2.12 \pm 0.04) \times 10^{5}$
k_d (s^{-1})	$(2.68 \pm 0.05) \times 10^{-2}$	$(2.45 \pm 0.02) \times 10^{-2}$
K_D (nM)	117	115
Chi^2	2.2	1.6
n	ND	

Supplementary Table 21

compound 7	RNA SEQUENCE
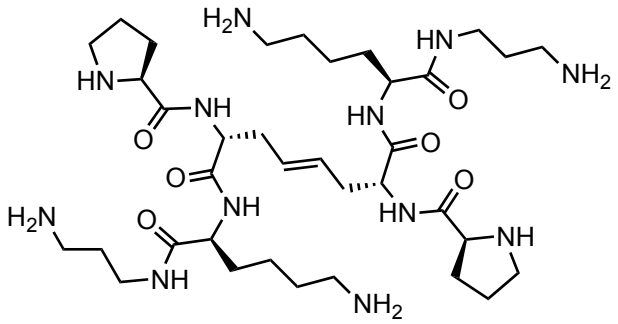	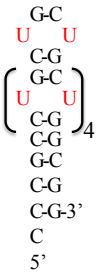 **(CUG)10**

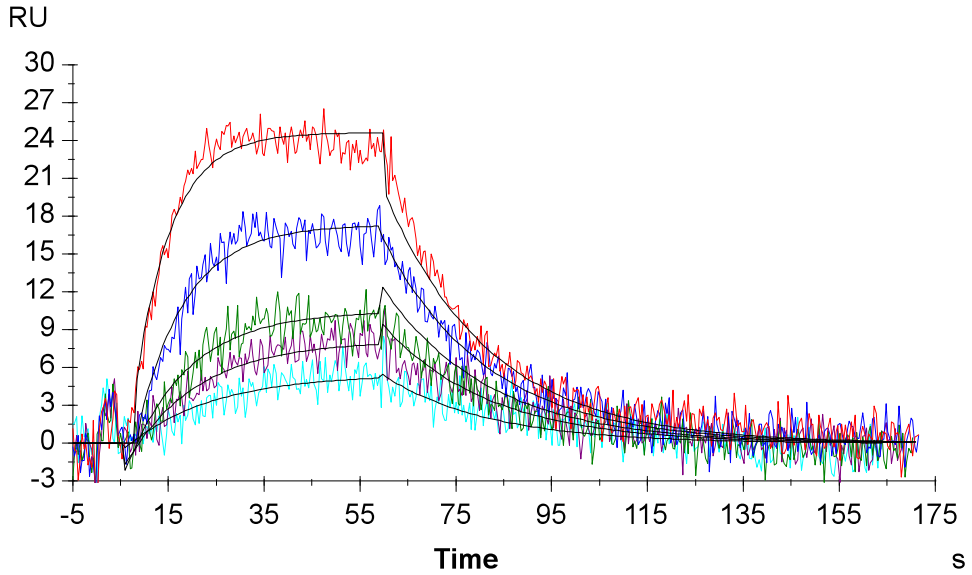

	Trial-1	Trial-2
k_a ($M^{-1}s^{-1}$)	$(1.08 \pm 0.03) \times 10^{5}$	$(1.09 \pm 0.03) \times 10^{5}$
k_d (s^{-1})	$(4.54 \pm 0.05) \times 10^{-2}$	$(4.61 \pm 0.05) \times 10^{-2}$
K_D (nM)	421	423
Chi^2	1.5	1.4
n	ND	

Supplementary Table 22

compound **7**	RNA SEQUENCE
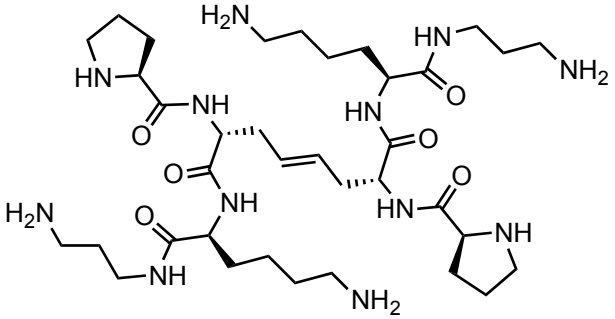	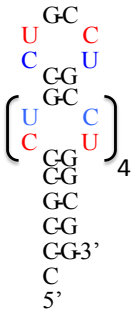 **(CCUG)10**
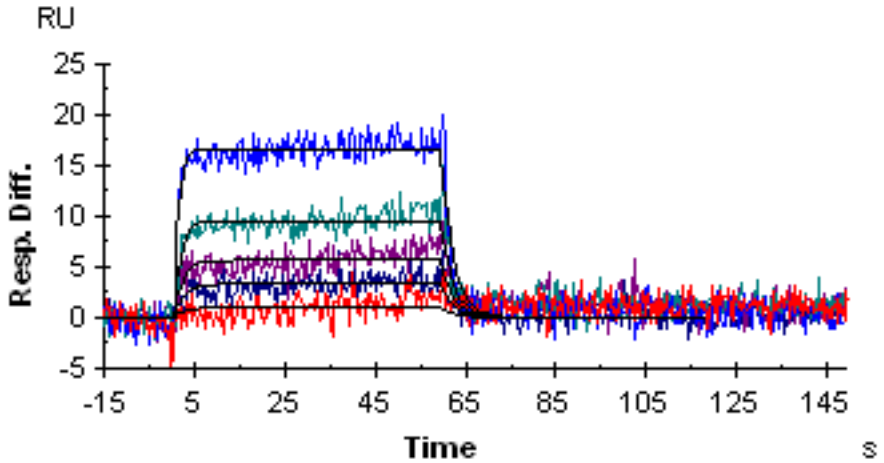	

	Trial-1	Trial-2
k_a ($M^{-1}s^{-1}$)	$(1.27 \pm 0.1) \times 10^{4}$	$(1.34 \pm 0.7) \times 10^{4}$
k_d (s^{-1})	$(3.93 \pm 0.1) \times 10^{-1}$	$(5.51 \pm 0.01) \times 10^{-1}$
K_D (nM)	31100	41100
Chi^2	1.5	1.4
n	ND	

Supplementary Table 23

compound **7**	RNA SEQUENCE
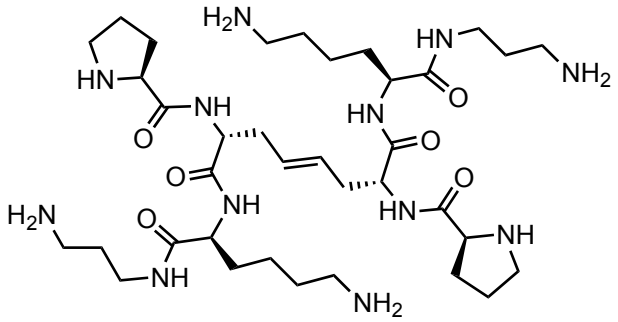	G-C A A C-G G-C A A C-G C-G 4 G-C C-G C-G-3' C 5' **(CAG)10**

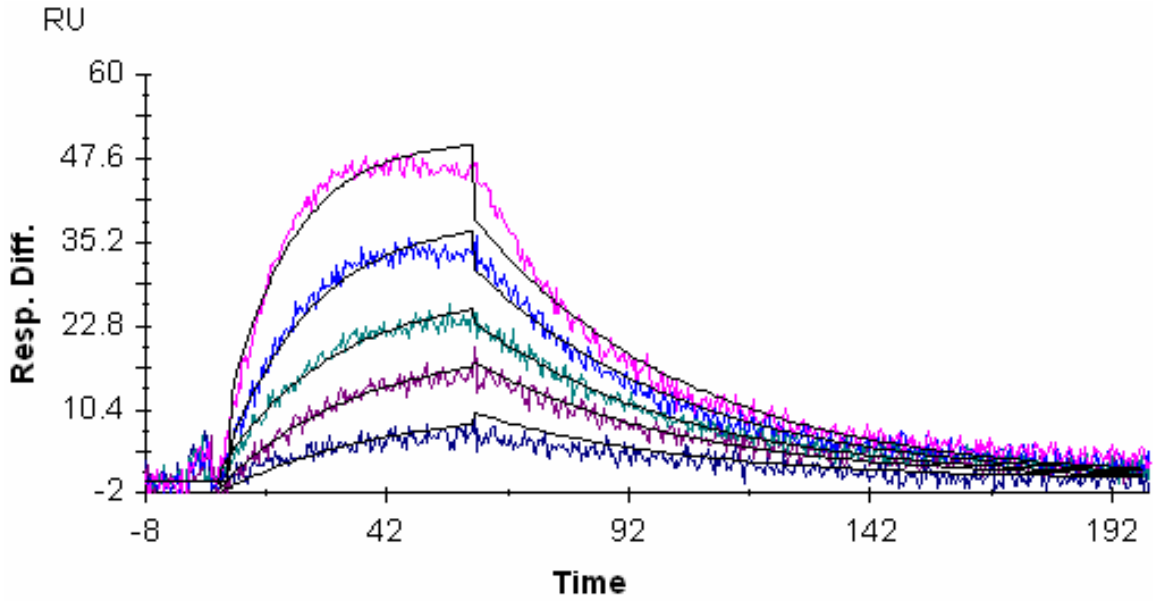

	Trial-1	Trial-2
k_a ($M^{-1}s^{-1}$)	$(6.5 \pm 0.9) \times 10^{4}$	$(8.6 \pm 0.1) \times 10^{4}$
k_d (s^{-1})	$(2.29 \pm 0.01) \times 10^{-2}$	$(2.34 \pm 0.01) \times 10^{-2}$
K_D (nM)	352	273
Chi^2	2.0	2.4
n	ND	

Supplementary Table 24

compound **7**	RNA SEQUENCE
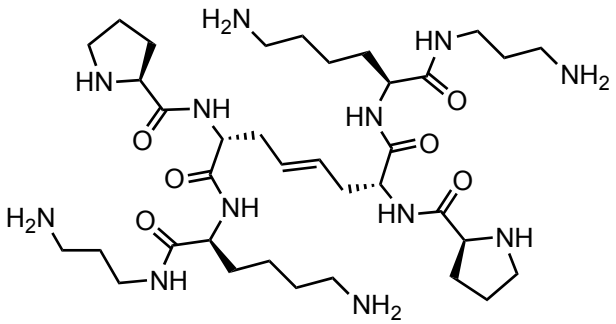	C-A A A C-G C-G C-G U-A U-A C-G C-G G-C G-C 3' 5' **HIV-1FSS**
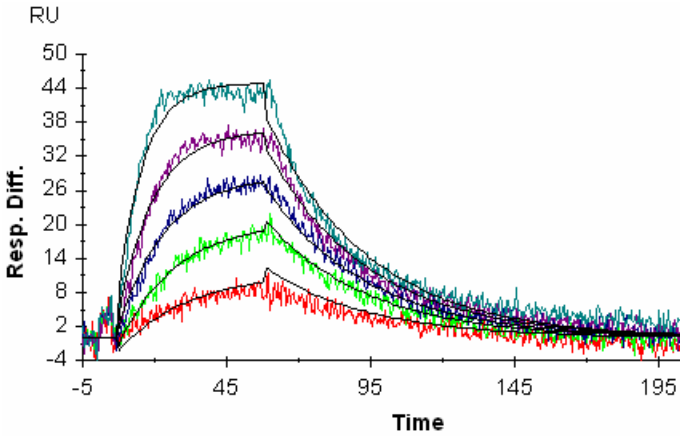	
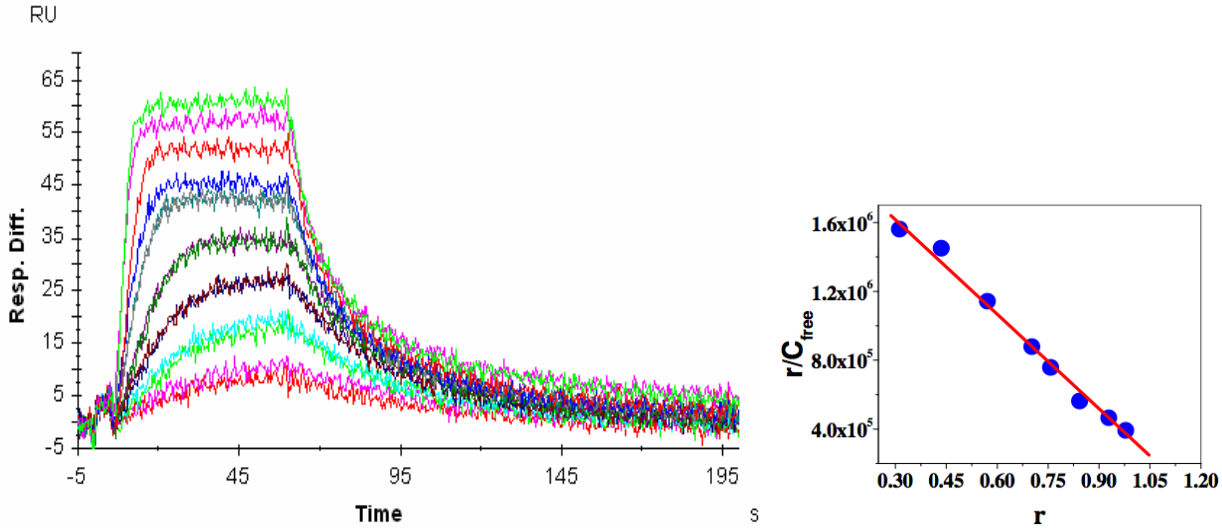	

	Trial-1	Trial-2
k_a ($M^{-1}s^{-1}$)	$(6.9 \pm 0.6) \times 10^{4}$	$(6.26 \pm 0.7) \times 10^{4}$
k_d (s^{-1})	$(2.07 \pm 0.06) \times 10^{-2}$	$(1.90 \pm 0.08) \times 10^{-2}$
K_D (nM)	302	303
Chi^2	2.2	2.1
n	1	

Supplementary Table 25

compound **8**	RNA SEQUENCE
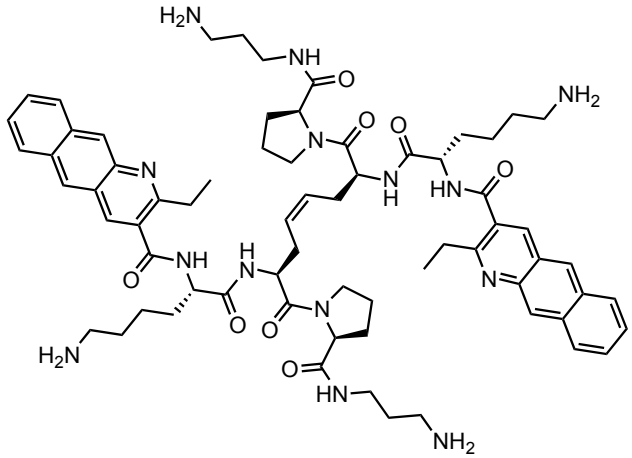	G-C U U C-G G-C U U C-G C-G G-C C-G C-G-3' C 5' $(CUG)_4$ **(CUG)10**

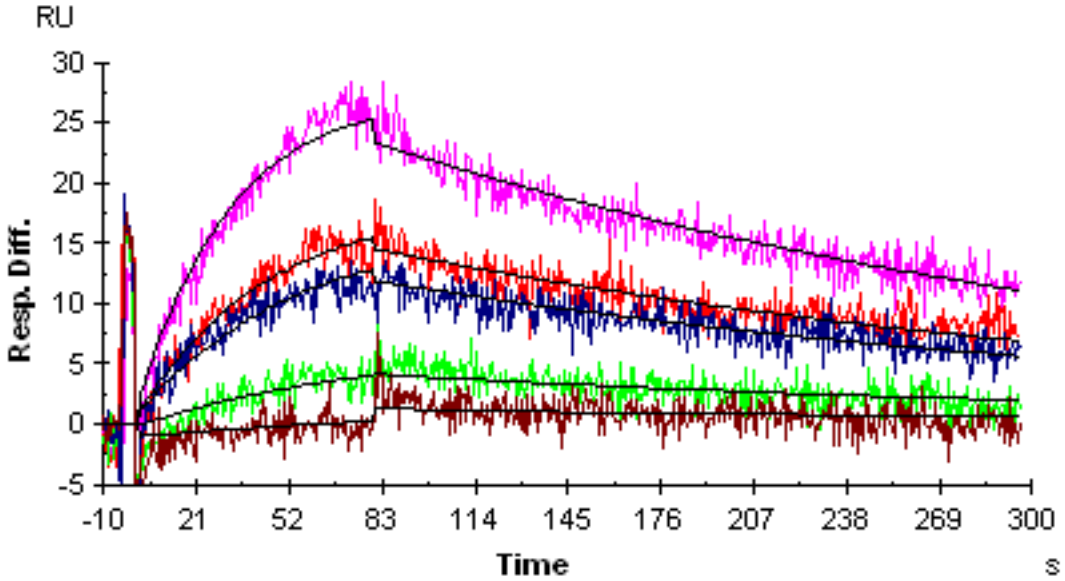

	Trial-1	Trial-2
k_a ($M^{-1}s^{-1}$)	$(2.0 \pm 0.3) \times 10^{4}$	$(2.8 \pm 0.5) \times 10^{4}$
k_d (s^{-1})	$(3.45 \pm 0.03) \times 10^{-3}$	$(2.58 \pm 0.05) \times 10^{-3}$
K_D (nM)	175	91.8
Chi^2	1.5	1.7
n	ND	

Supplementary Table 26

compound **8**	RNA SEQUENCE
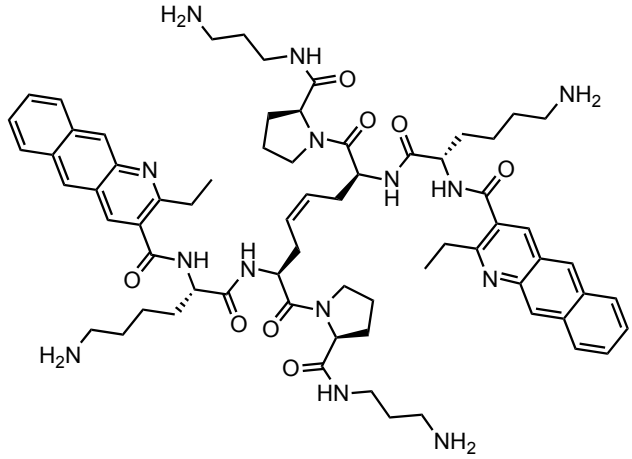	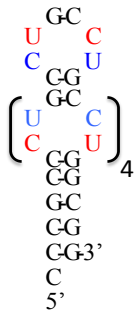 **(CCUG)10**

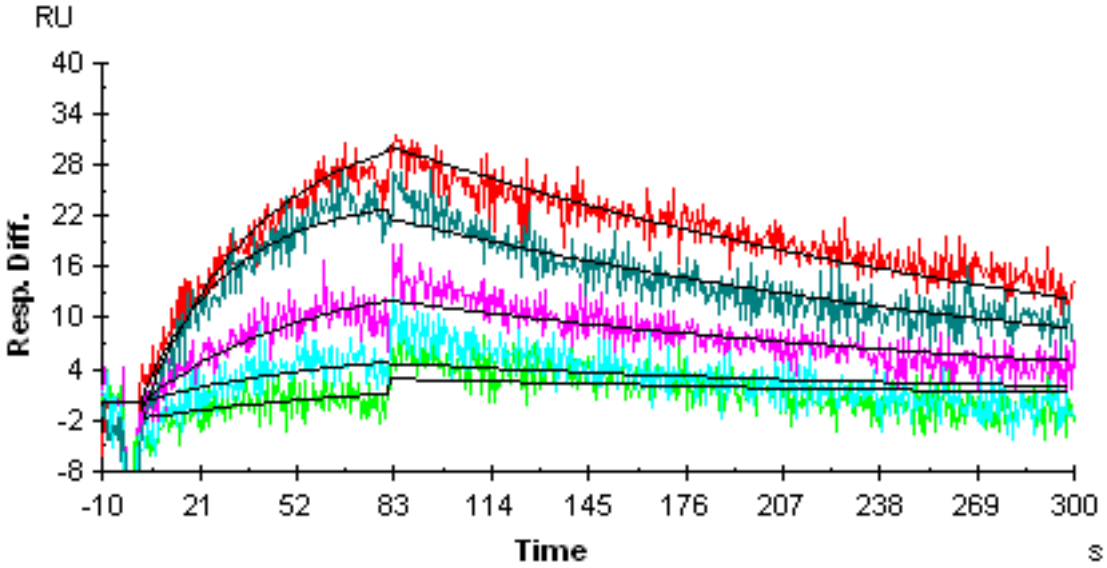

	Trial-1	Trial-2
k_a ($M^{-1}s^{-1}$)	$(1.51 \pm 0.7) \times 10^{4}$	$(1.57 \pm 0.7) \times 10^{4}$
k_d (s^{-1})	$(4.16 \pm 0.04) \times 10^{-3}$	$(4.90 \pm 0.04) \times 10^{-3}$
K_D (nM)	275	313
Chi^2	4.7	4.5
n	ND	

Supplementary Table 27

compound **8**	RNA SEQUENCE
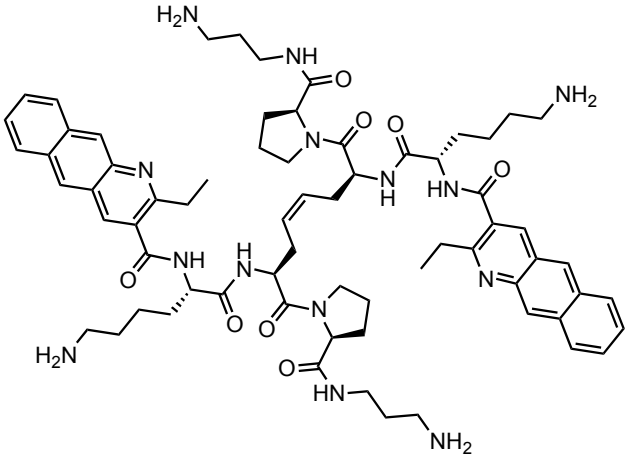	G-C A A C-G G-C (A A) C-G C-G 4 G-C C-G C-G-3' C 5' **(CAG)10**

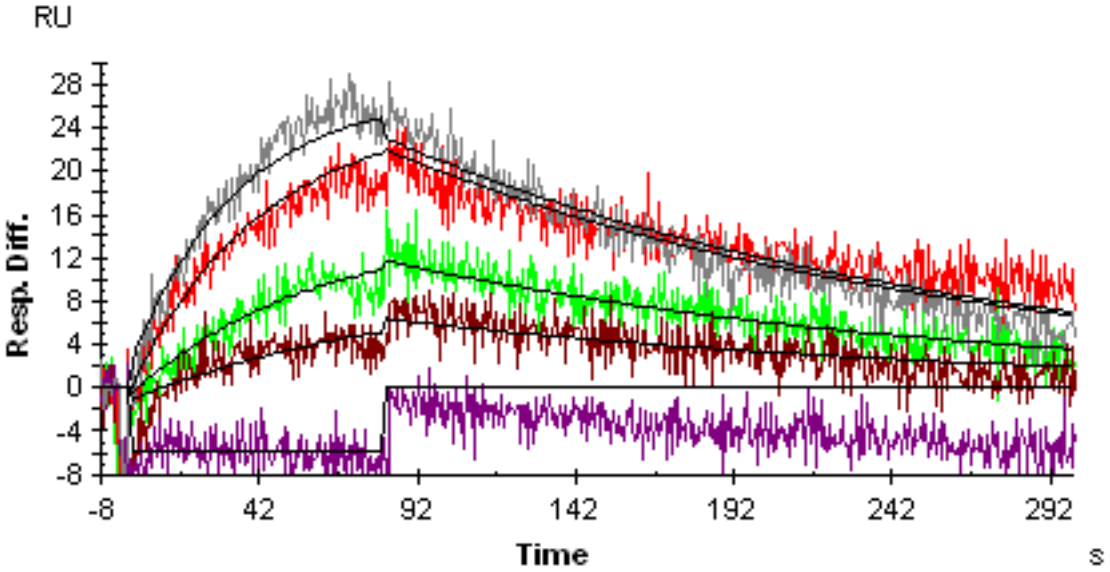

	Trial-1	Trial-2
k_a ($M^{-1}s^{-1}$)	$(1.3 \pm 0.4) \times 10^{4}$	$(1.23 \pm 0.04) \times 10^{4}$
k_d (s^{-1})	$(6.36 \pm 0.05) \times 10^{-3}$	$(5.49 \pm 0.03) \times 10^{-3}$
K_D (nM)	504	445
Chi^2	4.5	5.5
n	ND	

Supplementary Table 28

compound **8**	RNA SEQUENCE
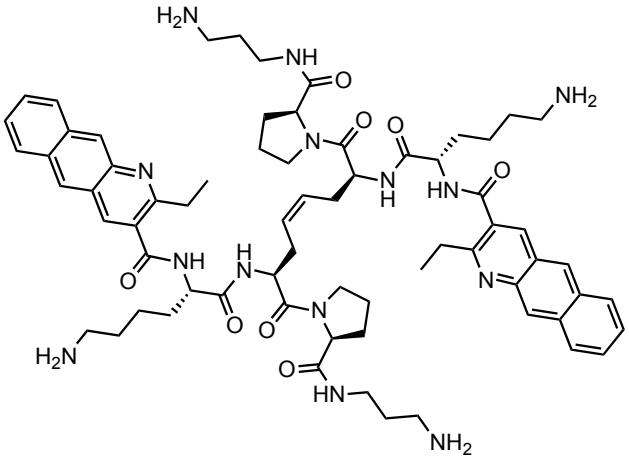	G-C U A C-G (G-C U-A C-G)$_4$ C-G G-C C-G C-G-3' C 5' **Duplex**
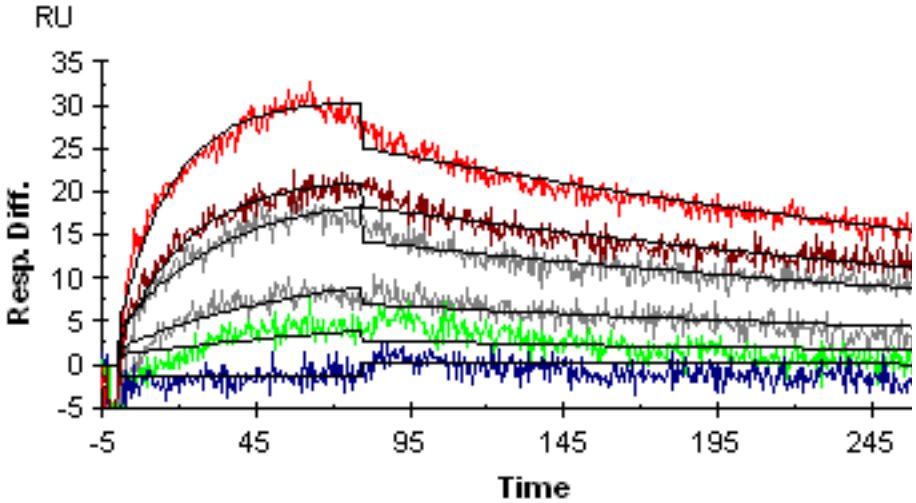	

	Trial-1	Trial-2
k_a ($M^{-1}s^{-1}$)	$(2.7 \pm 0.6) \times 10^{4}$	$(3.1 \pm 0.7) \times 10^{4}$
k_d (s^{-1})	$(2.71 \pm 0.03) \times 10^{-3}$	$(2.71 \pm 0.03) \times 10^{-3}$
K_D (nM)	99.9	87.8
Chi^2	1.9	2.6
n	ND	

Supplementary Table 29

compound **9**	RNA SEQUENCE
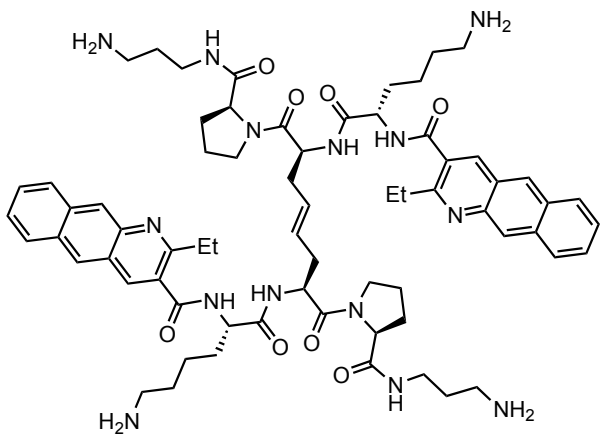	G-C U U C-G G-C U U C-G C-G G-C C-G C-G-3' C 5' **(CUG)10**

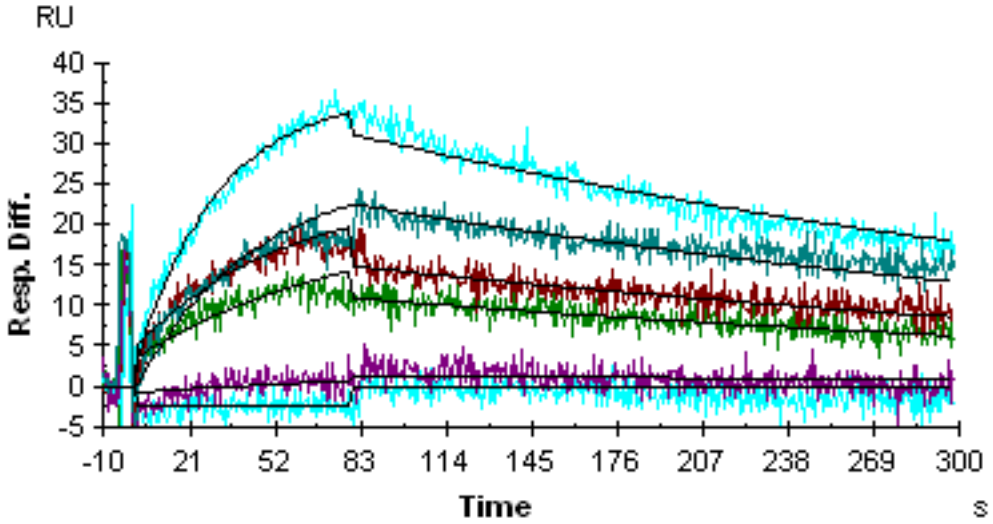

	Trial-1	Trial-2
k_a ($M^{-1}s^{-1}$)	$(2.40 \pm 0.5) \times 10^{4}$	$(2.1 \pm 0.5) \times 10^{4}$
k_d (s^{-1})	$(2.85 \pm 0.03) \times 10^{-3}$	$(2.55 \pm 0.02) \times 10^{-3}$
K_D (nM)	118	123
Chi^2	2.1	2.2
n	ND	

Supplementary Table 30

compound **9**	RNA SEQUENCE
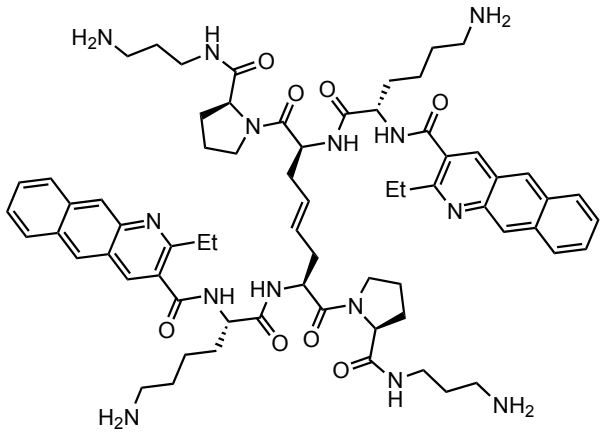	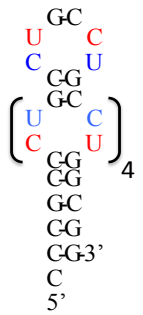 **(CCUG)10**

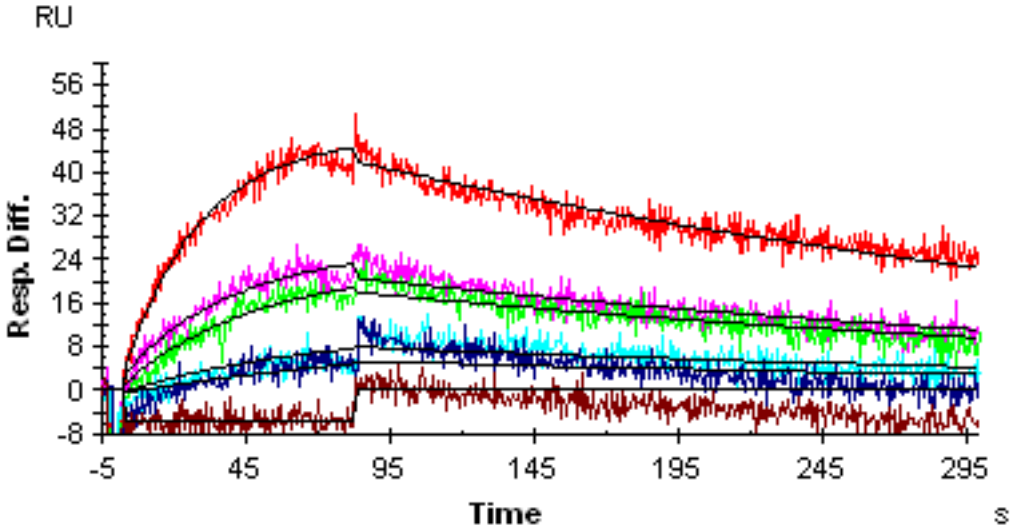

	Trial-1	Trial-2
k_a ($M^{-1}s^{-1}$)	$(2.32 \pm 0.5) \times 10^{4}$	$(1.66 \pm 0.2) \times 10^{4}$
k_d (s^{-1})	$(2.88 \pm 0.02) \times 10^{-3}$	$(2.53 \pm 0.02) \times 10^{-3}$
K_D (nM)	124	152
Chi^2	6.3	1.9
n	ND	

Supplementary Table 31

compound **9**	RNA SEQUENCE
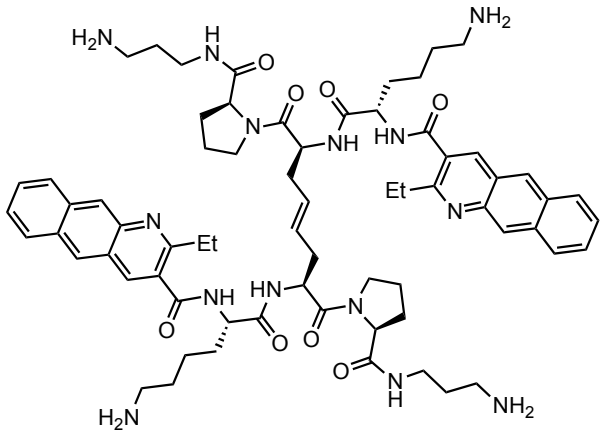	G-C A A C-G G-C A A C-G C-G 4 G-C C-G C-G-3' C 5' **(CAG)10**
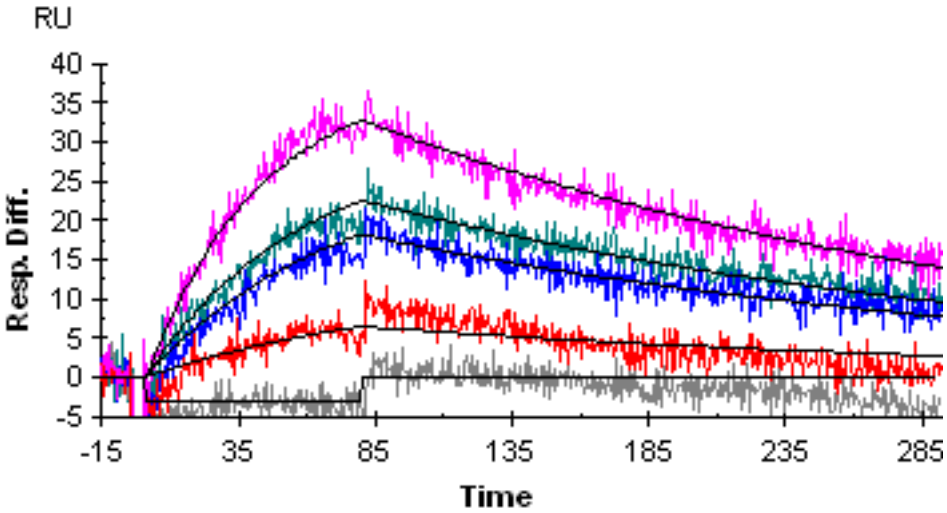	

	Trial-1	Trial-2
k_a ($M^{-1}s^{-1}$)	$(1.4 \pm 0.1) \times 10^{4}$	$(1.78 \pm 0.4) \times 10^{4}$
k_d (s^{-1})	$(4.03 \pm 0.02) \times 10^{-3}$	$(4.0 \pm 0.1) \times 10^{-3}$
K_D (nM)	298	228
Chi^2	3.2	7.2
n	ND	

Supplementary Table 32

compound **9**	RNA SEQUENCE
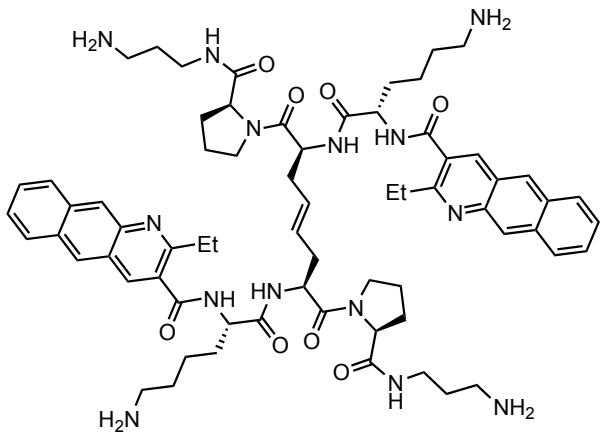	G-C U A C-G (G-C U-A C-G)$_4$ C-G G-C C-G C-G-3' C 5' **Duplex**

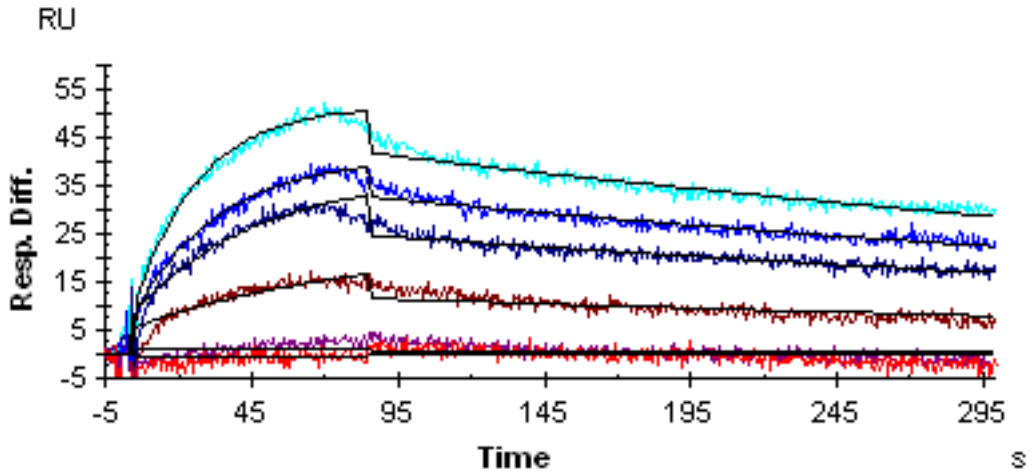

	Trial-1	Trial-2
k_a ($M^{-1}s^{-1}$)	$(2.7 \pm 0.6) \times 10^{4}$	$(2.1 \pm 0.2) \times 10^{4}$
k_d (s^{-1})	$1.92 \pm 0.02) \times 10^{-3}$	$(1.79 \pm 0.01) \times 10^{-3}$
K_D (nM)	70.6	80.3
Chi^2	1.7	1.8
n	ND	

Supplementary Table 33

compound **9**	RNA SEQUENCE
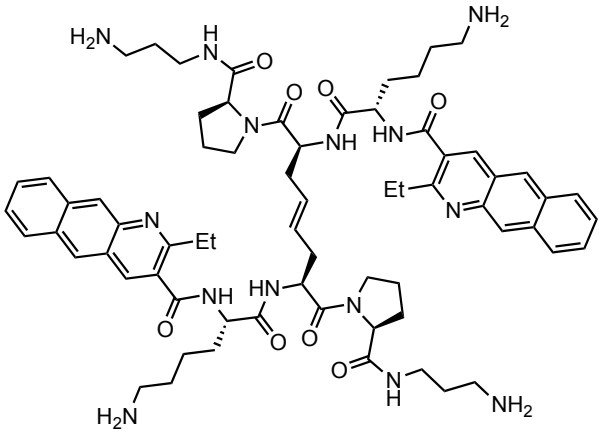	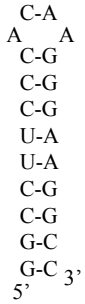 **HIV-1FSS**

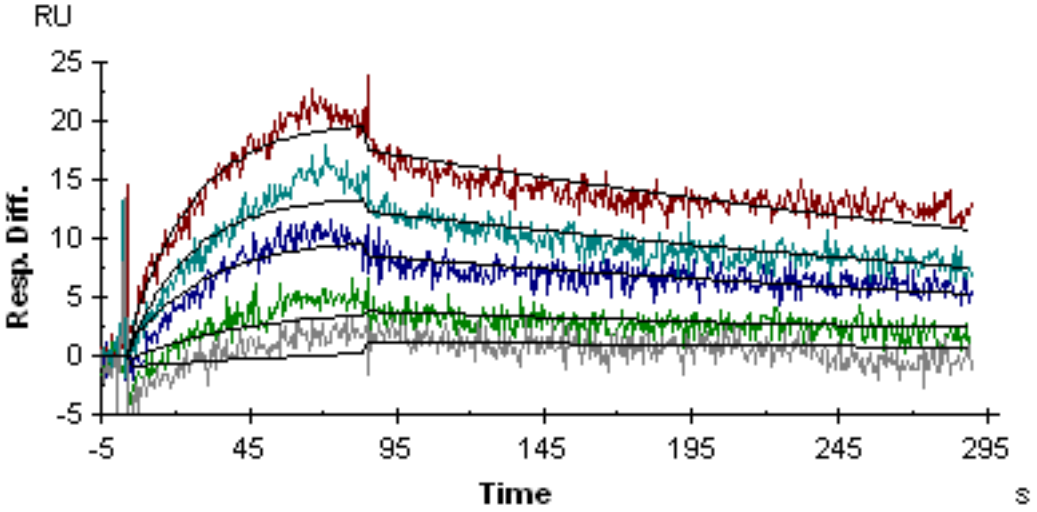

	Trial-1	Trial-2
k_a ($M^{-1}s^{-1}$)	$(2.0 \pm 0.5) \times 10^{4}$	$(4.48 \pm 0.7) \times 10^{4}$
k_d (s^{-1})	$1.59 \pm 0.03) \times 10^{-3}$	$(2.41 \pm 0.03) \times 10^{-3}$
K_D (nM)	80.4	53.9
Chi^2	1.1	1.4
n	ND	

Supplementary Table 34

compound **10**	RNA SEQUENCE
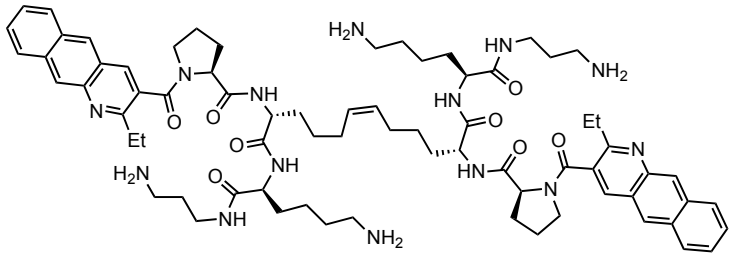	G-C U U C-G G-C U U C-G C-G G-C C-G C-G-3' C 5' (CUG)10

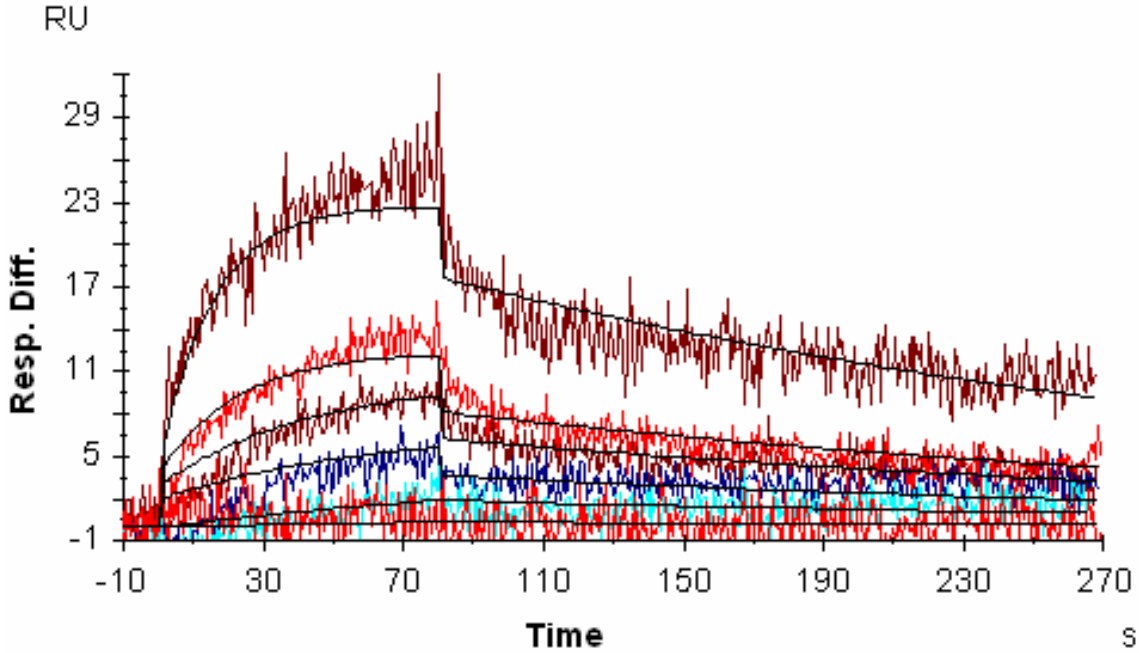

	Trial-1	Trial-2
k_a ($M^{-1}s^{-1}$)	$(4.2 \pm 0.9) \times 10^{4}$	$(4.7 \pm 0.9) \times 10^{4}$
k_d (s^{-1})	$(3.51 \pm 0.01) \times 10^{-3}$	$(3.68 \pm 0.02) \times 10^{-3}$
K_D (nM)	84.4	78.7
Chi^2	1.9	1.7
n	ND	

Supplementary Table 35

compound **10**	RNA SEQUENCE
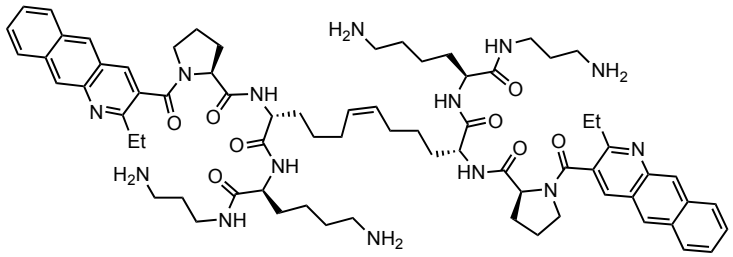	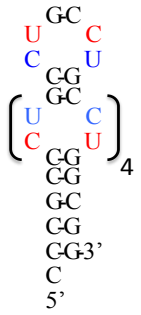 **(CCUG)10**

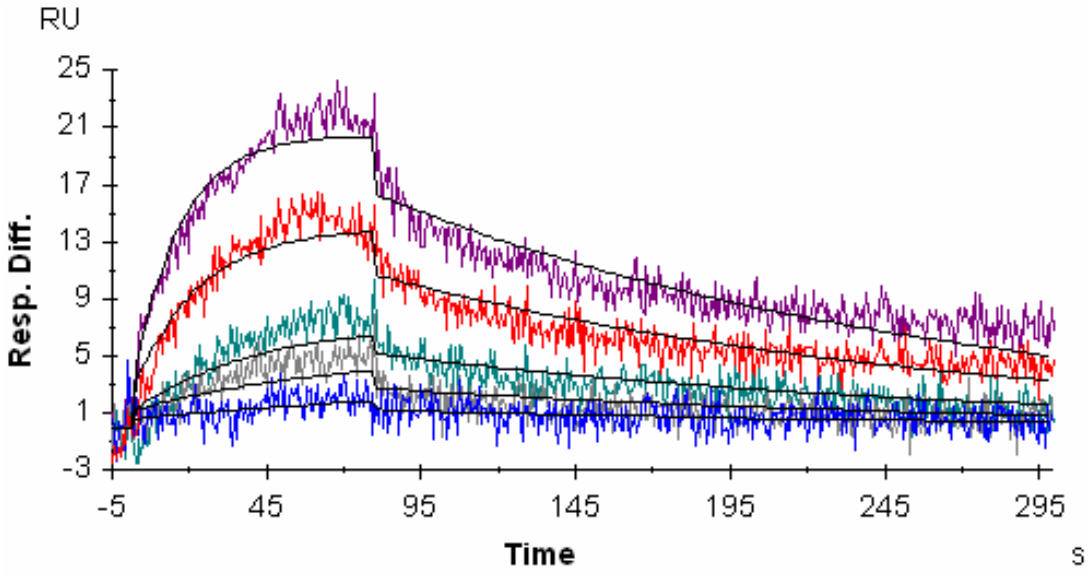

	Trial-1	Trial-2
k_a ($M^{-1}s^{-1}$)	$(2.0 \pm 0.4) \times 10^{4}$	$(1.8 \pm 0.4) \times 10^{4}$
k_d (s^{-1})	$(5.39 \pm 0.05) \times 10^{-3}$	$(5.29 \pm 0.04) \times 10^{-3}$
K_D (nM)	265	292
Chi^2	1.3	1.2
n	ND	

Supplementary Table 36

compound **11**	RNA SEQUENCE
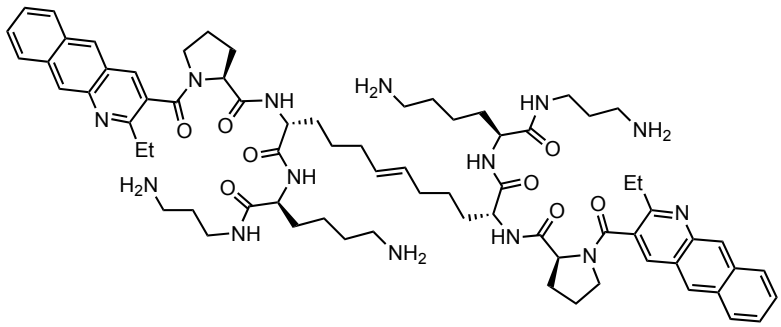	G-C U U C-G G-C (U U C-G)4 C-G G-C C-G C-G-3' C 5' **(CUG)10**
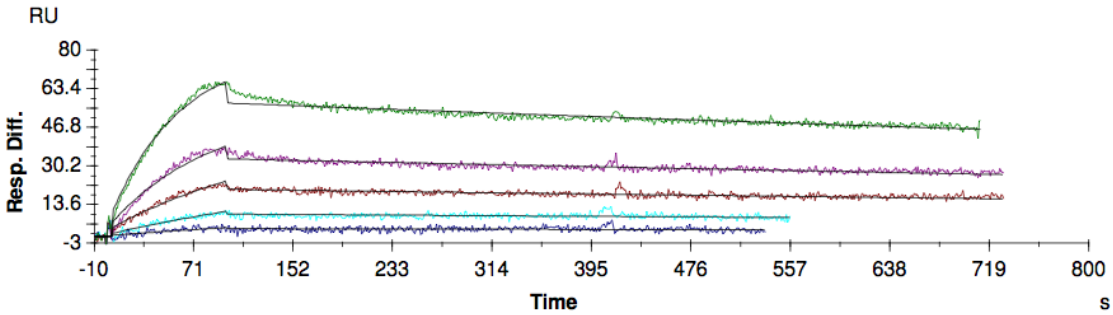	
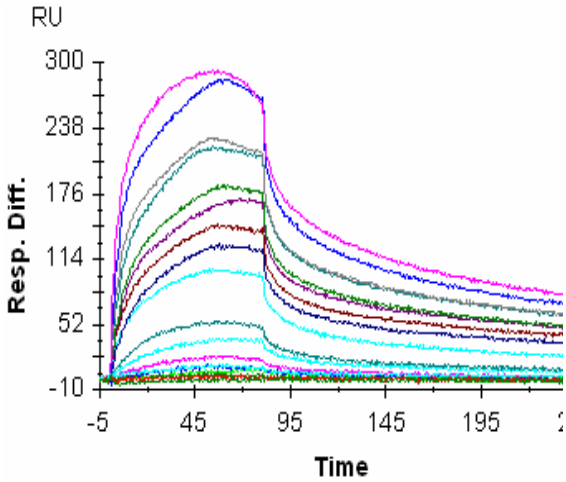 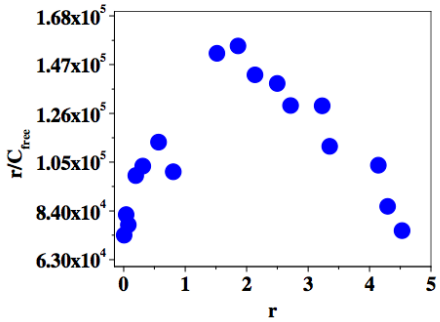	

	Trial-1	Trial-2
k_a ($M^{-1}s^{-1}$)	$(2.4 \pm 0.2) \times 10^{4}$	$(2.5 \pm 0.8) \times 10^{4}$
k_d (s^{-1})	$(3.6 \pm 0.2) \times 10^{-4}$	$(7.3 \pm 0.1) \times 10^{-4}$
K_D (nM)	16	29
Chi^2	1.3	1.6
n	5	

Supplementary Table 37

compound **11**	RNA SEQUENCE
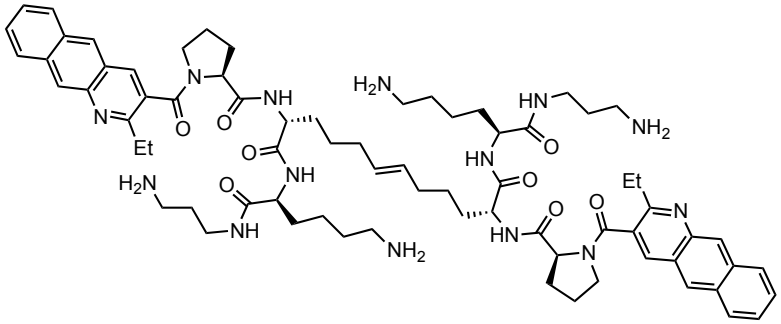	G-C U U C-G G-C U U C-G C-G G-C C-G C-G-3' C 5' **(CUG)4**
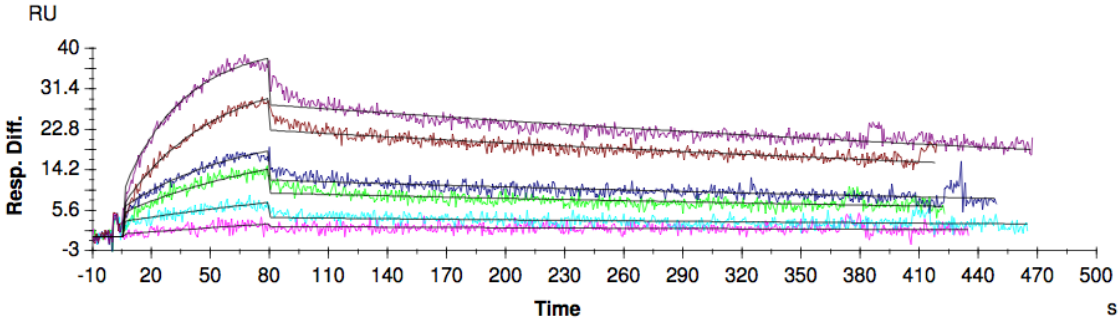	
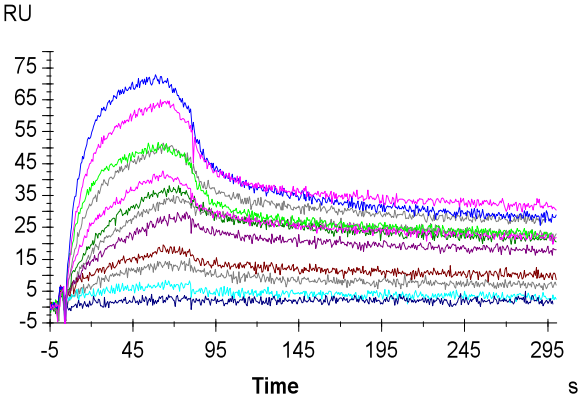 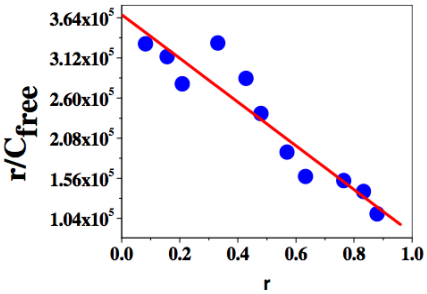	

	Trial-1	Trial-2
k_a ($M^{-1}s^{-1}$)	$(2.1 \pm 0.5) \times 10^{4}$	$(9.1 \pm 0.8) \times 10^{3}$
k_d (s^{-1})	$(1.1 \pm 0.7) \times 10^{-3}$	$(6.2 \pm 0.6) \times 10^{-4}$
K_D (nM)	51	69
Chi^2	1.0	1.8
n	1	

Supplementary Table 38

compound **11**	RNA SEQUENCE
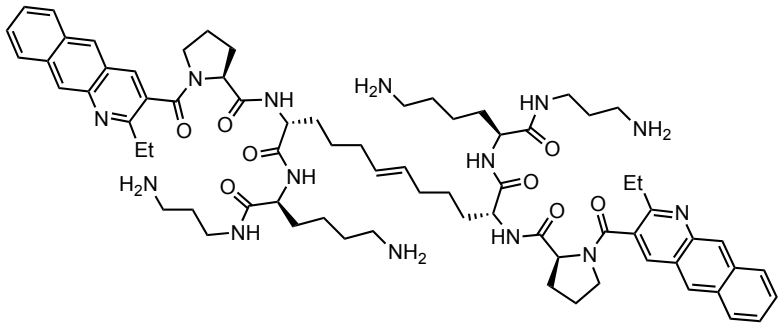	G-C U U C-G G-C C-G C-G-3' C 5' **(CUG)2**

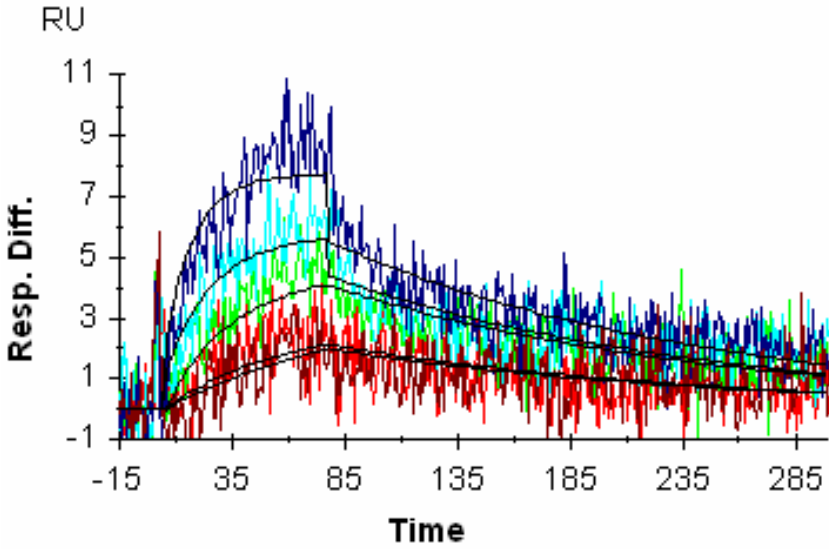

	Trial-1	Trial-2
k_a ($M^{-1}s^{-1}$)	$(9.1 \pm 0.5) \times 10^{3}$	$(9.85 \pm 0.2) \times 10^{3}$
k_d (s^{-1})	$(5.18 \pm 0.09) \times 10^{-3}$	$(7.57 \pm 0.09) \times 10^{-3}$
K_D (nM)	568	768
Chi^2	0.8	1.0
n	ND	

Supplementary Table 39

compound **11**	RNA SEQUENCE
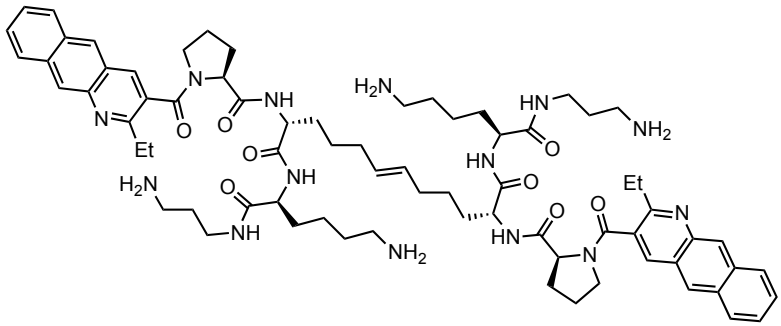	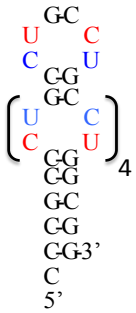 **(CCUG)10**
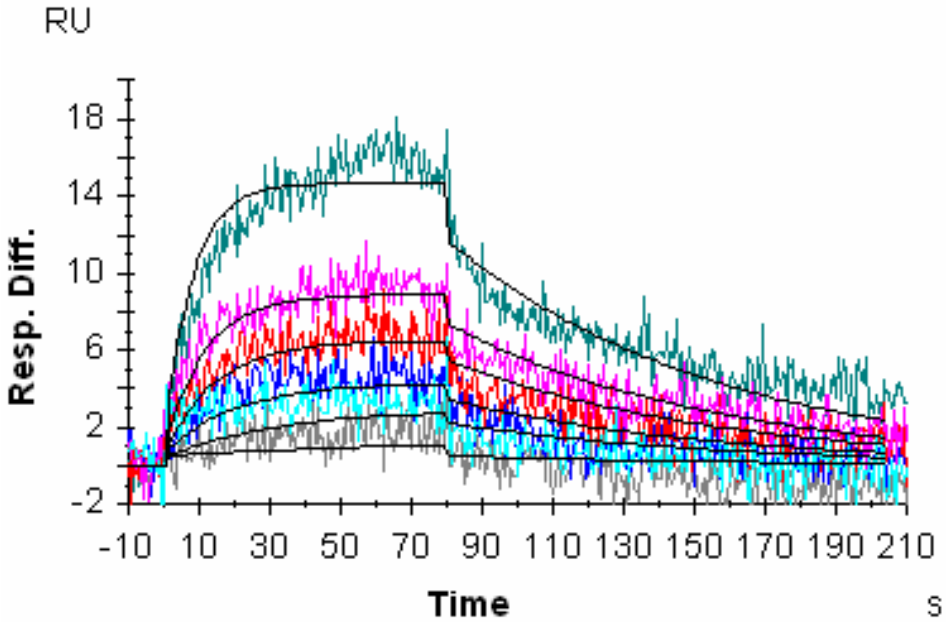	

	Trial-1	Trial-2
k_a ($M^{-1}s^{-1}$)	$(6.08 \pm 0.01) \times 10^{4}$	$(7.5 \pm 0.2) \times 10^{4}$
k_d (s^{-1})	$(1.51 \pm 0.01) \times 10^{-2}$	$(1.30 \pm 0.12) \times 10^{-2}$
K_D (nM)	248	172
Chi^2	1.4	1.3
n	ND	

Supplementary Table 40

compound **11**	RNA SEQUENCE
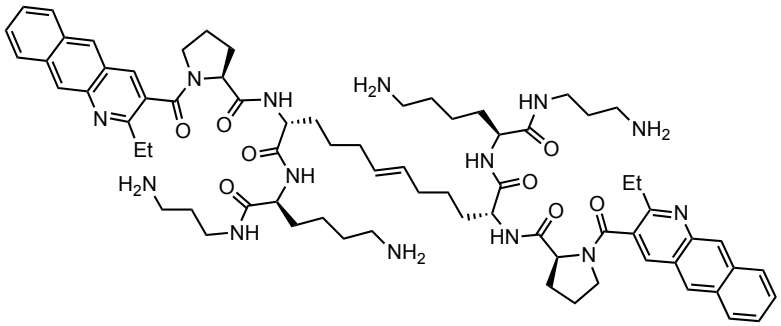	G-C A A C-G G-C (A A) C-G C-G 4 G-C C-G C-G-3' C 5' **(CAG)10**

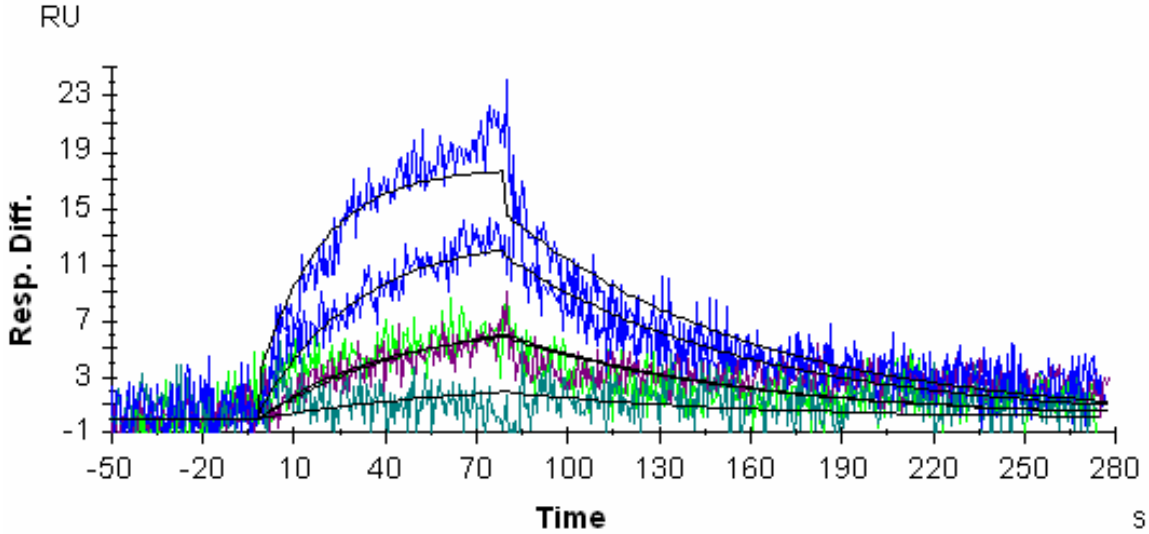

	Trial-1	Trial-2
K_a ($M^{-1}s^{-1}$)	$(1.6 \pm 0.6) \times 10^{4}$	$(1.29 \pm 0.1) \times 10^{4}$
K_d (s^{-1})	$(1.32 \pm 0.01) \times 10^{-2}$	$(1.14 \pm 0.08) \times 10^{-2}$
K_D (nM)	846	878
Chi^2	4.1	2.4
n	ND	

Supplementary Table 41

compound **11**	RNA SEQUENCE
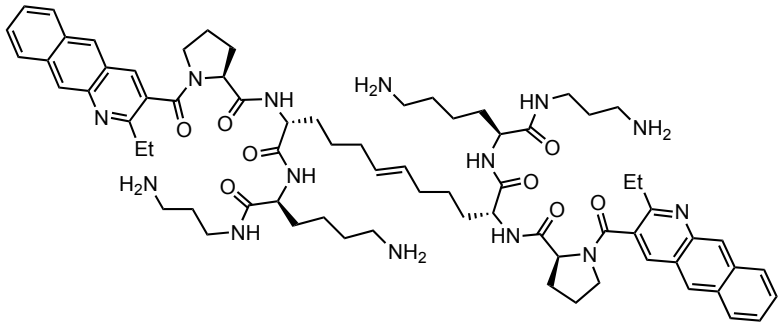	G-C U A C-G (G-C U-A C-G)$_4$ C-G G-C C-G C-G-3' C 5' **Duplex**
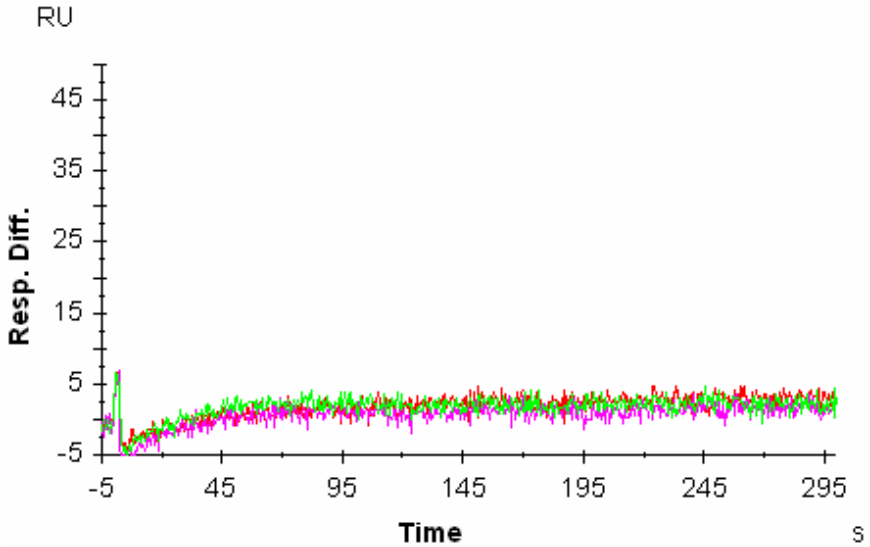	
k_a ($M^{-1}s^{-1}$)	-
k_d (s^{-1})	-
K_D (nM)	No Binding observed
Chi^2	-
n	-

Supplementary Table 42

compound **11**	RNA SEQUENCE
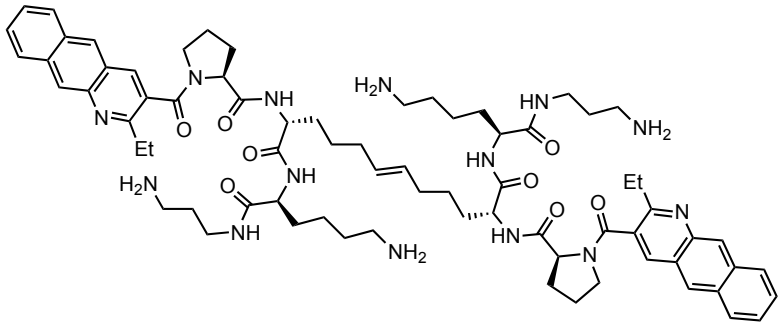	C-A A A C-G C-G C-G U-A U-A C-G C-G G-C G-C 3' 5' **HIV-1FSS**

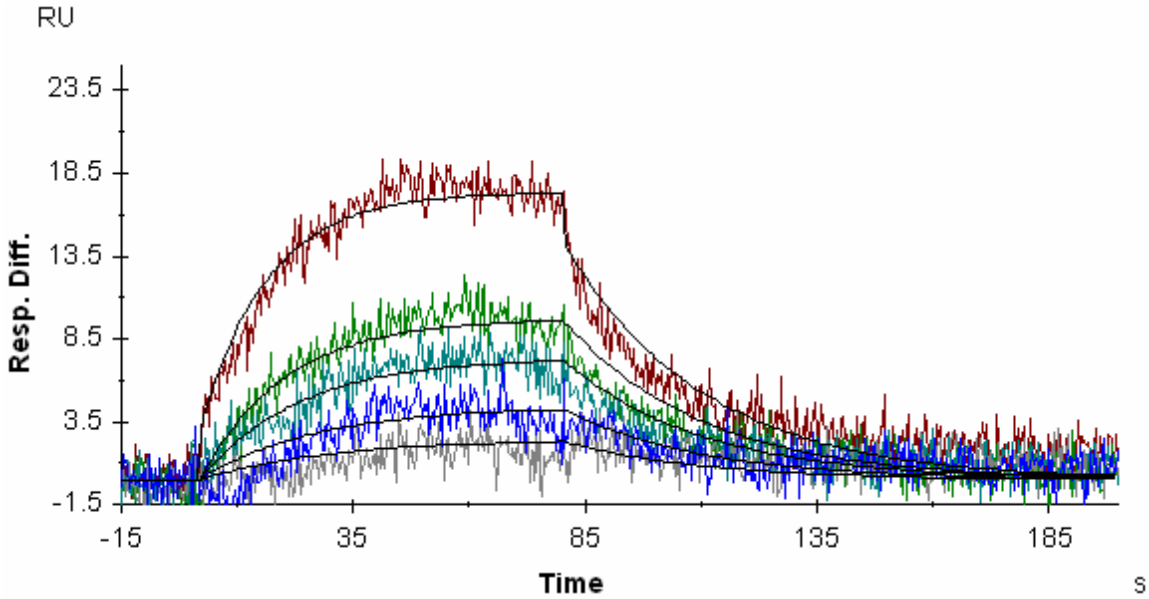

	Trial-1	Trial-2
k_a ($M^{-1}s^{-1}$)	$(9.6 \pm 0.3) \times 10^{3}$	$(2.0 \pm 0.8) \times 10^{4}$
k_d (s^{-1})	$(2.52 \pm 0.04) \times 10^{-2}$	$(2.71 \pm 0.03) \times 10^{-2}$
K_D (nM)	2620	1380
Chi^2	1.5	2.1
n	ND	

Supplementary Table 43

Neomycin B	RNA SEQUENCE
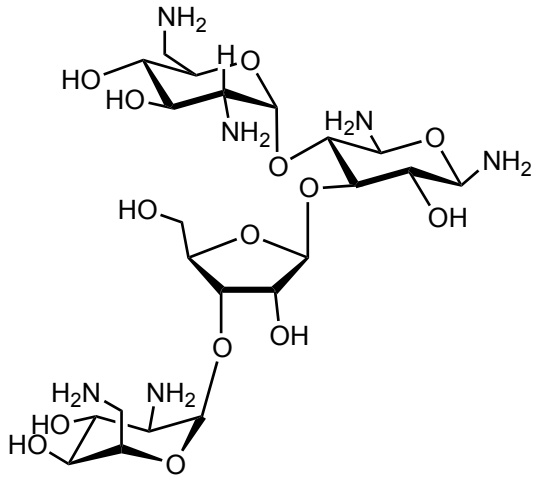	G-C U U C-G G-C U U C-G C-G G-C C-G C-G-3' C 5' **(CUG)10**
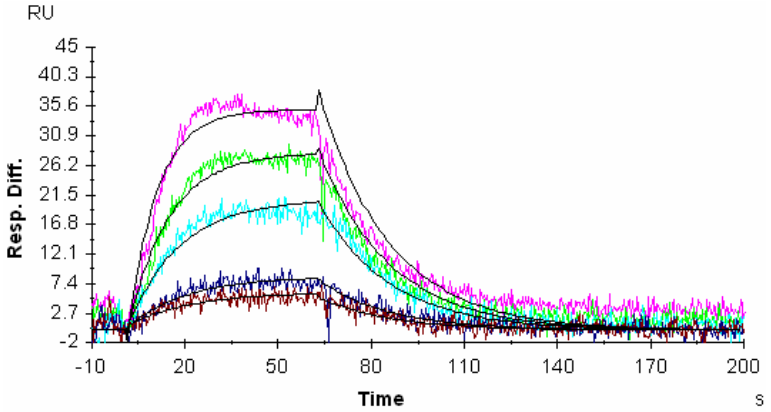	
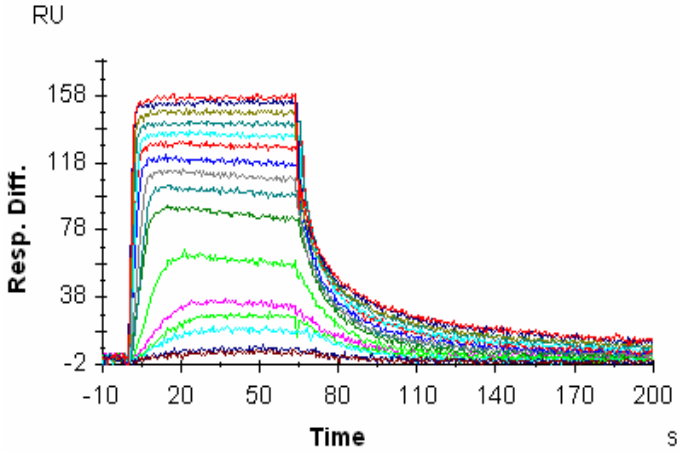 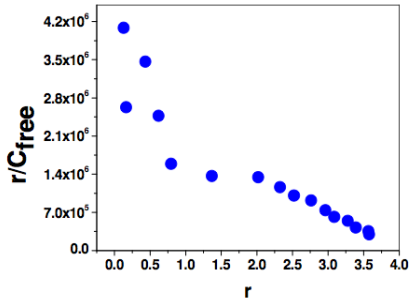	

	Trial-1	Trial-2
k_a ($M^{-1}s^{-1}$)	$(1.22 \pm 0.03) \times 10^{5}$	$(1.27 \pm 0.04) \times 10^{5}$
k_d (s^{-1})	$(5.74 \pm 0.04) \times 10^{-2}$	$(4.40 \pm 0.04) \times 10^{-2}$
K_D (nM)	472	346
Chi^2	0.6	2.3
n	4	

Supplementary Table 44

Neomycin B	RNA SEQUENCE
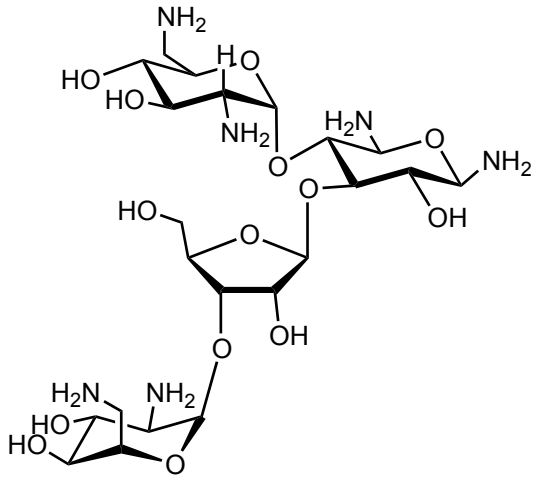	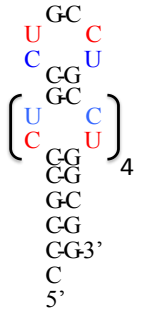 **(CCUG)10**

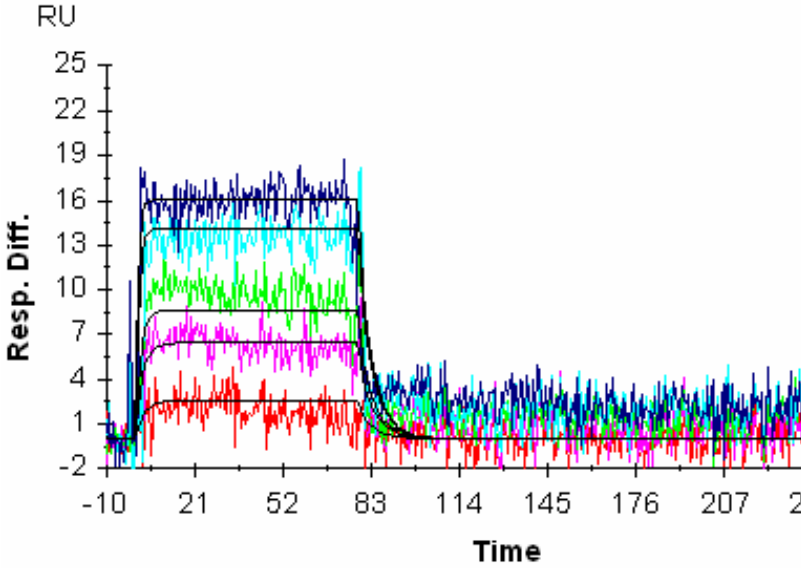

	Trial-1	Trial-2
K_a ($M^{-1}s^{-1}$)	$(7.39 \pm 0.2) \times 10^{4}$	$(1.44 \pm 0.05) \times 10^{4}$
K_d (s^{-1})	$(1.82 \pm 0.001) \times 10^{-1}$	$(2.08 \pm 0.06) \times 10^{-1}$
K_D (nM)	2460	1450
Chi^2	3.1	3.4
n	ND	

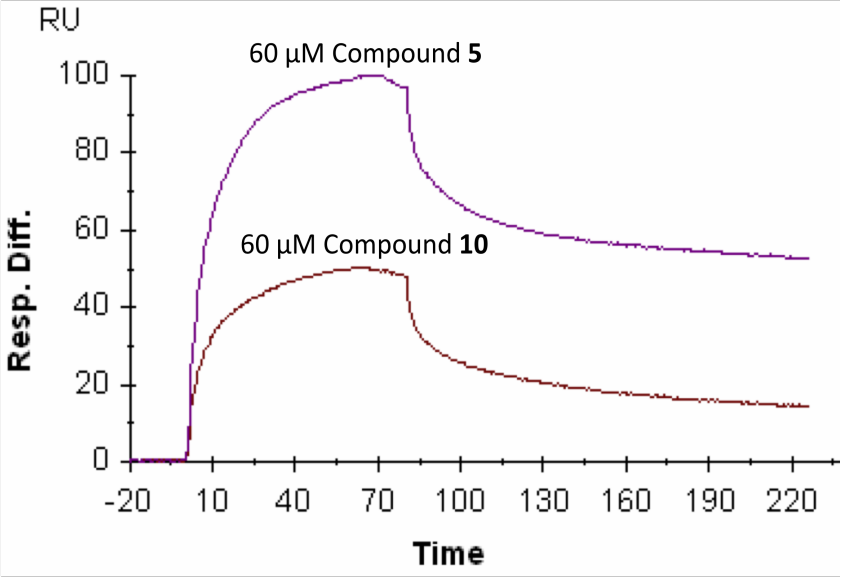

Supplementary Fig 2: An excess of **5** provides roughly double the SPR response for a $(CUG)_{10}$ chip of an equivalent concentration of **10**, consistent with the two-fold difference in stoichiometry deduced from Scatchard analysis.

Note: The Response Units (RU) has been normalized to 100.

Binding Analyses by Fluorescence

ANALYSIS OF (CUG) REPEAT BINDING BY DIRECT MONITORING OF BENZO[G]QUINOLINE FLUORESCENCE.

PROCEDURE

Compounds containing the benzo[g]quinoline heterocycle are inherently fluorescent, and hence can be assayed directly for RNA binding due to changes to their fluorescence properties. Fluorescence titration binding measurements were performed on a Cary Eclipse fluorescence spectrophotometer using a 10 mm path-length semimicro quartz fluorescence cell with 400 μL sample holding capacity. Absorbance measurements were carried out on a UV-Visible spectrophotometer (Shimadzu, UV-1601PC) using a 1 mL (1 cm path-length) quartz cell. Spectroscopic grade anhydrous methanol used in the measurement of relative quantum yield of the 2-ethyl benzo[g]quinoline carboxylic acid was purchased from Alfa Aesar and was used without further purification.

Relative Quantum Yield of 2-ethyl benzo[g]quinoline carboxylic acid (**2**) : the quantum yield of the ethyl benzo[g]quinoline carboxylic acid relative to quinine sulfate (sigma Aldrich) was measured by following literature procedure.[12,13] First, absorbance (0.0-0.06 A.U) and emission intensities were recorded for various concentrations (0 -30 μM) of **2** in methanol. **2** has two distinct excitation maxima at 260 nm and 362 nm respectively, and an emission maximum at 439 nm in methanol. (**Supplementary Fig. 3 a** and **b**). The 362 nm was used as excitation wavelength to record fluorescence spectra for various concentrations of (**1**) in methanol. Next, the number of photons emitted was determined by integrating the area under each fluorescence spectrum using Origin 7 graphical software. The gradient of the plot of integrated fluorescence intensity versus absorbance gives the quantum the quantum yield of the fluorophore.The above procedure was repeated for quinine sulfate by measuring absorbance values at 362 nm and fluorescence emission spectra also at 362 nm excitation wavelength using 0.1 M H_2SO_4 as solvent.

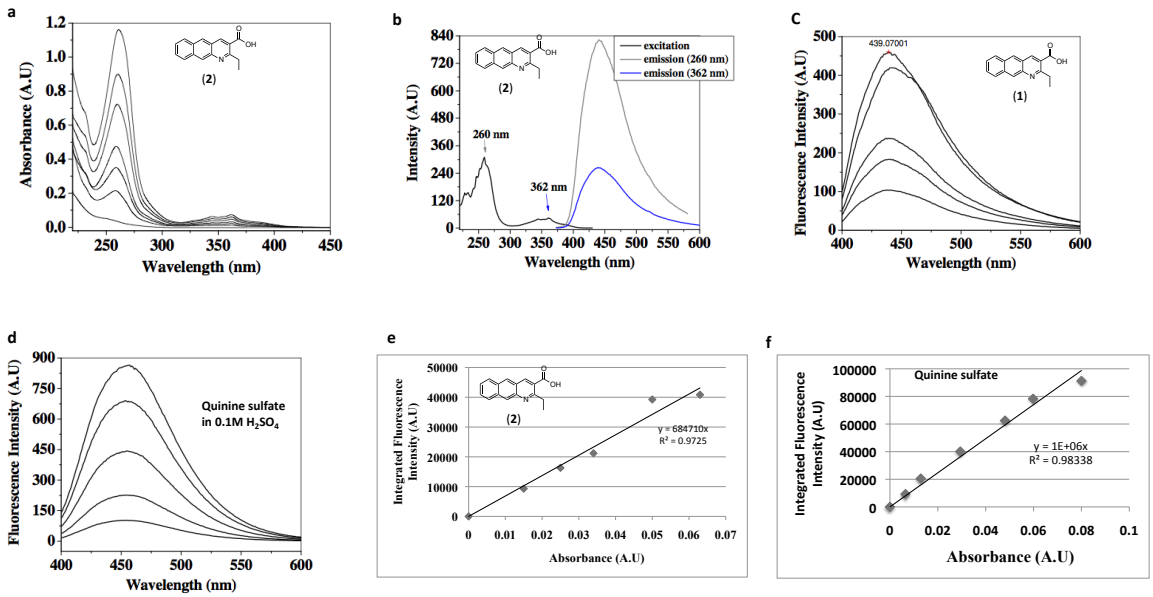

Supplementary Fig. 3: Determination of fluorescence quantum yield of 2-ethylbenzo[g]quinoline carboxylic acid. (a) absorption spectrum of (**2**) in methanol. (b) excitation and emission spectra of benzo[g]quinoline in methanol. (c) Emission spectrum of (**2**) in methanol. (d) Emission spectrum of quinine sulfate in 0.1 N H_2SO_4. (e, f) Plots of integrated fluorescence intensity versus absorbance for benzo[g]quinoline and quinine sulfate respectivly.

The fluorescence quantum yield (ϕ) of **2** relative to the quinine sulfate standard was calculated as 0.64 using the relation:

$$\Phi_{(X)} = \Phi_{ST}\left(\frac{Grad_X}{Grad_{ST}}\right)\left(\frac{\eta_X}{\eta_X}\right)^2 \qquad (1)$$

Where the subscripts ST and X denote standard (quinine sulfate) and test sample (**2**) respectively, and Φ is the fluorescence quantum yield. *Grad* is the gradient from the plot of integrated fluorescence intensity versus absorbance, and η is the refractive index of the solvents used. (1.3325 for water, and 1.3312 for methanol).

Binding analyses of compounds **3**, **4** and **5** by fluorescence based assay: fluorescence binding measurements were carried out in autoclaved 1x HEPES buffered saline (HBS-N) (0.01 M HEPES, 0.15 M NaCl, pH = 7.4). Rnase-free HPLC purified unlabeled $(CUG)_{10}$ repeat RNA was purchased from Integrated DNA Technologies Inc. A 10 μM solution of $(CUG)_{10}$ RNA in 1000 μL HBS-N buffer was heated to 70 $^{\circ}$C for 2 min and then allowed to cool slowly to room temperature in order to ensure that the RNA assumes its secondary hairpin structure. A 1 μM solution of compound was prepared in HBS-N and then 400 μL of this was taken in the cell and excited with a wavelength of 360 nM at a 10 nm slit width. The emission spectrum was collected from 430 nm to 580 nm wavelength range at a PMT voltage of 680 V and 20 nm slit width. The $(CUG)_{10}$ RNA in 1 x HBS was then titrated into the cell containing the compound starting from 1 μL from the 10 μM stock. After each addition, the solution was mixed thorough by pipetting up and down, then allowed to equilibrate for a minimum of 10 min before the fluorescence emission spectra were taken. Equilibrium was determined to be established after taking three similar fluorescence spectra at 1 min intervals. The decrease in the fluorescence intensity of the compound was noted at 468.5 nm for each added concentration of RNA. The fluorescence units (FU) were then corrected for dilution and the FU after each addition was subtracted from the FU at zero RNA concentration to give ΔFU. The titration was discontinued when the binding approached saturation, which was signified by little or no change in FU upon addition of RNA. This ΔFU was plotted against RNA concentration using Origin 7 (OriginLab Corp.). The data were fit to a one-site binding model (equation 2) to obtain apparent binding constants (K_D).

$$Y = \frac{B_{\max} X}{K_D + X} \qquad (4)$$

Where Y = bound ligand:receptor complex concentration, $B_{\max}$ is the total receptor concentration, X is the total ligand concentration and K_D is the dissociation constant. Each titration experiment was repeated at least two times. Representative titration curves as well as emission/excitation spectra for compound **4** and **5** are shown. (**Supplementary Fig. 4**)

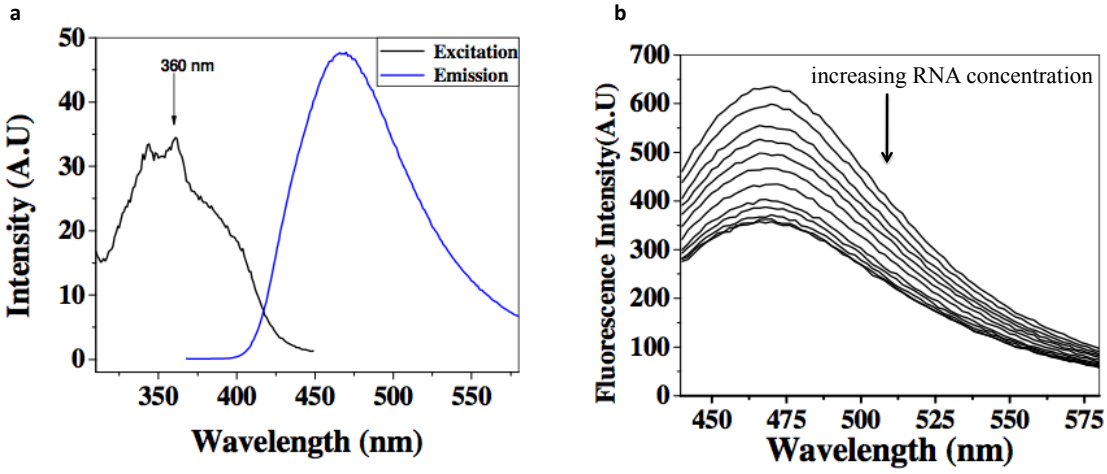

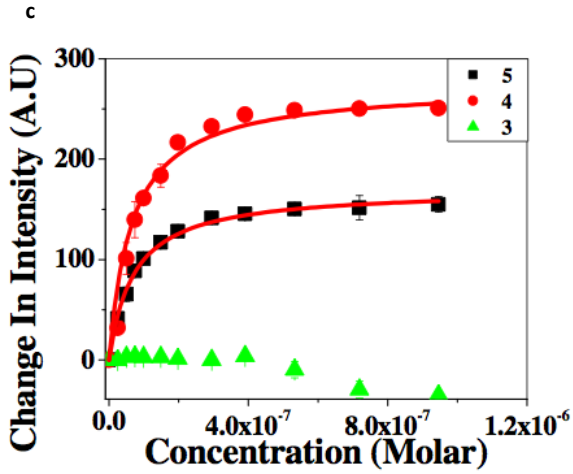

Compound	Binding constant K_D (nM)
3	No binding
4	70.42 ± 1.1
5	66.35 ± 2.1

Supplementary Fig. 4: **(a)** Excitation and emission spectra for **4** in HBS-N buffer. **(b)** Representative fluorescence emission intensity spectra for titration of unlabeled CUG10 RNA into 1μM solution of **4** in HBS-N buffer. The fluorescence intensity of the compound showed quenching upon addition of the target RNA. (**c**) Plots of change in fluorescence intensity units ($\Delta FU = F_o - F_n$) against concentration for titration of **3**, **4** and **5**, fitted with a onsite-binding fit (red line) to obtain apparent K_D (table at the bottom right). Error-bars are standard deviations for at least two separate titrations.

Binding analyses of compounds **10** and **11** by fluorescence based assay: The procedure for measuring the binding constant for **10** and **11** was the same as that used for compounds **3**, **4** and **5** above. The emission and excitation spectra as well as representative fluorescence titration intensity spectra are shown in **supplementary Fig. 5** below.

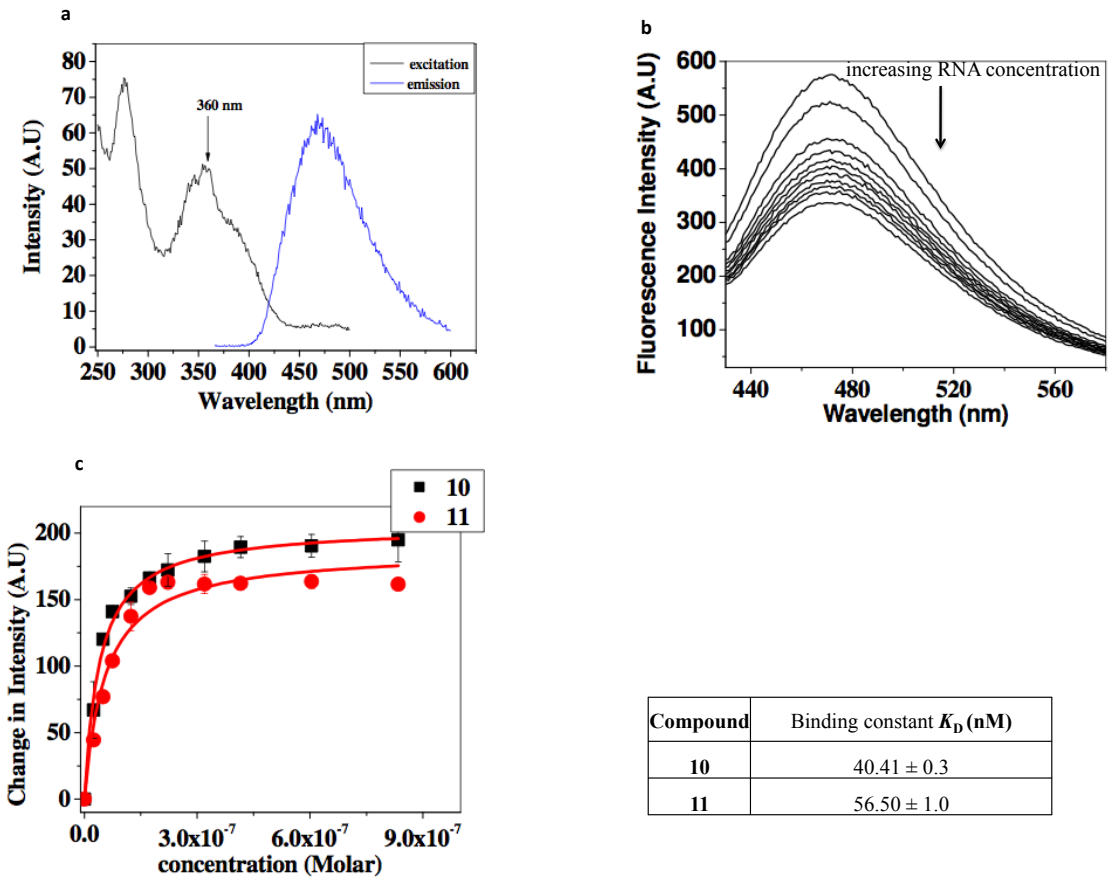

Compound	Binding constant K_D (nM)
10	40.41 ± 0.3
11	56.50 ± 1.0

Supplementary Fig. 5: Binding analysis of extended compounds **10** and **11** to $(CUG)_{10}$ RNA measured by direct monitoring of benzo[g]quinoline fluorescence. (**a**) Excitation and emission spectra for compound **10** in HBS-N buffer pH=7.4. (b) Representative emission spectrum showing the quenching of ligand fluorescence with increasing RNA concentration. (c) Plots of change in fluorescence intensity against concentration for the titration of **10** and **11**. The data were fitted to one-site binding equations (red line) to obtain the K_D shown in the table at the bottom left.

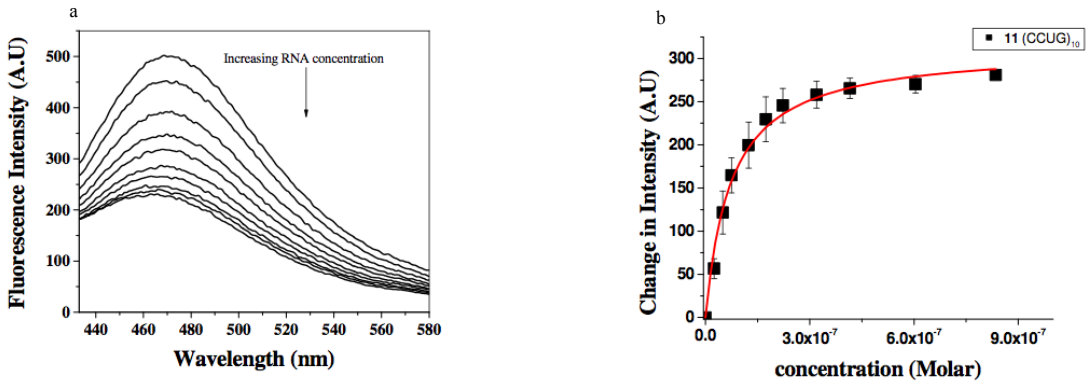

Supplementary Fig. 6: Binding analysis of **11** to $(CCUG)_{10}$ RNA measured by direct monitoring of benzo[g]quinoline fluorescence. (**a**) Representative emission spectra showing fluorescence quenching with increasing RNA concentration. (b) Plot of change in fluorescence intensity against concentration (black squares), fitted (Red line) to a one-site binding equation to obtain an apparent K_D of 73.62 ± 0.75 nM. The error represents an average of two separate titrations.

Cell permeation assessment

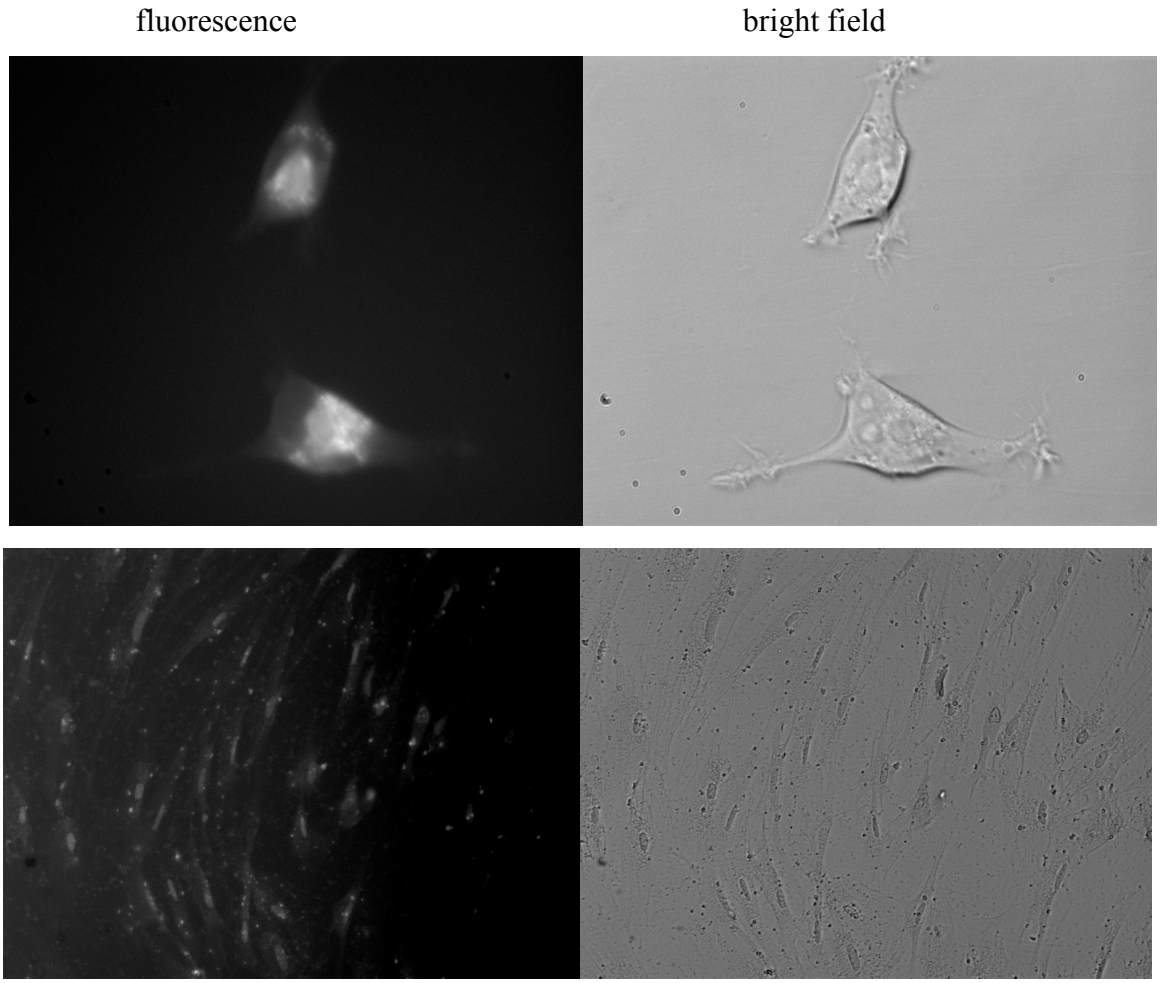

Supplementary Fig. 7. Top: mouse myoblasts (C2-12) incubated 12 h with 125 μM of **4**. (Exposure = 1.5 s). Bottom: human fibroblasts incubated with a mixture of **4** and **5.** Compound shows localization especially in the nucleus of cells.

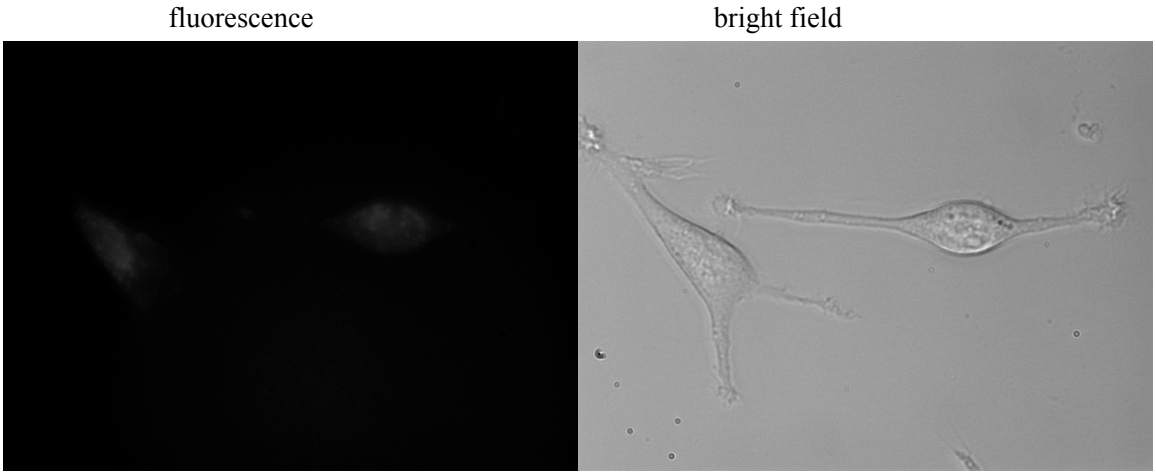

Supplementary Fig. 8. Mouse myoblast cells incubated 12 h with 125 μM of **9** (exposure = 1.5 s).

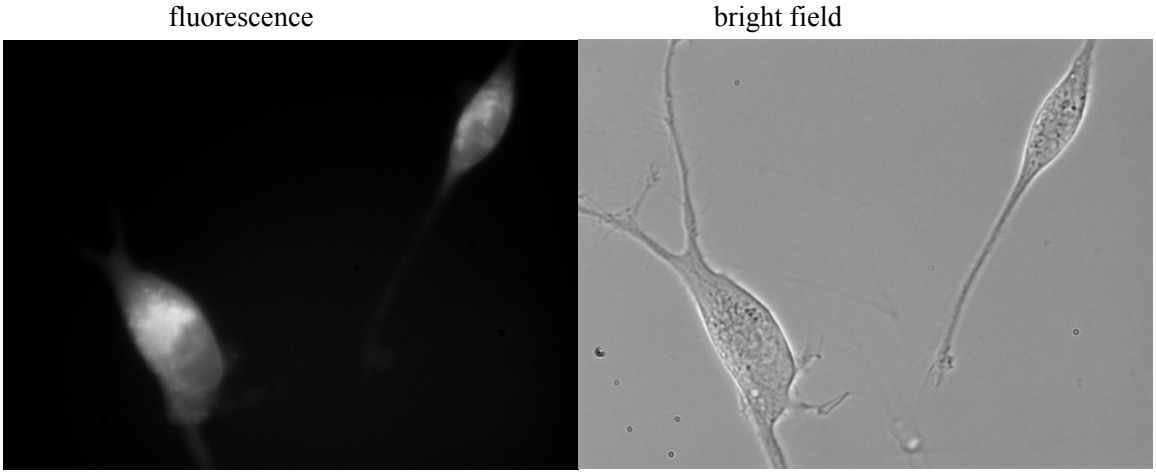

Supplementary Fig. 9. Mouse myoblast cells incubated 12 h with 125 μM of **11** (exposure = 1.5 s).

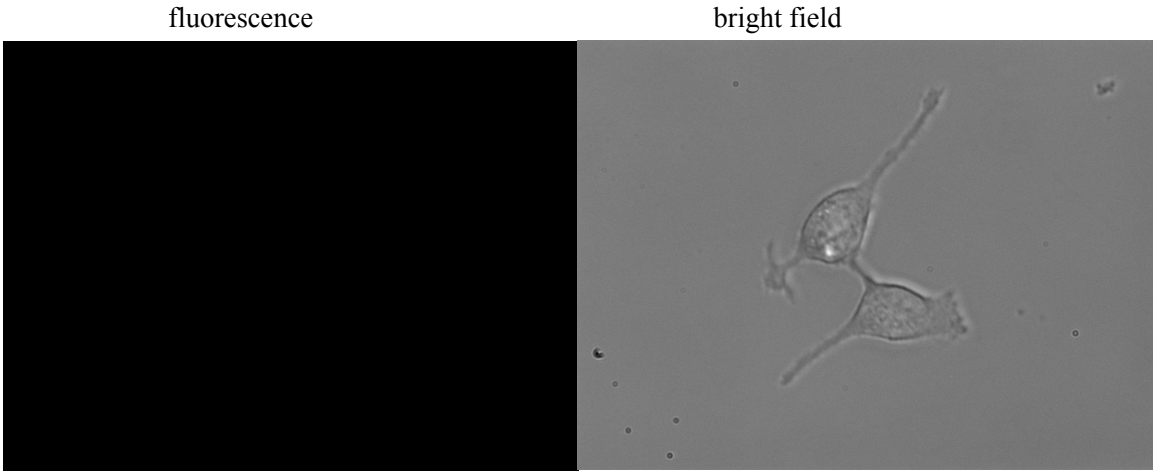

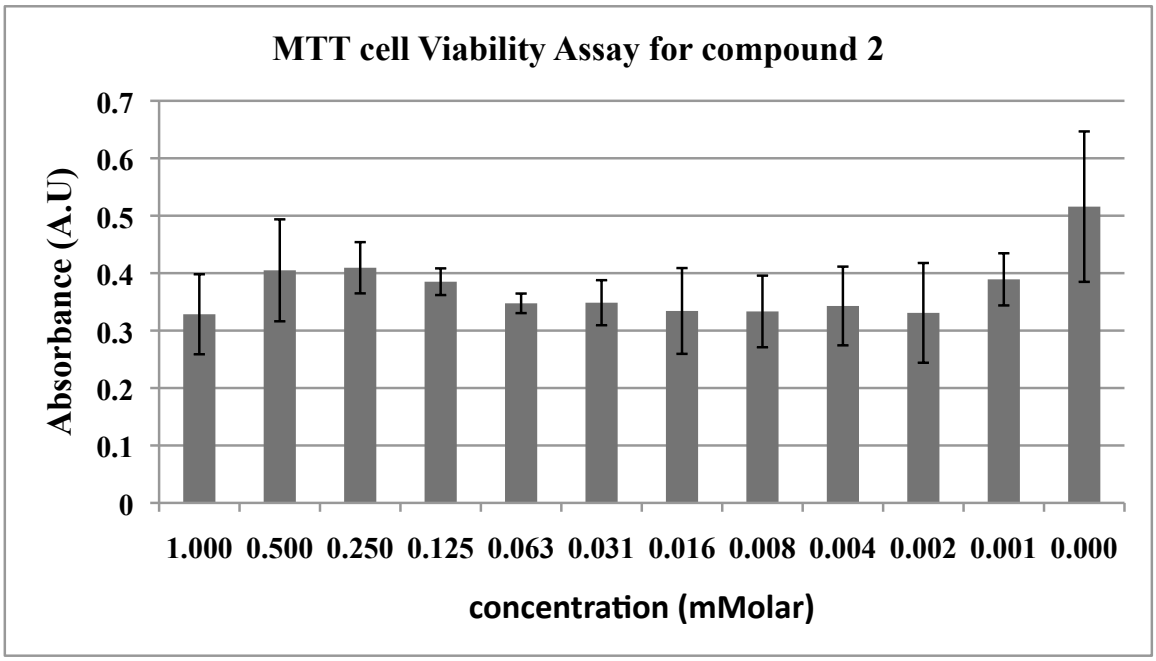

Supplementary Fig. 10. Top: Mouse myoblast cells incubated 12 h with 125 μM of **2** (exposure = 1.5 s). **2** was not internalized by cells. Bottom: MTT cell viability assay of 2-ethyl benzo[g]quinoline carboxylic acid (**2**) using human fibroblast cells

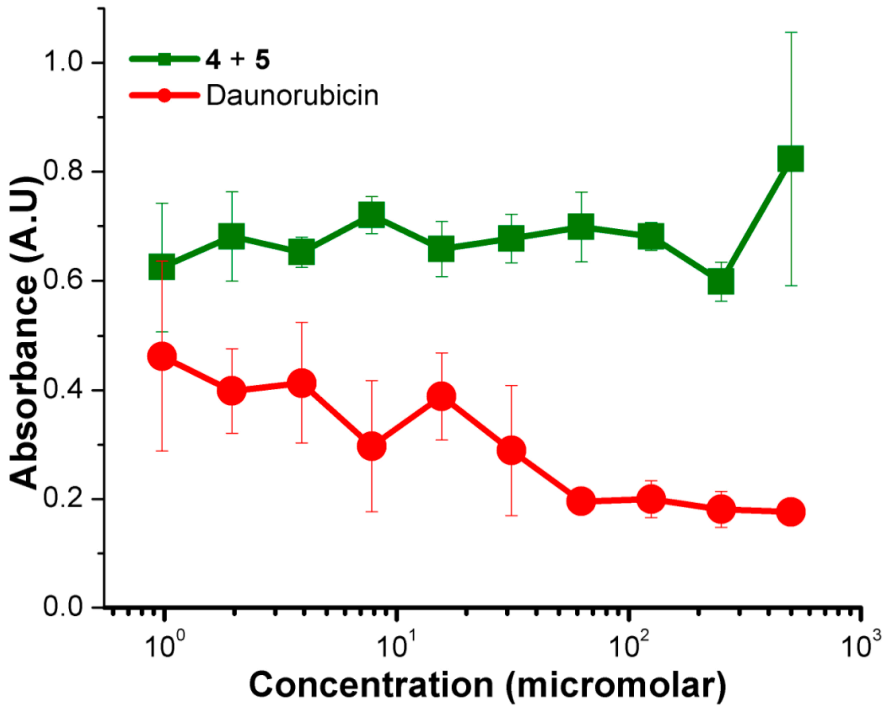

Supplementary Fig. 11. MTT cell viability assay of **4** and **5** (measured as a mixture) in human fibroblast cells. Toxicity of daunorubicin is shown for comparison.

Protein Quantitation by Bradford Assay.

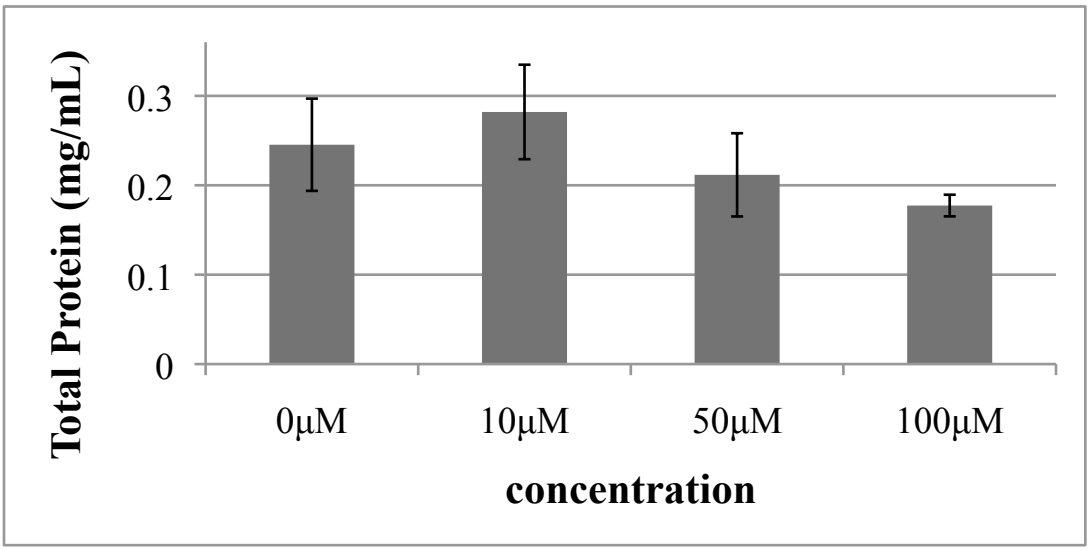

Supplementary Fig. 12. Total protein content of C1-S (mouse myoblasts incorporating a luciferase construct containing zero CUG repeat RNA) cells treated with various concentrations of compound **4.**

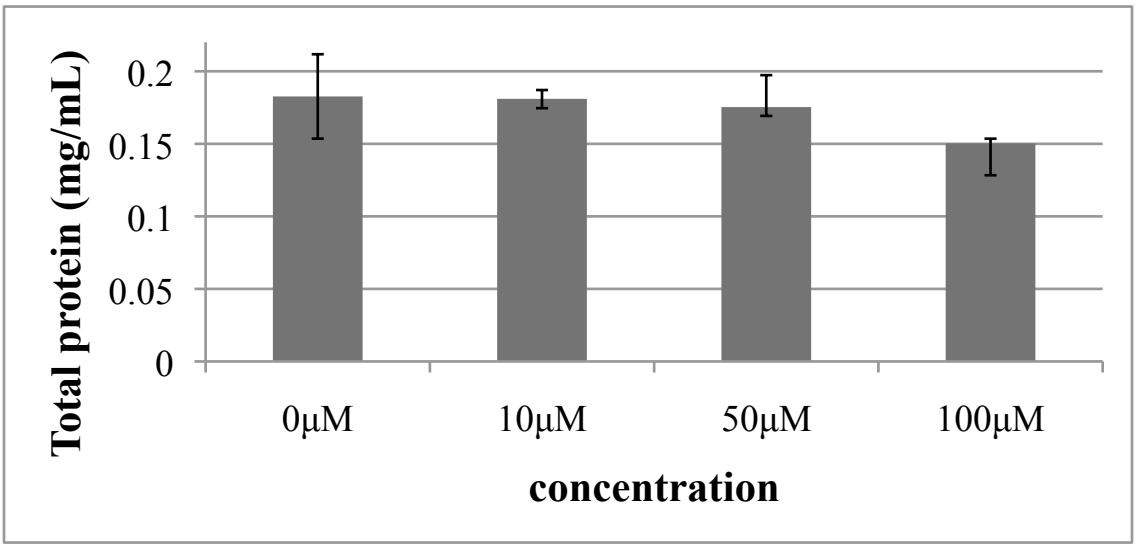

Supplementary Fig. 13. Total protein content of C5-14 (mouse myoblasts incorporating a firefly luciferase with 800 CUG repeats at the 3'-UTR) cells treated with various concentrations of compound **4.**

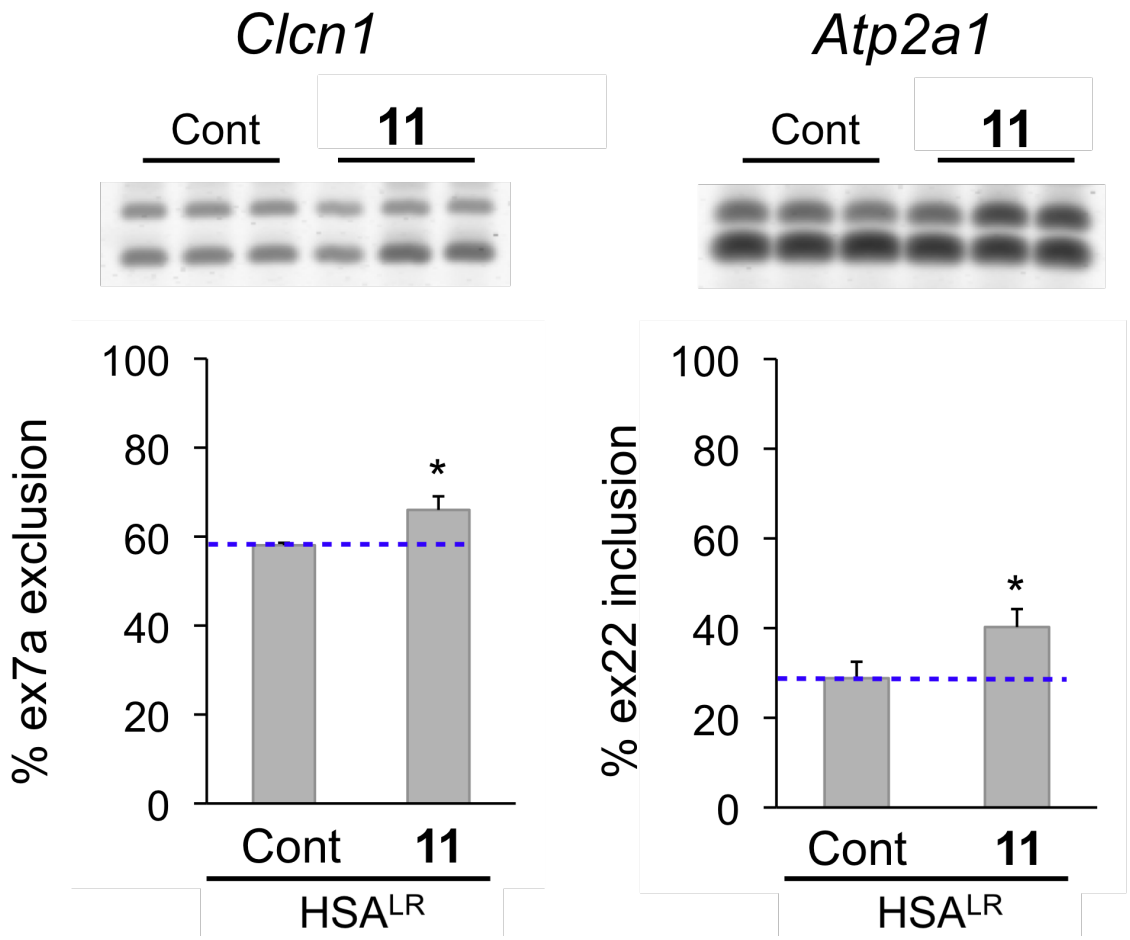

Supplementary Figure 14: Preliminary experiment demonstrating that compound **11** improves MBNL1-dependent splicing *in vivo*. Asterisks (*) indicate statistical significance (P = 0.0113 for *Clcn1* and P = 0.0230 for *Atp2a1*); the dashed line is provided as a reference to splicing levels for *HSA*^{LR} mice in the absence of compound (control; n = 3 each for experimental and control). A repeat of this experiment in which 5 experimental and control mice were examined is shown in Figure 7 of the main text.

Supplementary References:

1. Silva, P.C., Costa, J.S. & Pereira, V.L.P. AN EXPEDITIOUS SYNTHESIS OF 3-NITROPROPIONIC ACID AND ITS ETHYL AND METHYL ESTERS. *Synthetic Communications* **31**, 595–600 (2001).
2. Kienzle, F. Kienzle, F. (1980) The reaction of phthalaldehydes with 3-nitropropionates. A simple route to 3-nitro-2-naphthoic acids. *Helv. Chim. Acta 63*, 2364-2369. *Helv. Chim. Acta* **63**, 2364–2369 (1980).
3. Kokotos, G. & Noula, C. Selective One-Pot Conversion of Carboxylic Acids into Alcohols. *J. Org. Chem.* **61**, 6994–6996 (1996).
4. Pyridinium Chlorochromate-Efficient Reagent for Oxidation of Primary and Secondary Alcohols to Carbonyl-Compounds. (1975).
5. Palde, P.B., Ofori, L.O., Gareiss, P.C., Lerea, J. & Miller, B.L. Strategies for recognition of stem-loop RNA structures by synthetic ligands: application to the HIV-1 frameshift stimulatory sequence. *J. Med. Chem.* **53**, 6018–6027 (2010).
6. Knothe, G., Bagby, M.O. & Weisleder, D. Fatty alcohols through hydroxylation of symmetrical alkenes with selenium dioxide/tert.-butylhydroperoxide. *J Am Oil Chem Soc* **72**, 1021–1026 (1995).
7. Kremminger, P. Asymmetric synthesis of unsaturated and bis-hydroxylated (S,S)-2,7-Diaminosuberic acid derivatives. *Tetrahedron,* Vol. 53, No. 20, pp. 6925-6936*,* (1997).
8. McNaughton, B. R. Bucholtz, K. M.; Camaano-Moure, A.; Miller, B. L. "Self-Selection in Olefin Cross Metathesis: The Effect of Remote Functionality" *Org. Lett.*, **2005**, *7*, 733-736.
9. Silverstein, R.M., Webster, F.X. & Kiemle, D.J. *Spectrometric identification of organic compounds*. Seventh Edition: page 85-120 502 (Wiley: 2005).
10. Myers, A.G., Gleason, J.L., Yoon, T. & Kung, D.W. Highly Practical Methodology for the Synthesis of d- and l-α-Amino Acids, N-Protected α-Amino Acids, and N-Methyl-α-amino Acids. *J. Am. Chem. Soc.* **119**, 656–673 (1997).

11. Ryan, S. J.; Zhang, Y.; Kennan, A. J., Convenient Access to Glutamic Acid Side Chain Homologues Compatible with Solid Phase Peptide Synthesis. *Org. Lett.* **2005,** *7*, (21), 4765-4767.
12. Lee, M. & Grissom, C.B. Design, Synthesis, and Characterization of Fluorescent Cobalamin Analogues with High Quantum Efficiencies. *Org. Lett.* **11**, 2499–2502 (2009).
13. Joseph R. Lakowicz, Principles of Fluorescence Spectroscopy, 2nd ed (Kluwer Academic/Plenum Publishers, 1999).